THESIS

Development and Evaluation of a Compliant Polyurethane, Endothelial Cell Seeded Vascular Graft for use in Infrainguinal Arterial Bypass.

Submitted for the degree of Master of Surgery (University of London)

by

Nigel Tai MBBS FRCS (Eng)

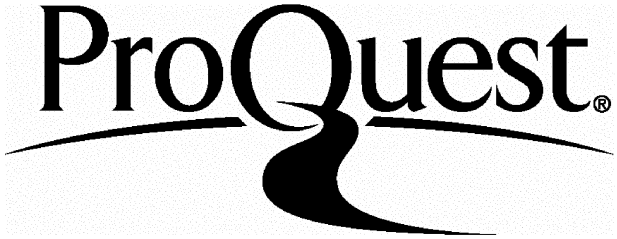

CONTENTS page number

CONTENTS **page number**

CONTENTS **page number**

CONTENTS **page number**

Abstract

Lower-limb vascular by-pass undertaken with prosthetic graft does not have the longevity associated with use of autologous saphenous vein. This work evaluates a new prostheses made from Chronoflex, a compliant polyurethane (CPU), with regard to its compliance, endothelial cell (EC) seeding, and biostability characteristics.

The *in vivo* compliance range that the Chronoflex CPU graft should simulate was determined in 33 human subjects with and without peripheral vascular disease (PVD). The compliance of the femoropopliteal artery was 2.2 - 14.1 % mm Hg^{-1} x 10^{-2} ; PVD was associated with a reduction in compliance. The compliance of grafts made from polytetrafluoroethylene (ePTFE), Dacron and Chronoflex CPU was measured *in vitro* and compared to human artery and vein. Chronoflex CPU and artery had similar compliance values (mean ± SD: 8.1 ± 0.4 and 8.0 ± 5.9 % mm Hg^{-1} x 10^{-2} respectively). The requirements for successful EC seeding of the Chronoflex CPU graft were sought by seeding graft segments over a range of concentrations and incubation periods prior to washing, gamma counting and scanning electron microscopy. Densities beyond 18 x 10^5 cells/cm^2 did not result in greater residual cell retention; the saturation density of Chronoflex CPU was found to be 9.65 ± 1.2 x 10^5 cells/cm^2. Maximal cell retention was observed with 240 minutes incubation. Seeding under these conditions, 72.2 ± 2.5 % of initially attached cells remained adherent following 6 hours of perfusion using a pulsatile flow circuit. Chronoflex CPU grafts, incubated in degenerative media for 70 days and assessed for change by SEM and compliance measurement resisted degradation better than poly (ether) grafts although immersion in t-butyl oxidative solutions caused environmental surface cracking.

It is concluded that the new graft is likely to diminish graft-artery compliance mismatch, is suited to EC seeding applications and possesses superior biostability compared to poly (ether) grafts.

Dedication

This thesis is dedicated to my wife Celestine, my parents and to Nicholas Ingledew.

Acknowledgements

I am indebted to Dr Alex Seifalian for providing me with unceasing theoretical and practical guidance in the design and interpretation of the experiments undertaken for this thesis. I fully acknowledge the help and support of Dr Henryk Salacinski and Mr Alberto Giudiceandrea in the same respect. My thanks to Mrs Karen Cheetham, Mr Geoffrey Punshon and the staff of the University department of Surgery at the Royal Free Hospital and Medical School for their abundant assistance. Dr Buscombe of the department of nuclear medicine provided help with the nuclear medicine image processing system. The electron microscopy unit of the Royal Free Hospital kindly processed samples for scanning electron microscopy and developed the micrographs. Dr Fiona Lampe provided help with the statistical analyses.

I wish to thank my supervisors – Mr George Hamilton and Professor Marc Winslet - for their great help in steadily directing my research with considered advice, instruction and humour.

I acknowledge the financial support of the South Essex Medical Education and Research Trust and Cardiotech Ltd, Wrexham, UK.

Note:

With the above provisos, I was responsible for the great majority of the experimental work conducted in this thesis. I undertook patient recruitment, ultrasound measurements, operation of the walltracking system; acquistion of tissue samples, assembly and operation of the flow circuit, graft preclotting; harvesting, culture and radiolabelling of endothelial cells, seeding of graft material, gamma counting, formulation of degradative media, and compliance testing of the graft specimens. Data collation and input, graph production, statistical analysis and interpretation was carried out by me. The manuscript and text was written by myself and any remaining errors are my responsibility.

Hypothesis

The hypothesis under study in this thesis is that vascular grafts made from Chronoflex, a poly(carbonate) urethane, are suitable for use as endothelial cell-seeded compliant prostheses in arterial bypass procedures undertaken for lower-limb ischaemia.

List of Abbreviations

ABPI	Ankle brachial pressure index
AC	Activity (cell supernatant)
ACE	Angiotensin converting enzyme
ADP	Adenosine diphosphate
AS	Activity (control supernatant)
AIH	Anastomotic intimal hyperplasia
AK	Above knee
AKPA	Above knee popliteal artery
ANOVA	Analysis of variance
AU	Arbitrary units
β	Stiffness index
BCPM	Background counts per minute
BK	Below knee
cAMP	Cyclic adenosine monophosphate
C	Diametrical compliance
CA	Cells adherent
CE	Cholesterol esterase
CFA	Common femoral artery
CF	Correction factor
CPU	Compliant polyurethane
CS	Seeding density
CR	Percentage cells adherent
CV	Coefficient of variation
DNA	Deoxyribonucleic acid
e	Error of a single estimation
EC	Endothelial cells
ECM	Extra-cellular matrix
EDAX	Electron dispersive analysis by X-Ray
Ep	Petersen's elastic modulus
ESC	Environmental surface cracking
FGF	Fibroblast growth factor
FTIR	Fourier transform infra-red spectroscopy
FWC	Flow waveform conditioner
G/B/Co	Glutathione/t-butyl peroxide/cobalt chloride
GCPM	Graft counts per minute
GPC	Gel permeation chromotography
H202/Co	Hydrogen peroxide/cobalt chloride
HUV	Human umbilical vein
HUVEC	Human umbilical vein endothelial cells
MABP	Mean arterial blood pressure
MIH	Myointimal hyperplasia
MC	Mesothelial cells
MDI	Methylene diiodocyanate
NMIP	Nuclear medicine image processor
NO	Nitric Oxide
NS	Non significant
PA	Popliteal artery
PBS	Phosphate buffered saline
PDGF	Platelet derived growth factor
PEG	Polyethylene glycol
PF	Plasma fraction
PLE	Percentage labelling efficiency
PHZ	Para-anastomotic hypercompliance zone
PLA	Phospholipase A2
PSFA	Proximal superficial femoral artery
PTA	Percutaneous transluminal angioplasty
PTFE	Polytetrafluoroethylene
PU	Polyurethane
PVD	Peripheral vascular disease
RGD	Arginine-glycine-D-aspartate
Re	Reynolds number
RF	Radiofrequency
SEM	Scanning electron microscopy
SD	Standard deviation
SMC	Smooth muscle cell
TMF	Transonic medical flow meter
WSS	Wall shear stress
XPS	X-ray photo spectrometry

Table of Figures

Chapter 1.

Introductory review of scientific literature pertaining to the aetiology and prevention of prosthetic vascular graft failure, with particular reference to the issues of endothelial cell seeding and compliance mismatch.

1.1. The problem of lower-limb arterial occlusive disease

1.1.1. Epidemiology and natural history

Occlusive lower-limb peripheral arterial disease is widespread amongst the adult population of developed nations. Approximately 5% of the population aged above 50 suffer from intermittent claudication, the commonest symptomatic manifestation[1,2,3]. The prevalence of asymptomatic disease is much higher ; 22% of the 55-74 age-group who are claudication-free have an abnormal resting or post-exercise ankle-brachial pressure index [2,3] . Patients with intermittent claudication may be considered to have relatively benign disease : under half will experience a deterioration in their symptoms and less than 5% will progress to major amputation [1,2] . However, of those that progress to critical limb ischaemia, which affects 1 in 2500 of the UK population, over two-thirds will require operative revascularisation procedures in order to improve tissue perfusion [4]. The ischaemia is defined as critical if the rest pain has persisted over a two-week period, or if ulceration has occurred; additional features of critical ischaemia include an ankle systolic pressure less than 50 mmHg. In diabetics, this latter criterion is replaced with absence of peripheral ankle pulses because of the unreliability of pressure measurement due to arterial calcification [5]. Altogether, 50 000 admissions are made annually to hospitals in England and Wales as a consequence of peripheral arterial disease, with 15 000 patients undergoing major surgical intervention [6].

1.1.2. Overview of atherosclerosis

Symptomatic lower-limb ischaemia largely results from occlusion of the lower-limb arterial vasculature, occurring due to the progressive development of vessel stenoses or as a consequence of sudden luminal obliteration following thrombosis or embolism. Atherosclerosis is the commonest causative pathology of lower-limb arterial stenoses, and is characterised by intimal lipid accumulation and smooth muscle cell proliferation [7]. Tobacco smokers have up to

a fourfold increased risk of intermittent claudication than non-smokers [8] and the odds are also raised in patients with elevated serum cholesterol [9], hypertension [10] and diabetes [11]. A disease that has afflicted mankind for millennia [12], the pathogenesis of atherosclerosis remains poorly understood. The pathognomonic lesion of atherosclerosis is a fibrous plaque, characterised by a central core of lipid and necrotic debris overlain by a cap of macrophages and smooth muscle cells. The progenitor lesion has yet to be identified although candidates include the fatty streak, a linear accumulation of subendothelial lipid-filled smooth muscle cells (SMCs) or macrophages; and the intimal cell mass, a focal accumulation of intimal SMCs [13]. The aetiology of plaque maturation is likely to be multi-factorial and involve endothelial insult with loss of anticoagulant function, secretion of SMC mitogens and macrophage chemoattractants, and abnormal uptake or accumulation of circulating lipid [14]. Accumulation of activated platelets at the site of injury may compound SMC proliferation. Eventually the core becomes necrotic and the plaque may fissure or ulcerate, causing exposure of thrombogenic material, which results in localised thrombosis or distal embolisation, remodelling and plaque progression. As the plaque develops, the vessel lumen is progressively encroached and, although compensatory vessel dilatation can offset diminished flow, this mechanism is ineffective once the plaque occupies 40% of luminal cross-sectional area [15]. Finally, as a consequence of plaque rupture and the rapid formation of thromboses, complete vessel occlusion may occur. The most commonly affected regions of the lower limb arterial tree are the above-knee popliteal artery as it passes through the Adductor canal, the midgenicular popliteal artery, popliteal trifurcation and the proximal portions of the tibial vessels [16,17].

1.1.3. Clinical features

The clinical picture is dependent upon whether the arterial occlusion develops chronically or is the result of an acute process. Likewise, the severity of ischaemia can be classified according to the risk of limb-loss.

Claudication (derived from the Latin *to limp*) is a characteristic feature of chronic lower-limb ischaemia. The patient typically experiences calf or thigh pain reproducibly precipitated by exercise; moreover the pain is quickly relieved upon cessation of exercise [18]. Persistent foot pain, particularly pain in the toes and metatarsal heads, is a sign of declining perfusion, worsening ischaemia and the possibility of tissue death or limb-loss. In early cases the pain typically occurs at night and may be relieved by the patient placing the foot in a dependent position either by hanging the foot over the bed or rising and walking [19]. Acute lower limb ischaemia that occurs in the absence of preformed collateral vessels presents with severe lower limb pain; paraesthesia and then paralysis develop as nerve and muscle function diminish respectively. On examination the leg appears pale and cold to touch. Pulses will be absent distal to the level of occlusion. Eventually the skin will become mottled and stained and the muscle bellies tense; such features usually indicate irreversible ischaemia [20]. In those with a past history of claudication, the effects of an acute arterial occlusion may be diminished by the presence of a pre-existent collateral circulation.

1.1.4. Surgical management

In general, claudication should be managed by ensuring that the patient stops smoking [21] and undertakes regular, structured exercise [22]. Any hyperlipidaemia or thrombophilia must be identified and treated as part of an overall strategy to manage the other clinical manifestations of atherosclerosis in the cardiac or extracranial circulation. Aspirin should be started [23].

After identifying the extent and level of disease with Duplex ultrasound and contrast arteriography, patients with disabling claudication or critical ischaemia may be treated with percutaneous transluminal balloon angioplasty or reconstructive surgical bypass. Angioplasty of proximal stenoses can be used to convert multi-level into single segment disease thus converting critical ischaemia to claudication or reducing the length of distal bypass required [20]

The first recorded episode of successful arterial reconstuction was when José Luis Goyanes carried out popliteal vein grafting for a popliteal artery aneurysm in 1906 [24]. In 1949 Jean Kunlin (a protégé of René Leriche) described the first successful series of arterial bypasses with saphenous vein as a treatment for chronic lower-limb ischaemia [25]. The technique was further developed by DeBakey in the 1950s [26] and nowadays the surgical bypass of diseased arterial segments is an established means of increasing blood flow within lower limb arteries.

1.1.5. Indications for surgical bypass

Correct selection of the patients who require surgical bypass is necessary in order to reduce the chances of graft failure. Indications for surgical bypass [27] include unilateral disabling claudication that has not responded to other measures, presence of critical ischaemia pain and deteriorating ischaemia in a patient with contralateral amputation. Contraindications include poor inflow or outflow (as judged on contrast arteriography) and disabling angina, stroke or limb paralysis.

1.1.6. Outcome of infrainguinal bypass

Whittemore has analysed the results of four recent series and obtained mean patency data corrected for variations in the number of patients treated in each series [28]. When autologous saphenous vein is utilised mean primary patency rate at 5 years is 75% for a bypass to above-knee (AK) popliteal artery and 67% when a distal – i.e. infrapopliteal – reconstruction is undertaken. Expanded polytetraflouroethylene, (ePTFE) is the prosthetic material most commonly employed if autologous vein is not available and the equivalent mean 5 year patencies are 50% for AK and 14 % for distal bypass (based on data summarised from 9 and 4 studies respectively). As acknowledged by Whittemore, the studies differed in such factors as the proportions of patients with claudication or critical ischaemia and type of vein bypass utilised (*in situ* or reversed saphenous vein). However, this summary illustrates the fact that

prosthetic material does not perform as well as vein, particularly if the bypass is distal or undertaken for critical ischaemia. Ideally, vein should be used in all bypasses, even in the above knee position where the performance of prosthetic grafts approaches that of vein [29]. Unfortunately, in 30% of patients a prosthetic graft is required because no suitable vein is evident [30] typically because the patient has already undergone prior lower limb re-vascularisation or coronary artery by-pass .

1.1.7. Consequences of failed bypass

A vascular graft, interposed within the arterial circulation and exposed to pulsatile flow, can be described as having failed when it no longer conducts any blood to the distal tissues. Prior to outright cessation of flow, a failing graft is one which is patent to some degree but whose function has so deteriorated that the patient experiences symptoms of lower-limb ischaemia [31]. This definition should be broadened to include grafts where diminishment of flow has led to reduction in objective markers of distal perfusion (such as diminished ankle pressures as measured by hand-held Doppler) that precede the symptoms of ischaemia.

Patients with a failing or occluded graft will encounter a number of deleterious consequences. Of those in whom the graft was performed as a treatment for claudication, one in four will experience ischaemia worse than that which existed prior to bypass [32]. If the limb becomes threatened then urgent re-intervention is required, and so the patient will become exposed to the attendant morbidity and mortality of treatments such as thrombolysis and angioplasty, or operative graft exploration, revision and replacement. The outlook is particularly poor for patients with failed distal prosthetic bypass as all suitable sources of vein are likely to have been exhausted, thus the 3 yr patency of secondary reconstructions of PTFE grafts is around 12%[33]. Furthermore, there is evidence that patients with failed distal bypass will require a higher level of amputation than if they had undergone amputation as a primary procedure [34], although such evidence is disputed [35]. Some 50% of amputees will have died within 3 years of

their amputation [36] and as few as 5% are satisfactorily rehabilitated [37]. Patients who eventually undergo amputation because of a failed graft have frequently endured the distress of several operative procedures for no obvious net gain.

1.2. Causes of failure of surgical bypass

The miscellaneous causative factors in graft failure can be classified as either patient, surgeon or graft-related.

1.2.1. Surgeon and patient-related causes of failure

Patient-associated factors in graft failure include progression of the patient's occlusive vascular disease, either proximal or distal to the graft, which may lead to sufficient reduction in graft inflow or runoff such that flow diminishes and thrombus is formed. This process accounts for 30% of all failures when using PTFE grafts [38] and is a frequent cause of late-onset failure occurring 18 months or more following reconstruction. A similar reduction of graft inflow due to fall in cardiac output or hypotension caused by cardiac ischaemia may also produce graft thrombosis. A hypercoaguable state predisposes to graft failure [39]. Patients who continue to smoke have a heightened incidence of subsequent prosthetic graft failure and in one series graft patency at 2 years was 21% lower for smokers against non-smokers [40].

Surgeon-related factors in graft failure concern the proficiency of the clinician in selecting the patient and performing the by-pass. These determinants are of prime importance in achieving a successful outcome, especially so when autogenous vein is no longer available. The absolute prerequisites to reconstruction are a sufficiently pressing operative indication (rest pain, tissue necrosis, disabling claudication or a threatened limb) plus adequate inflow and run-off in a patient who will be able to withstand the stress of surgery. Failure to observe these requirements will result in early graft failure. Likewise, technical deficiency in performing the

anastomoses or other key parts of the surgery will manifest as graft failure, usually within 30 days of operation.

1.2.2. Graft-related causes of failure

Modern prostheses are disadvantaged by several characteristics likely to precipitate eventual failure of the bypass.

1.2.2.1. Contemporary Graft Materials and Design

The overwhelming majority of prosthetic vascular grafts in clinical use today are fabricated from either expanded polytetrafluoroethylene (ePTFE) or Dacron. Grafts made from ePTFE are the most widely utilised despite the existence of modern evidence demonstrating that Dacron performs adequately in infrainguinal bypass [41,42] . Although textile PTFE had been used for vascular prostheses in the early 1960's, it was not until Robert Gore developed a method of producing extruded, expanded PTFE [43] that use of this material for infrainguinal repair became a realistic proposition. It consists of solid nodes of PTFE – a polymer of carbon bonded to fluorine atoms – from which extend longitudinally arranged fibrils. ePTFE is highly porous, with the ePTFE node-fibril structure accounting for 15-20% of the total volume of the material [44] , but is hydrophobic and thus does not require pre-clotting; current grafts have a pore size of 30μm. The expanded material has better tensile strength with less deformation under load than unexpanded PTFE. Circumferential strength is maintained by the addition of an ePTFE wrap to the outer surface. ePTFE vascular grafts are highly resistant to creep, have a high burst pressure and retain sutures well. ePTFE is inert and stable to biologic degradation. Since Campbell and colleagues' first use of ePTFE grafts for infrainguinal bypass in 1976 [45], the original specification by W.L Gore has been modified, and a variety of wall thicknesses, fibril lengths and supported or wrapped designs are available.

The alternative prosthetic material for infrainguinal reconstruction is a yarn of Dacron, (polyethylene terephthate) knitted into a textile graft. The yarn itself is multifilamentous and texturised to impart elasticity and softness. Knitted yarns are used for their greater porosity over woven yarns; they have greater compliance and superior handling qualities but require pre-clotting to seal the interstices of the cloth and are less strong than their woven counterparts; because of slippage of the knit pattern progressive dilatation may occur [46]. The material may be crimped to impart additional elasticity and kink resistance although such a treatment may disrupt laminar blood flow and provoke thombogenesis [47]. Externally supported uncrimped material is often used when crimping may compromise the patency of a small diameter prosthesis. Knitted Dacron grafts require pre-clotting in order to reduce transmural leakage although collagen or albumin-impregnated grafts are commercially available; such grafts do not require pre-clotting and may be less thrombogenic than untreated prostheses [48].

Although not in widespread clinical use, human umbilical cord vein (HUV) has attracted much investigation as a conduit for lower-limb revascularisation. The graft consists of a length of stripped umbilical vein that has undergone several tanning procedures with glutaraldehyde and ethanol to impart strength and decrease antigenicity. The graft is then enclosed in a Dacron mesh. The so called "Dardik" graft has been reported to have favourable 5 year patency rates of 26-28% in the infrapopliteal position [49], although there is dispute over whether the patencies associated with HUV grafts are superior to those of ePTFE prostheses [50,51]. However, despite its satisfactory patency profile, problems concerning graft handling, lack of graft uniformity and a preponderance for long-term aneurysmal degeneration [49] have limited surgical enthusiasm for this type of prosthesis.

1.2.1.2. The concept of the ideal vascular graft

As discussed in section 1.1.6., use of prosthetic grafts instead of autologous saphenous vein affects the likelihood of long-term bypass patency, especially if distal reconstruction is undertaken. The goal of graft development is to engineer a prosthetic graft that has limitless patency *i.e.* to create an "ideal" graft [52]. The concept of the ideal graft is a useful brief to consider when evaluating new vascular prostheses. Such a graft should be a conduit of pulsatile blood flow that easily integrates into host tissues and is non-toxic. Flawlessly matching the biomechanical properties of human artery, the ideal graft should have an actively non-thrombogenic luminal surface, be resistant to infection and aneurysmal deformation, possess good suture retention and handling features, and be of low cost but easily obtainable in sterile form.

1.2.1.3. Disadvantages of current grafts

Graft failure occurs though one principal mechanism: intra-luminal formation of thrombus with cessation of bloodflow. This may occur due to the inherent thrombogenicity of the graft, or as a consequence of lowered flow through the outflow tract due to the progression of native disease or the development of anastomotic intimal hyperplasia (AIH). Assuming patient selection has been adequate, primary graft thrombosis accounts for the majority of early graft failures (< 30 days) whilst thrombosis secondary to diminished outflow is responsible for later failure [33]. Therefore graft factors likely to influence patency include the inherent thrombogenicity of the graft material and the extent to which the graft is incorporated by the host as this may affect the degree to which the graft becomes endothelialised and thus non-thrombogenic. Equally important is the degree to which the bypass generates anomalous mechanical and shear stress in the adjacent distal vessel as such stresses have been postulated to induce AIH.

1.2.1.3.1. Graft thrombogenicity

The graft may have a high potential for causing intra-luminal accretion of thrombus, either by the inherent thrombogenicity of the material used to fabricate the graft, or because the graft fails to encourage a host response that could lead to formation of a non-thrombogenic intima.

1.2.1.3.2. Material thrombogenicity

A graft destined for infrapopliteal use should have as low a *thrombotic threshold* [53] as possible *i.e.* remain patent even in the face of very low velocity blood-flow. Following exposure to blood-flow all prostheses will develop a luminal layer of plasma proteins, fibrinogen and fibrin. This layer has potential to activate platelets and initiate clot formation [54]. Smaller-diameter grafts in low-flow situations have a propensity for developing a relatively thicker layer of fibrin; it is therefore advantageous for grafts in this situation to either have low thrombogenicity or be actively antithrombogenic. Unfortunately neither ePTFE or Dacron can be regarded as anti-thrombogenic: within 1 hour of exposure to flow an irregular fibrin/platelet structure forms on the luminal surface [55] ; within 3 days this interface has incorporated leucocytes and still continues to attract red blood cells. Dacron is especially thrombogenic; such grafts cause greater platelet deposition than ePTFE [56], are able to systemically activate platelets [57], induce *in vitro* procoagulant macrophage activity [58] and are subject to persistent platelet accumulation for years post-implantation [59].

1.2.1.3.3. Host Tissue Response

The ideal end-result of successful incorporation of a prosthetic graft is the spontaneous development of a confluent lining of actively antithrombogenic endothelial cells at the luminal surface. Endothelialisation would be facilitated through "fall-out" deposition of endothelial cells carried in circulating blood, at the adventitial surface *via* a vasa vasorum of vascularised tissue elements growing through the graft interstices, or by the migration of cells from

contiguous artery. Additionally, the graft should be incorporated such that it is anchored firmly but not constrained excessively so that graft elasticity is preserved. Unfortunately, neither Dacron or PTFE grafts implanted within humans exhibit endothelial colonisation beyond the immediate juxta-anastomotic area [60,61]. The reason for this is not known but many factors are likely to be involved; endothelial cells preferentially adhere to flattened rather than to fibrillar surfaces [62] ; graft complement activation can in turn activate polymorphonuclear (PMN) leucocytes which then mitigates against graft EC colonisation [63]; and compared to animal cells, human endothelial cells may lack sufficiently robust reproductive capacity to spontaneously colonise prosthetic graft material *in vivo* [64]. Additionally, it has been hypothesised that microporous grafts do not allow for adequate tissue ingrowth. Conventional ePTFE has an average internodal distance of 30μm and shows poor potential for tissue ingrowth [61] which may be further restricted by the presence of an outer supportive wrap possessing internodal distances of 5-10μm.

1.2.1.4. Anastomotic intimal hyperplasia (AIH)

AIH is characterised by a proliferation of subintimal smooth muscle cells (SMC), with deposition of excess extracellular matrix, in the native artery just distal to the lower anastomosis [65]. The resulting luminal encroachment impedes bloodflow, causes stagnation and thence graft thrombosis, and is responsible for the majority of graft failures that occur beyond 30 days post-implantation [66]. Dacron and ePTFE bypasses are equally likely to develop AIH [67]. The pathogenesis of AIH is unclear, but the key events appear to be an initial insult to the endothelium with SMC migration and hyperplasia occurring in response to mitogenic stimulation produced by interaction between the overlying injured endothelium and elements of flowing blood [66]. In this respect, AIH resembles the migrational and hyperplastic response by SMC's provoked by endothelial damage sustained during balloon angioplasty or following vein grafting, known as myointimal hyperplasia (MIH). Neville and Sidawy have

compared and contrasted these pathological entities [66]. Damage during angioplasty, vessel arthrectomy or endarterectomy, or placement of luminal stents, typically leads to extensive endothelial denudation. Thrombus is deposited, nitric oxide and heparan sulphate levels diminish, and SMC proliferation begins. Macrophages secrete growth factors such as platelet derived growth factor (PDGF), Angiotensin II, and basic fibroblast growth factor; these peptides attract SMC's and draw them across the internal elastic lamina. SMC proliferation peaks by four weeks post injury, but the deposition of extracellular matrix continues for up to a further year, despite re-establishment of endothelial continuity.

In bypass grafting where autologous vein is used, the injury is less extensive, and re-endothelialisation is achieved more quickly. However, SMC proliferation continues despite an intact endothelium; it occurs over a longer time course as compared with the response to balloon angioplasty, and there is a larger medial contribution to the proliferative response. Two proposed causative factors in MIH in this situation include vein wall ischaemia due to interruption of the vasa vasorum and the increased tangential wall stress that the vein is exposed to when placed within the arterial tree. Indeed, recent research conducted by Angelini's group has shown that intimal and medial hyperplasia can be reduced in vein grafts by positioning the vein segment within an oversized external polyester stent [68]. Using a porcine saphenous vein model, they demonstrated diminished wall thickness together with less neointimal and medial hyperplasia plus lower levels of cellular proliferation as compared to normal, unstented vein grafts. Interestingly, they also found higher levels of PDGF protein in the unstented grafts. The authors have suggested that the stents serve to reduce excessive vein deformation produced by exposure to arterial pressures, thereby limiting the medial and intimal hyperplasia that is a frequent response to increased tangential wall stress. Furthermore, the stent provokes formation of a densely vascular neoadventitia in the space between stent and graft. Although the vascularity progressively diminishes with time, it may be sufficient to reduce the ischaemia that the vein wall experiences due to interruption of the

vasa vasorum. As well as suggesting a means of improving the performance of coronary artery by-pass grafting with autologous vein, this paper serves to emphasize the importance of mechanical-haemodynamic factors in the development of intimal and medial hyperplasia. However, the relevance to peripheral arterial bypass has yet to be demonstrated.

Anastomotic intimal hyperplasia can be considered to be a variety of MIH, although the combination of initiating and sustaining factors is particular to the specific situation of arterial bypass with prosthetic material. Some damage to endothelium will occur due to gentle instrumentation of the arterial wall and suture placement. Other important factors thought to predispose current prostheses toward the development of AIH are the generation of abnormal shear-stresses at the site of the anastomosis, caused as blood passes from graft to artery, and the acute disparity in elastic behaviour of graft and artery evident in the para-anastomotic region.

1.2.1.4.1. Anomalous shear-stress as a contributory factor

Arteries are able to regulate their diameter in response to changes in blood flow, with decreased flow leading to lowered diameter and *vice-versa* [69,70]. There is an extensive body of evidence to suggest that this response is governed by the endothelium [71], which is able to sense wall shear-stress (WSS) *i.e.* the friction produced by the flow of blood at the luminal surface. Sensors are probably multiple and interlinked, and include focal cell membrane-bound receptor tyrosine kinases, G-protein coupled receptors and shear-sensitive ion channels [72]. Change in shear stress causes cytoskeletal re-alignment [73] and the upregulation of genes encoding enzymes producing vasoactive mediators such as nitric oxide (NO) [74,75] and receptors for PDGF [76,77], a key mitogen in the cascade of events leading to AIH [66]. Studies have demonstrated that regions of low or unusually oscillatory shear stress result in

SMC proliferation [78], are injurious to endothelium [79] and are generated at the toe, heel and floor of end-to-side anastomoses [80] where AIH is frequently observed [81].

1.2.1.4.1.1. Vein cuffs

The interposition of a collar or strip of vein between graft and artery was originally performed in order to ease the technical difficulty of performing an exacting anastomosis. There is good evidence that patency is improved by such a procedure [82], and when such grafts do fail the extent of AIH is less [83]. Such cuffs may abolish the low WSS found in the anastomotic region by generating stable, high velocity vortices thus suppressing AIH [84]. They may also act by cushioning the abrupt change in compliance that occurs between graft and artery.

1.2.1.4.2. Compliance mismatch as a contributory factor

The specialised structure of arteries bestows inherent elasticity *i.e.* the ability to deform when a stress is applied and to regain the original configuration when stress is removed [85]. Circumferential elasticity facilitates energy-efficient transmission of pulsatile blood-flow, the simultaneous damping of excessive pressure fluctuations and the matching of the impedance characteristics of the proximal arterial tree to distal branches [85-87]. The mechanical properties of ePTFE and Dacron grafts do not reproduce these favourable characteristics. Indeed, implantation of an incompliant graft into the lower-limb arterial tree (analogous to the introduction of an impedance in to an oscillating electrical circuit) diminishes flow pulsatility [88] and perfusion efficiency [89] which in low-flow situations may itself lead to critical reduction in flow and thus graft thrombosis.

Interestingly, a higher rate of lower-limb bypass failure has been shown to correlate with low graft compliance [90,91]. It must be noted that these analyses may merely reflect the fact that the flow surfaces of Dacron and ePTFE prostheses are more thrombogenic than the smooth intimae possessed by the more compliant HUV and saphenous vein grafts. However, as will

be discussed, experimental evidence suggests that endothelial and smooth muscle cells can perceive the mechanical effects caused by abrupt change in compliance at the distal anastomosis, and cellular response to compliance change is part of the pathogenesis of AIH.

1.2.1.4.2.1. Definition of arterial compliance

Many indices have been derived to describe the change in arterial distension with respect to alteration in intra-luminal pressure and there has been substantial debate amongst investigators as to the most appropriate description [92-94].

In 1960 Petersen and co-workers defined the elastic modulus *Ep*, an index of arterial stiffness, which describes the relationship of strain to intra-luminal pressure in an open-ended vessel [95]. The original description referred to the change in vessel volume, but as arterial lumina are generally circular in cross-section the equation has been modified to :

$$Ep = Ps - Pd / Strain \qquad [1.1]$$

Where strain is defined as the fractional pulsatile diameter change that occurs in an artery exposed to a given change in intra-luminal pressure and is defined as:

$$Strain = (Ds - Dd) / Dd \qquad [1.2]$$

Where D and P are diameter and pressure and d and s denote diastole and systole respectively. The inverse of Petersen's elastic modulus is known as cross sectional, or diametrical compliance C [96].

$$C\ (\%\ mmHg^{-1} \times 10^{-2}) = (Ds - Dd / Dd) \times 10^{4} / Ps - Pd \qquad [1.3]$$

Compliance is thus defined as the ability of a vessel to undergo pulsatile diametrical deformation at a specific pressure for a specific pressure change.

1.2.1.4.2.2. Tubular and anastomotic compliance

Compliance mismatch may adversely affect graft blood flow in two principal ways. As stated, an inherently stiff graft with poor tubular (radial) compliance acts as an impedance to the

propagation of pulsatile flow leading to increased peripheral resistance and stiff grafts have thus been postulated to diminish end-organ perfusion [97,98]. Secondly, the disparity of compliance at the anastomotic interface leads to local changes in the physical microenvironment of adjacent endothelial and smooth muscle cells (SMC's) that may predispose to AIH.

The increased wave reflection that is known to occur as a result of sudden change in vessel impedance may be a cause of vibratory damage to adjacent endothelium [86]. It has been demonstrated that, whilst the suture ring itself creates a region of very low compliance at the anastomosis, the immediately neighbouring artery exhibits excessive compliance [99,100] . This para-anastomotic hypercompliance zone (PHZ), a region approximately 5mm in length, has been postulated to promote AIH through a number of mechanisms. Cyclic stretching of cultured endothelial cells has been reported to influence endothelial morphology [101], activate secondary messenger systems [102] and upregulate transcription of the PDGF-B gene [103] demonstrating that EC may be very sensitive to periodic mechanical strain. Although the strain-perception apparatus has yet to be fully understood, SMC's appear to be similarly sensitive and both cell proliferation and production of extracellular matrix, two key histopathological features of AIH, are influenced by repetitive, cyclic stretching [104,105]. Flow visualisation experiments suggest that compliance mismatch creates an area of low shear at the anastomosis [106], with prolonged particle residence time [107] and platelet trapping. Interaction of such platelets with endothelium injured by exposure to low shear stress created by turbulent bloodflow across the PHZ may trigger SMC replication [79,108]. AIH thus appears to result from a multitude of co-dependent and mutually aggravating triggers, some resulting from anomalous mechanical strains and others resulting from localised disturbances in blood flow.

1.3. Strategies for improving the performance of arterial prostheses

The vast majority of methods intended to improve the design of prosthetic grafts have concerned modification of the luminal interface or the mechanical properties of the graft. Pharmacologic therapies designed to modify haemostasis (such as prolonged administration of warfarin) or surgical manoeuvres intended to increase graft bloodflow (such as the creation of distal arterio-venous fistulae) do not directly pertain to graft design and are not explored in this review.

1.3.1. Luminal surface modification

There has been substantial research in to the reduction of graft thrombogenicity. Attachment of antithrombogenic agents to the luminal interface, the degassing of potentially thrombogenic bubbles from graft interstices and the promotion of a functionally antithrombogenic cellular neointima are the main strategies in this regard.

1.3.1.1. Bonded antithrombogens

This approach attempts to render the graft luminal surface antithrombogenic by fixing inhibitors of coagulation to the luminal interface. Candidate antithrombogens should be readily attachable to the graft material, efficiently prevent formation of intra-luminal thrombus, and resist wash-out following exposure to blood-flow and deactivation or adsorption by circulating plasma proteins.

Heparin is a heterogeneous mixture of sulphated polysaccharides that prevents thrombin formation via the formation of a heparin-antithrombin III complex and binding with heparin cofactor II. Thrombin is necessary for the formation of fibrin from fibrinogen, catalyses the formation of factors V, VIII and XIII from their inactive precursors and induces platelet aggregation [109]. Initial studies carried out in the 1970's demonstrated the feasibility of reducing graft platelet adhesion by impregnating heparin in to the surface of the graft and it is this

compound that has received most attention [110-112]. Heparin treatment has been shown to reduce the post-implant thrombogenicity (up to 4 hours) of heparin treated ePTFE and polyurethane (PU) carotid artery interposition grafts in sheep [113]; to elevate the 3 month patency of PU aorta grafts in dog [114] and to decrease 1 month graft failure rates with reduction in size and number of microthrombi generated by iliac artery ePTFE grafts in the rat [115,133]. Infrainguinal use of heparin-bonded Dacron grafts is practical and gives acceptable results [116] although superiority over non-bonded grafts has yet to be demonstrated. Indeed, *in vitro* work has suggested that the antithrombogenic character of heparin-bonded grafts may be transient and moderated by prolonged exposure to flow, as heparin is inhibited naturally by platelet factor 4 and fibrin monomer [117,118]. In a study of collagen-coated polyester grafts implanted in to the iliac artery of 24 dogs [119], no differences in 6 month patency rates were observed between heparin-bonded grafts and controls, although heparin grafts did have a thinner neo-intima and the high iliac artery flow-rates may have helped preserve the patency of the unbonded grafts. Furthermore, heparin-bonded grafts may leach sufficient heparin to cause platelet aggregation in heparin-sensitised individuals [120].

Hirudin is an antithrombin III independent polypeptide that inhibits thrombin and is not subject to natural inactivation. *In vitro* models have confirmed the anticoagulant activity of graft-bonded hirudin and demonstrated that inhibition of fibrin formation is more durable than is the case with heparin [117,121]. To date there are no randomised, controlled clinical trials evaluating the benefits of heparin or hirudin-bonded grafts compared to unbonded grafts.

The effect of bonding anti-platelet agents to vascular prostheses has also been investigated. ePTFE grafts treated with forskolin – which raises platelet cyclic adenosine monophosphate (cAMP) levels thus reducing platelet aggregation – had a higher patency rate than untreated controls at 3 months in sheep [121]. Encouraging results obtained from animal studies have been described for PTFE grafts coated with acetyl salicylic acid and polyurethane grafts coated with adenosine diphosphate protease (ADP-ase), an enzyme which deactivates

platelet organ-zone ADP and reduces aggregation [122,123]. Other antithrombogenic agents found to experimentally lessen graft thrombogenicity include fibrinolytic compounds such as tissue plasminogen activator [124] and urokinase [125], non-thrombogenic acrylic copolymers [126], pyrolytic carbon [127], phospholipids [128] and immobilised, thrombin-binding plasma proteins [129].

The only one of these compounds to have undergone controlled clinical study is pyrolytic carbon; in a randomised multicentre trial 167 patients underwent bypass to the infragenicular popliteal or distal vessels with carbon-coated or standard ePTFE grafts [130]. At twelve months there was a trend toward higher limb salvage in the carbon-impregnated ePTFE group compared to the standard ePTFE group (57 vs 47% respectively), with similar trends in primary (45% vs 35%) and secondary patency (53 vs 36%) although none of these differences were statistically significant.

Thus, whilst the concept of graft-bonded antithrombogenic compounds appears practical and such agents have proved experimentally advantageous, their clinical benefit remains to be proven. None of the coatings appear to have any particular advantage.

1.3.1.2. Graft denucleation

Air accounts for around 80-85% of ePTFE graft wall volume and gas bubbles at the luminal interface are thrombogenic. It has thus been postulated that denucleating prosthetic materials may pacify graft thrombogenicity. In one study of ethanol-washed, degassed dacron incubated in human plasma, such grafts showed significantly less platelet aggregation and C3a/C5 activation than untreated controls [131]. In a study of 46 dogs implanted with de-gassed prosthetic ePTFE grafts (treated by immersion in degassed saline and exposure to negative pressure) early patency was significantly higher than control grafts [132]. Unfortunately the advantageous effect of denucleation was not durable; the authors suggested that the late absorption of gas from the control grafts accounted for this feature. Similar conclusions were drawn in a subsequent study of microvascular prostheses used in a rat model where the effect

of degassing the grafts was considerably limited when compared to heparin treated control grafts [133]. Additionally, a potentially significant drawback of denucleation is that the "wetting" procedure removes the hydrophobic barrier that normally prevents trans-mural leakage. Thus there is a heightened risk of haemorrhage, seroma formation and infection in grafts that have been treated in this way [134].

1.3.1.3. Luminal neo-endothelialisation

It is unlikely that bonded antithrombogens will ever approach the anticoagulative potential of stable quiescent endothelium, which normally serves to maintain blood flow even in the high viscosity, very low-flow environment of the capillary lumen [86,135]. Therefore, the concept of prosthetic graft lined with a functional endothelial neo-intima is highly attractive.

Normally, the endothelium has a number of distinct antithrombotic roles [136,137,138]. Firstly, endothelium prevents platelet degranulation by cloaking the underlying extracellular matrix (ECM) proteins and by presenting a negatively charged glycocalyx at the flow surface. Secondly, the endothelial luminal surface contains antithrombogens such as heparan sulphate (which potentiates the action of antithrombin III and heparin co-factor II), thrombomodulin (a receptor for thrombin which acts with proteins S and C to deactivate factors Va and VIIIa) and tissue factor pathway inhibitor (which blocks the direct activation of factor X). Endothelium actively secretes vasoactive, antithrombotic prostaglandins such as prostacyclin. Additionally, endothelium binds and converts plasminogen to plasmin through the action of endothelial synthesized tissue-type plasminogen activator (tPA), thereby initiating fibrinolysis.

Two approaches to graft endothelialisation have been developed. Firstly, graft porosity has been manipulated in order to encourage adventitial ingrowth of vascularised, endothelial cell-laden tissue elements in order to promote luminal colonisation. Secondly, immediate luminal coverage prior to implantation has been sought by the direct deployment of "seeded" endothelial cells previously harvested from autogenous donor tissue.

1.3.1.3.1. Graft porosity and auto-endothelialisation

The evidence regarding the benefits of high porosity in vascular grafts is contradictory. Initially, early animal and clinical experience with synthetic vascular grafts suggested that a good degree of porosity enhanced tissue ingrowth which in turn promoted patency [139,140]. Thus the use of ultra-thin, highly porous Dacron grafts was advocated but these grafts were found to be structurally weak and very difficult to pre-clot, with an excess risk of trans-graft haemorrhage [141]. The case for porous ePTFE was similarly lessened when it was experimentally demonstrated that pore size greater than 22μ resulted in reduced patency – possibly because of the larger pores' tendency to cause local blood stagnation and initiation of clot formation [142]. In two related studies [127,143], no difference in the accumulation of radiolabelled platelets was found between standard and highly porous (pore size 90μ) ePTFE grafts inserted into the large arteries of dogs. However, a trend toward better patency at 18 weeks post-implantation with significantly better histological evidence of endothelialisation was observed in the highly porous grafts. The authors of a similar study, utilising 60μm ePTFE grafts in dogs, also found a trend supporting the conclusion that patency was promoted by porosity [144]. Clowes and colleagues, encouraged by their finding of enhanced endothelialisation of 60μm ePTFE grafts implanted in baboons [145], implanted 10 grafts composed of equal lengths of highly porous and standard ePTFE in 8 patients who underwent femoropopliteal reconstruction [146]. ^{111}Indium-labelled platelet uptake was undertaken to assess graft thrombogenicity at 1 week and 3 months. The results were disappointing – no differences were observed between control and test graft segments. In two patients re-operation for bypass thrombosis afforded histological examination of porous graft samples but transmural capillary penetration was scanty and luminal endothelial cells were absent. The authors blamed the presence of an outer wrap deemed necessary to provide structural integrity to the highly porous grafts used in their study.

Proposed strategies to enhance capillary ingrowth include the fabrication of hybrid ePTFE grafts that possess a highly porous adventitial surface and a finely pored luminal surface, connected by tapered channels designed to accommodate vascular elements [147]. Endothelialisation might be encouraged by augmenting the graft with growth factors: fibroblast growth factor (FGF) has been reported to promote tissue ingrowth and endothelialisation in ePTFE [148] and microporous polyurethane grafts [149] implanted in animal models. Experimental co-impregnation with heparin has a synergistic effect on endothelial cell growth whilst retarding smooth muscle cell proliferation [150].

It remains to be seen if these strategies can result in spontaneously endothelialised grafts in vascular patients, in whom tissue ingrowth and EC function and reproduction may be constrained by age and underlying disease.

1.3.1.3.2. Endothelial cell seeding

The goal of endothelial cell seeding is to establish a confluent endothelial cell monolayer on the graft intima prior to implantation by directly depositing such cells onto the luminal surface of the graft.

1.3.1.3.2.1. Experimental and animal studies

Since the pioneering work of Herring and colleagues in 1978 [151] many well designed animal studies have demonstrated the feasibility and benefit of implanting prosthetic grafts that have undergone endothelial cell seeding. Enhanced patency in seeded grafts has been demonstrated in a number of animal studies [151,153,157,160]. Analysis of surrogate outcome markers has shown that seeded grafts enjoy higher flow rates [152, 153] and exhibit greater thrombus-free surface areas on histological examination following explantation [152,154-156]. Platelet deposition is also reduced [153,154,157,158], although not as low as that observed in native artery [158] and does not develop for at least two weeks following implantation [153,156]. Early

attachment of white cells and fibrinogen is unaffected by seeding [159], and platelet deposition on seeded grafts may actually be higher in the immediate post operative period than on unseeded grafts [153]. Seeded grafts produce less thromboxane A2 [158] and more prostacyclin [160] than unseeded controls and explanted seeded grafts perfused in a bioassay system have been reported to actively produce other vasoactive compounds such as 6-keto prostaglandin F1 alpha and C-type natriuretic factor [161]. Seeded grafts benefit from enhanced resistance to early post-implantation bacterial infection [162], although this effect becomes less conspicuous in chronically implanted mature grafts [163].

1.3.1.3.2.2. Clinical studies – single stage seeding

Following experimental success, Herring and others transferred the cell seeding concept into the clinical domain, with initially promising results. Enzymatically harvested endothelial cells, derived from excised segments of autologous external jugular vein, were immediately seeded onto the ePTFE grafts of 17 out of 28 patients undergoing femoropopliteal by-pass procedures [164]. One year patency rates were significantly higher for seeded grafts with most benefit experienced amongst smokers and those with infra-geniculate grafts; the same author also documented histological confirmation of a confluent endothelial monolayer 90 days post-seeding [165]. A subsequent prospective randomised trial investigating the patency rates of 66 seeded ePTFE and 53 autologous vein grafts used for femoropopliteal bypass was devised but cell seeding was not found to influence short or mid-term patencies [166]. Herring explained his results by suggesting that the single-stage technique – which employed the immediate seeding of cells onto PTFE graft material with a 10-20 minute incubation period prior to implantation – did not allow sufficient time for adequate cell spreading and attachment. The efficacy of single-staged seeding has also been investigated in clinical studies using scintigraphy to evaluate platelet activation; Ortenwall and colleagues have reported reduced platelet deposition in seeded dacron and PTFE grafts used in aortobifemoral [167] and lower-

limb [168] arterial reconstruction. Others have found no scintographic evidence of reduced graft thrombogenicity [169] or decrease in plasma markers of platelet activation [170] in patients with seeded prostheses.

1.3.1.3.2.3. Clinical studies – two stage seeding

More encouraging results have been reported utilising a two-stage seeding process, whereby the endothelial donor tissue is harvested from the patient several weeks preceding the date of planned reconstruction. After extraction the endothelial cells are aseptically cultured *in vitro* in order to ensure optimal cell viability and number before seeding onto the graft, which is then incubated for several days to allow the cells to become firmly attached to the material prior to implantation. A prospective, controlled but unrandomised study utilising the two stage seeding technique in 13 of 26 patients undergoing ePTFE infrapopliteal bypass for failed prior revascularisation reported significant differences in patency. Four of the seeded grafts against 8 of the unseeded grafts failed by the end of the first year with a reduction in the 18 month amputation rate from 31 to 15% in the seeded group compared to controls [171]. After reporting disappointing results [172] utilising the single staged seeding technique, Zilla and colleagues switched to a two-staged approach. Forty-nine patients with either critical ischaemia or disabling claudication were randomised to seeded or unseeded ePTFE grafts precoated with fibrin glue in order to aid cell adhesion. The authors reported that the 34 month actuarial patency was significantly higher at 84.7% for seeded grafts versus 55.4% for unseeded grafts [173]. Significant advantage in ankle-brachial pressure index and lowered radiolabelled platelet uptake was also described in the seeded group. The authors emphasised that, although their method required *in vitro* cell culture facilities, the culture/seeding process itself was practical, reproducible and advantageous. However, they conceded that two-stage seeding excluded patients who required emergency by-pass; moreover in a third-to-half of elective patients two stage seeding may not be feasible due to technical difficulties with the *in vitro* culture process

[171]. What is not in doubt is the patency benefit that a confluent endothelium endows. On the basis of their randomised study, Zilla and his group took the decision to cease randomisation and to offer all non-acute patients without suitable vein an endothelialised graft [174]. A further 116 patients received 83 above-knee and 33 below-knee femoro-popliteal endothelialised grafts with 5 year primary patencies of 64 and 76% respectively – data which suggests that seeded grafts have the longevity of autologous vein [28].

1.3.1.3.2.4. Optimisation of seeding protocols

These studies demonstrated the clinical benefit of luminal endothelialisation achieved by two-stage seeding; the challenge now being addressed is to formulate an effective single-stage seeding protocol applicable to all vascular patients and all surgical institutions. This would extend the benefits of seeding to patients in all vascular units, dispensing with the need for costly *in vitro* cell culture facilities and staff. Studies have sought to determine the underlying behaviour and biology of the seeded cell, and to establish the optimal conditions required of each step in the single-stage seeding process to ensure maximal cell adhesion and function once the graft has been implanted.

1.3.1.3.2.4.1. Donor tissue and purification

A successful protocol will harvest easily obtained autogenous donor tissue which yields excess microvascular endothelial cells, enabling cell densities sufficient to provide immediate confluency – at least 1.4×10^5 cells/cm^2 for PTFE [175] – to be readily achieved. Fat retrieved from subcutaneous [176-178] or omental sites [179-181] provides a source of abundant microvascular endothelial cells for seeding purposes. Such cells have been used to saturate the graft with endothelial cells at supraconfluent densities, by flushing cell-laden medium through the graft interstices so as to encourage cell-graft interaction whilst providing a reserve of cells to replace those washed out following exposure to blood flow [182]. Although percoll centrifugation

[177] or filtration can be used to purify adipose or omental tissues, a more specific cell extraction system is desirable if contamination with other cells is to be avoided. Paramagnetic beads coated with ligands such as Ulex Europaeus Agglutinin 1 or anti-CD 31 directed at specific EC membrane residues have been successfully utilised in this respect [183, 184]. Mesothelial cells (MC), lining the omental fat have been advocated as suitable for seeding since they can express antithrombogenic function [185,186]. However, MC have also been shown to be pro-thrombogenic [187,188]. The case for the preferential use of MC over EC has also been substantially weakened by a recent trial that failed to show any diminution in neointimal formation or graft occlusion in MC seeded ePTFE grafts compared to controls grafts that eventually autoendothelialised in a canine model [189].

1.3.1.3.2.4.2. Cell deployment

Ensuring that the utmost number of cells adhere to the graft surface, and remain adherent in the face of pulsatile flow has been addressed by refining the deployment of the cell-laden inoculums and pre-coating the graft with agents to enhance cell adhesion. Early methods relied upon gravity to induce graft-cell interaction but application of pressure to the cell inoculums [182], or a partial vacuum [90] to the graft exterior is appealing as cells are drawn into graft interstices. Recently, application of an electrostatically-induced positive charge on the graft lumen has also been used to trap endothelial cells, resulting in increased cell attachment and spreading [191,192].

1.3.1.3.2.4.3. Graft coatings and pre-conditioning

Pre-coating the graft luminal surface with substances capable of anchoring cells to the graft is obligatory as only 1-14% [193-195] of seeded cells remain attached on uncoated surfaces once flow is initiated. Luminal coatings composed of extracellular matrix glycoproteins have been shown to markedly improve cell attachment, particularly fibronectin [195-199] which also fosters

the production and release of tissue plasminogen activator by endothelium [200]. Cell adhesion, superior to that achieved with fibronectin, has been reported in grafts lined with synthetic peptides containing the [aginine-glycine-D-aspartate] moiety [201], which constitutes the terminal domain of many extracellular matrix glycoproteins. Linings composed of $F(ab')_2$ monoclonal antibody fragments directed at specific EC membrane antigens have excellent adhesive properties with minimal platelet activation [202]. Combining cell growth factors such as fibroblast growth factor with tissue glues to provide a pre-coat that stimulates both adhesion and proliferation has also been investigated [203], as has naturally derived extracellular matrix [204] .

In vitro experiments have shown that endothelial cell attachment can be heightened by exposing the seeded graft to a low level of shear-stress for a number of hours prior to implantation[197, 205] and this approach has been shown to produce significantly less cell loss in an animal model [206].

It would seem that the most practical solution to enhancing cell adhesion would be to covalently attach the RGD molecule to the graft. This ubiquitous molecule is commercially available, is substantially cheaper than antibody fragments, and offers high rates of cell attachment and adhesion without the necessity for complicated pre-implantation perfusion protocols.

1.3.1.3.2.4.4. Genetic manipulation

Deploying genetically modified EC specifically engineered for seeding purposes is an interesting if under-exploited idea. Cells destined for seeding have been modified for increased tPA production in order to lower graft thrombogenicity [207] or endow heightened proliferation [208]. Unfortunately a number of studies have shown that, compared to normal cells, transduced EC adhere poorly to grafts once exposed to bloodflow [209-211].

1.3.2. The compliant vascular graft and the compliance hypothesis

Seeded graft surfaces reduce luminal thrombogenicity but their role in inhibiting AIH is unproven. Seeded aortic ePTFE grafts have been reported to produce platelet derived growth factor (PDGF) [212], a smooth muscle mitogen implicated in the pathogenesis of intimal hyperplasia [66]. Furthermore, AIH has been found to be a frequent cause of occlusion in seeded prosthesis [213]. Thus the establishment of a non-thrombogenic lining can only be part of the approach toward improving the performance of prosthetic vascular grafts.

As stated in section *1.2.1.4.2.* compliance mismatch has been implicated in the development of AIH. Furthermore, stiff grafts compromise tissue perfusion. Thus the ideal graft should possess biomechanical qualities that reproduce those of native artery in the expectation that this will elevate graft patency. This is known as the compliance hypothesis, and was first proposed by Baird and Abbott in 1976 [97].

1.3.3. Experimental evidence for the compliance hypothesis

Investigating the influence of compliance by performing *in vivo* comparative studies between different graft types is fraught with difficulty. This is because any observed association between compliance and patency may be confounded by differences in flow surface or diameter amongst the grafts under study. Abbott and colleagues addressed this problem by developing a process to render stiffness into canine carotid artery segments *via* immersion in 10% glutaraldehyde. Equivalence in surface morphology and chemistry was achieved by treating the lumina of stiffened and normal arterial segments alike with 0.025% glutaraldehyde [214]. Using this protocol the patency of bilateral femoral artery interposition autografts using stiffened and normal carotid segments was assessed in 14 dogs. To further ensure that compliance was the only variable under test, control and test vessel segments were derived from the same vessel. Cumulative life table patencies were significantly different at 85% and 37% for compliant and stiff grafts respectively, and the authors concluded that even with near-

optimal flow surfaces, compliance mismatch was detrimental to graft patency [215]. In a more recent study, Trubel and colleagues performed 36 femoropopliteal bypasses in 18 sheep using autologous vein grafts, where each animal had one graft stiffened by means of an externally applied dacron mesh. The sheep were sacrificed at 8 months and histopathological examination of grafts revealed significantly less intimal hyperplasia in unconstricted grafts [216]. Further evidence in support of the hypothesis was supplied by Zenni *et al* who implanted stiff and elastic aortic polypropylene grafts into rabbits. Stiffer grafts were associated with significant elevation in the mitotic index of infiltrating myofibroblast cells and inner capsule thickness, and a trend in decreased patency [217]. This data might be seen to be at odds with results from Angelini's group, who discovered that covered, stented saphenous vein grafts subjected to end-to-end anastomosis with the carotid artery exhibited less neointimal and neomedial hyperplasia than unstented grafts [68]. However, this study cannot be used as evidence against the compliance hypothesis. The stents used were oversized and were designed to limit, and not tightly constrain expansion of the vein. Furthermore, the authors did not set out to investigate the compliance hypothesis and no attempt was made to formally evaluate the mechanical properties of stented and unstented vein grafts

This is not to say that the the validity of the compliance hypothesis remains unquestioned. Uchida *et al* studied compliant and noncompliant microporous polyurethane grafts inserted as carotid interposition grafts in dogs, and found no significant differences in either patency or degree of AIH between the two groups (although a trend toward increased patency in elastic prostheses was reported) [218] . Interestingly, the authors noted a loss of elasticity in the compliant grafts as the study progressed, such that at the end of the 14 week study period it had halved. This finding may account for the patency data reported. Wu and colleagues reported no differences in patency and intimal thickness between dacron grafts sited in the carotid artery and control autogenous carotid artery autografts sited in the femoral artery in 11 dogs [219]. However, the design of this latter study has been criticised [96]. Firstly, the control

grafts qualitatively differed from test prostheses in terms of flow surface; and secondly, control grafts were exposed to haemodynamic forces that differed from those experienced by the test grafts because they were sited in a different region of the arterial tree.

1.3.4. Fabrication of compliant vascular prostheses

The majority of investigators have used polyurethane or silicone to develop compliant vascular prostheses, although attention has also been directed at engineering compliant warp-knitted dacron [220] or longitudinally compliant ePTFE prostheses [221]. Silicone rubber or silicone-containing polydimethylsiloxone prostheses have been fashioned using the replamineform process, whereby shape and porosity is imparted by using a tubular sea-urchin spine as the graft template. Animal studies suggest that such grafts maintain their compliance and are biostable [222,223]. Silicone and polyurethane are virtually the only biocompatible, commercially available substances able to undergo substantial deformation in response to stress and thence return to the original configuration once the stress is removed. This type of deformation is termed *elastomeric*, and materials possessing this quality termed *elastomers*. It has thus become possible to engineer prototype prostheses with elastic qualities that match those of arterial tissue over certain physiological pressures [96].

1.3.5. The polyurethanes

The presence of a repeating urethane [- NH (CO) O -] group in the polymer chain is the characteristic feature of this family of polymers, which are highly divergent in terms of their physical properties. Medical polyurethanes generally consist of two linked polymeric components [224]: a "hard" segment consisting of the aromatic or aliphatic urethane and a soft segment of poly(ester), poly(ether) or poly(carbonate). The polyurethane is generated by reaction of the soft segment, or macroglycol, with an isocyanate prior to extension of the polymeric chain with a chain extender. The ratio of macroglycol to chain extender / isocyanate

determines the relative hardness and elasticity of the urethane. The material itself can be formed into shapes by solution or melt processes and can be spun, cast into porous or solid structures and extruded [225]; as such polyurethanes have found numerous biomedical implantation applications including pacemaker lead insulation, pacemaker connectors and breast implant capsules.

1.3.5.1. Poly(ester) and poly(ether) urethanes

The hard segment of most polyurethanes is generally considered to be biostable but the soft segment may be vulnerable to *in vivo* degradation. Poly(ester) polyurethanes are susceptible to hydrolysis *i.e.* cleavage of susceptible carbonyl groups with water [226]. Poly(ether) urethanes were introduced as a hydrolysis-resistant polyurethane but are now known to be susceptible to oxidative degradation; in the latter case chain cleavage is a direct result of oxidation of the vulnerable alpha-methyl group [224,227] . This manifests as environmental stress cracking (ESC) and is thought to be a consequence of free radicals generated by inflammatory cells activated during tissue incorporation [225,228] catalysed by plasma proteins such as alpha-2-macroglobulin and caeruloplasmin [229]. As ESC develops, the polyurethane becomes crazed and fissured with loss of mechanical integrity.

This phenomenon had yet to be fully understood when the first animal studies were conducted upon compliant polyurethane vascular grafts, and a number of prostheses made from poly(ether) polyurethanes were developed and tested. How and colleagues developed compliance matched grafts composed of fibrillar Biomer - a poly(ether) urethane - and evaluated patency in a canine carotid interposition model [230]. They reported that of 26 grafts, 17 (65%) were patent at 2 years but the authors did not formally assess the grafts for ESC or chemical change. Using the same animal model, Uchida *et al* found evidence of material degradation of sponge-configured Biomer grafts following 6 weeks implantation [218].

Mitrathane is also a poly(ether) urethane that has been used in two graft configurations: either as an impervious, closed-cell microporous hydrophilic type or as a fibrillar, open weave hydrophobic variety. Martz *et al* initially reported promising results, with a 75% patency rate over an 18 month evaluation of the impervious graft sited in the canine infrarenal aorta, but then observed a 100% failure rate of such prostheses when used in the carotid position [231,232]. Marois *et al* studied the hydrophobic, fibrillar variety of Mitrathane graft and found that patency could not be maintained beyond one month [233]. The same group also studied another poly(ether) graft made from Tecoflex: 7 out of 16 (44%) of canine aortic grafts had either partially or totally excluded in a study conducted over 6 months [234]. In the only clinical trial of poly(ether) grafts, Bull implanted 15 Mitrathane closed pore vascular femoropopliteal prostheses in patients with severe limb threatening ischaemia. They reported 5 early occlusions and a limb salvage rate of 66% at 6 months. The authors expressed concern over graft biostability and concluded that no further recommendation for use of this graft could be made [235].

1.3.5.2. Poly (carbonate) urethanes

The disappointing results associated with the use of first generation CPU grafts may merely reflect the susceptibility of poly(ester) and poly(ether) polyurethanes to *in vivo* degradation. Investigators and industrial concerns have therefore attempted to enhance polyurethane biostability. To this end, vulnerable soft-segment ether/ester linkages have been replaced with carbonate groups and poly(carbonate) polyurethanes have been produced.

Braun-Melsungen AG developed a poly (ester) carbonate porous prosthesis composed of spun, hydrophobic polyurethane microfibres that was putatively biostable. *In vitro* evaluation of the graft after prolonged exposure to protease solutions showed minor changes in the surface chemistry of the soft segment but no loss of structural integrity [236]. Animal studies confirmed these changes, which were related to loss of the soft-segment carbonate groups, but more

worryingly also revealed breakage of the microfibres, particularly in the anastomotic zones [237]. In a pilot study of the graft, implanted as a below-knee prosthesis, 8 out of 15 grafts had occluded by 12 months. Chemical analysis of failed grafts showed external surface carbonate loss similar to that reported in the animal studies, with limited deterioration in surface microstructure in a graft implanted for 12 months. No sub-surface change in chemical composition was found, but because the short and medium-term performance was no better than that of standard grafts it was decided to terminate graft development [238].

Corethane, a microporous polycarbonate CPU graft composed of spun fibres, has produced encouraging results when combined with an outer bonded wrap of warp-knitted Dacron applied to impart structural stability. Animal studies demonstrated 100% and 60% 1 year patencies for heparinised and non-heparinised femoral grafts respectively [239]. In 53 femoropopliteal bypasses performed in patients where the Corethane prosthesis was implanted the overall 6 month cumulative patency was 59% (79% for those grafts with good inflow or a distal anastomoses performed at or above knee-level) [240]. Unfortunately, graft chemical stability was not assessed in either the animal or human Corethane trials. No data is available on the extent to which the dacron wrap constrained the degree of compliance-match achieved with these grafts.

1.3.5.3. Chronoflex

Chronoflex is a poly(carbonate) polyurethane that was developed by Cardiotech Ltd of Wrexham, Wales. It is synthesised from methylene diidocyanate (MDI), polycarbonate diol and ethylene diamine in the molar ratios 2:1:0.97 [241]. Grafts are fabricated using a patented method where a mixture is made of the Chronoflex solution, a water-soluble porosifier and a surfactant. This is then extruded onto the surface of an electronically-controlled, rotating, stainless steel rod, such that a uniform coat of mixture is laid around the rod. During this process, the rod is advanced into a water bath maintained at 40°C [242]. The porosifier/filler

dissolves into the water whist the polymer is coagulating, thereby producing a graft with an open-pored, single-layered, sponge-like cross-section (fig 1.1). The graft is then simply slid off the rod, air-dried and subject to quality control procedures. Different gauges of graft may be produced by altering the diameter of the steel rod, and by varying other stages in the production process it is possible to change the degree of porosity and thus the mechanical properties of this graft [243]. This new poly(carbonate) has around half the soft-segment ether linkages associated with poly(ether) urethanes and is thus potentially more resistant to oxidative and hydrolytic degeneration.

Biostability has been the subject of preliminary evaluation by Cardiotech. In these studies, segments of mechanically stressed CPU graft were implanted subcutaneously into dogs for 18 months. The grafts were mechanically stressed in order to maximise the potential for ESC, and this was achieved by stretching them over outsized stainless steel mandrels, with subsequent implantation of mandrel plus overlying graft in the subcutaneous tissue. Analysis of the explants did not reveal any evidence of ESC [244]. Similarly, grafts were tested *in vitro* by stretching them on to outsized mandrels and exposure to a mixture of hydrogen peroxide / cobolt chloride solutions. Whereas all the polyether control grafts eventually decayed (such that the underlying steel mandrel became visible through the rotten graft wall), none of the Chronoflex grafts had done so by the end of the 250 day test period [245]. In the *in vivo* arm of the same study, two aorto-iliac bypass grafts implanted for 20 months (and patent at sacrifice) were retrieved from a single animal and assessed. In comparison to virgin grafts, no evidence of ESC or change in chemical composition was observed using scanning electron microscopy (SEM) and gel-permeation chromatography (GPC).

As well as exhibiting potentially favourable biomechanical qualities, the Chronoflex graft may be suited for endothelial cell seeding. Comparison of the behaviour of seeded Chronoflex and ePTFE grafts, exposed to pulsatile flow demonstrated significantly enhanced cell retention on

Opposite:

Fig. 1.1. Low (x50) and high (x220) power views of Chronoflex CPU graft.

Fig 1.1.

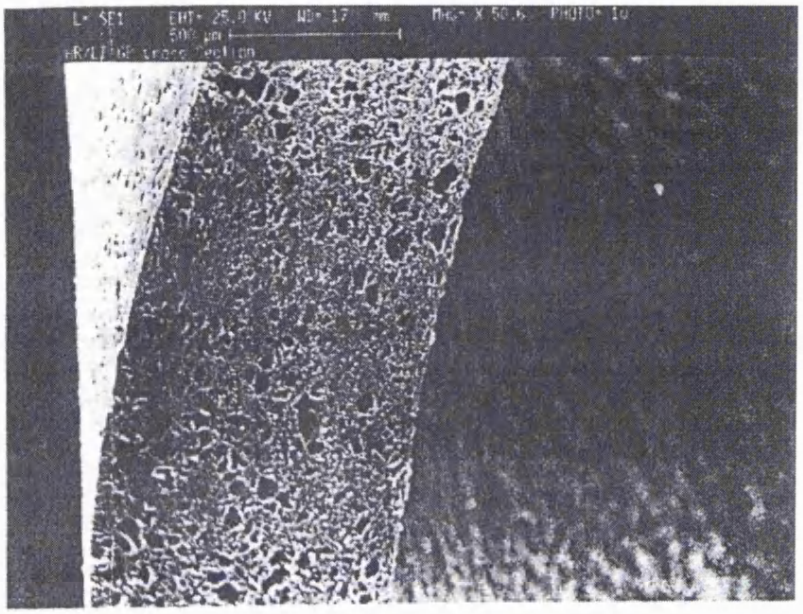

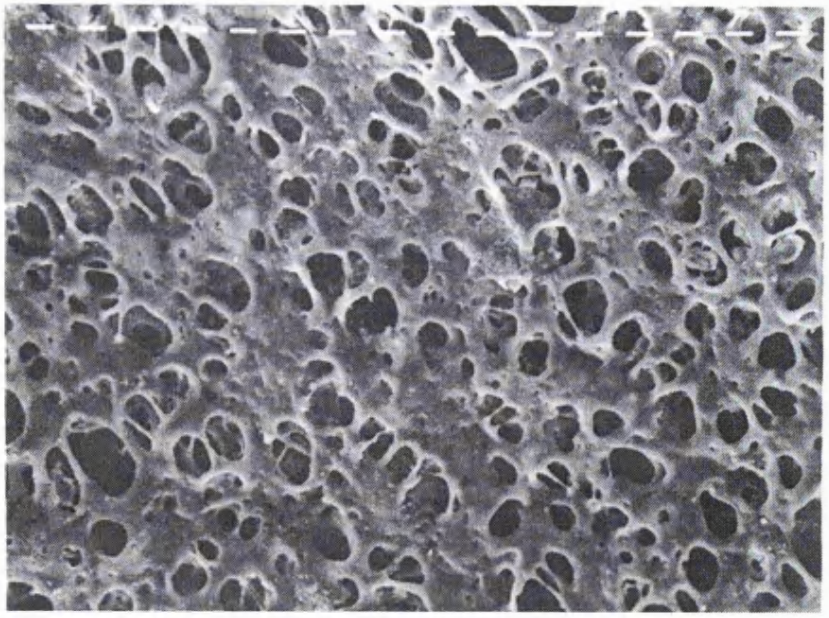

the CPU prostheses [246]. The authors postulated that the pitted, indented luminal surface affords a degree of shelter to seeded cells in the face of shear-stress generated by flow.

1.4. Conclusion of introductory review

The frequent development of graft thrombosis or anastomotic intimal hyperplasia in prosthetic bypass is a serious cause of morbidity and mortality in patients with lower-limb ischaemia. Although incompletely understood, graft failure appears to result from the summation of different aetiological factors which compound and aggravate one another. Current prostheses, whilst durable and mechanically strong, are especially lacking with regard to non-thrombogenicity, tissue incorporation and compliance characteristics. Two approaches to prolonging graft longevity are the development of a successful endothelial cell seeding protocol and the creation of grafts which diminish compliance mismatch. Regarding this, polyurethane grafts have the merit of a more realistic compliance profile but concerns over biostability have limited their clinical application. Poly(carbonate) grafts are more promising and preliminary studies of one such graft made from Chronoflex suggest increased biostability.

Given the evidence supporting the beneficial effects of endothelial cell seeding and compliance-matching, the proposition of a compliance-matched, cell-seeded graft is entirely logical. Such a graft would simultaneously address the mechanical and rheological factors implicated in the failure of ePTFE and Dacron grafts, thus raising the possibility that clinical use of a seeded CPU graft would extend the longevity of infrainguinal revascularisation.

Chapter 2

An assessment of the *in vivo* compliance characteristics of the femoropopliteal segment in patients with and without lower-limb vascular disease.

2.1. Introduction

In order to engineer a compliant graft and avoid anastomotic compliance mismatch, it is necessary to know the compliance of the vessel that the graft is to replace. Unfortunately, there are no studies dedicated to describing the compliance characteristics of the lower-limb muscular arteries in subjects suffering from lower limb PVD (*i.e.* the likely recipients of vascular bypass) although the *in vivo* elastic properties of the common femoral artery in young, aged and hypertensive populations [246-250] have been previously described. Therefore, the purpose of this study was to accurately survey the local *in vivo* compliance of the femoropopliteal vessel in a sample of patients with confirmed lower-limb PVD. Because the influence of atherosclerosis on vessel wall mechanics is disputed [251,252], a secondary aim was to test the hypothesis that the presence of PVD is associated with lowered vascular compliance. Furthermore, to validate the results against previously published data, a group of healthy young control subjects were surveyed. The hypothesis in this case was that vessels in disease-free, elderly individuals would be no stiffer than those in younger subjects as has been reported [246-248].

2.2. Methods and Materials.

2.2.1. Theoretical considerations

As stated in Chapter 1 both Ep and C are useful indices of functional vascular distensibility in the presence of a change in blood pressure as they describe the relative diameter change of a vessel for a given pressure change. However, if comparisons between individuals are necessary, then arterial wall stiffness index (β), as formulated by Kawasaki [253] and colleagues is useful. This is because it is less dependent on quantitative pressure change in describing the elasticity of an artery operating within physiological pressure ranges [254,255]. Thus the stiffness index (β) may be the same for two individuals even though their respective blood pressures may be different. Conversely, their measured compliance values would not be similar, as compliance is a highly pressure dependent variable. β is calculated as:

$$\beta = [\log_e (Ps/Pd)] \times Dd / (Ds - Dd) \qquad [2.1]$$

In this chapter arterial wall stiffness index (β) as well as diametrical compliance (C) are used to assess the vessel wall properties in patients with lower-limb PVD and control subjects free from symptomatic lower-limb PVD.

2.2.2. Subjects

Eleven patients with peripheral vascular disease (PVD), 11 age and sex-matched control subjects, and 12 young adult subjects were prospectively recruited (groups 1, 2 and 3 respectively). Informed signed consent was obtained from all subjects prior to undertaking any investigations. The study was performed after the protocol was discussed with the Chairman of the Royal Free Hospital Research Ethics committee. All study participants were non-smokers at the time of the study. Control subjects were allowed to participate providing they had absolutely no evidence of lower-limb PVD upon clinical examination or evidence of vessel calcinosis on ultrasound imaging of arterial segments. Additional exclusion criteria included a diagnosis of diabetes mellitus; one subject from the PVD group was diagnosed as

a non-insulin dependent diabetic at the time of this study and was thus retrospectively excluded. Control subjects were also excluded if ankle-brachial pressure index (ABPI) as measured by hand-held Doppler was less than 1.0. All group 1 patients had previously been diagnosed as suffering from symptomatic lower-limb occlusive vascular disease and had subsequently undergone lower-limb percutaneous transluminal angioplasty (PTA) in the previous year with good radiological and clinical outcome. In total, PTA had been undertaken on 3 common iliac arteries, 2 common femoral arteries, 7 superficial femoral arteries, 2 popliteal arteries and 1 tibioperoneal trunk, with a mean elapsed period since angioplasty of 25 weeks (range 3-48 weeks). Mean ABPI prior to angioplasty was 0.6 (range 0.5-0.75). PVD patients were excluded from the study if ABPI in the treated limb was less than 1.0 or if post-PTA angiograms revealed the presence of significant stenoses between aorta and mid-geniculate popliteal artery. Measurements were taken in 12 previously angioplastied limbs in group 1, 11 putatively healthy limbs in Group 2 and 12 putatively healthy limbs in group 3.

2.2.3. Measuring procedures

For each subject height and weight were recorded. All measurements were performed after 15 min of rest in the supine position to allow pulse and blood pressure to stabilise. Electrocardiographic leads were placed. Arterial blood pressure was recorded non-invasively in the right brachial artery using an automatic blood pressure monitor (Dinamap Compact TS, Johnson and Johnson Medical, Newport, Gwent UK).

Change in vessel wall diameter with respect to each cardiac cycle was measured at discrete sites along the femoropopliteal artery, with measurements taken in the sagittal plane at 90 degrees to the long axis of the vessel. Segments of the artery were imaged using a specially adapted duplex colour flow ultrasound system (Pie 350, Pie Medical Systems, Maastricht, Netherlands) with signal output to a high resolution echo-locked wall tracking system (Wall Track, Pie Medical Systems, Maastricht, Netherlands) This system allowed measurement of

vessel wall movement over time by automatically tracking assigned points of the induced radiofrequency signal deemed to be representative of anterior and posterior arterial wall. Real time M-Mode images of the arterial wall obtained via a 7.5MHz linear array probe were acquired (Fig 2.1). With the M-Mode cursor positioned perpendicular to the long axis of the vessel, the change in induced radiofrequency (RF) signal received from the vessel walls was sampled (Fig. 2.2). The data were transferred to a personal computer for real-time display of the displacement wave forms of the anterior and posterior artery walls (Fig. 2.3). End-diastolic and end-systolic intraluminal diameters were automatically determined for each cardiac cycle .

Vessel wall motion was recorded at common femoral artery (CFA), 2 cm proximal to the bifurcation; proximal superficial femoral artery (PSFA), 2 cm distal to the bifurcation; Above-knee popliteal artery (AKPA), 2 cm distal to the adductor hiatus; and mid-genicular popliteal artery (PA) (Fig. 2.4). Three registrations of vessel wall movement, each lasting 5 seconds, were made at each site. Brachial blood pressure was recorded simultaneously with each registration. For imaging and compliance sampling of group 1 vessel segments the ultrasonographer and the operator of the vessel wall-track system were blinded to the site of the original angioplasty procedure.

2.2.4. Data analysis and statistical methods

Vessel wall movement (over the three cardiac cycles in each registration) was averaged, and compliance and stiffness index calculated according to the blood pressure measured at the time of registration . The compliance and stiffness data from three registrations were then averaged to obtain mean values for each site along the vessel in each subject (each mean value being derived from 9 measurements of vessel wall motion).

Opposite:

Fig. 2.1. B-Mode and M-Mode image of common femoral artery in a Group 3 subject.

Fig. 2.2. A typical radiofrequency (RF) signal acquired from the artery is analysed to locate and mark the anterior and posterior luminal surfaces (denoted "A" and "P" respectively).

Fig. 2.3. Vessel distension over 4 cardiac cycles is displayed.

Fig 2.1.

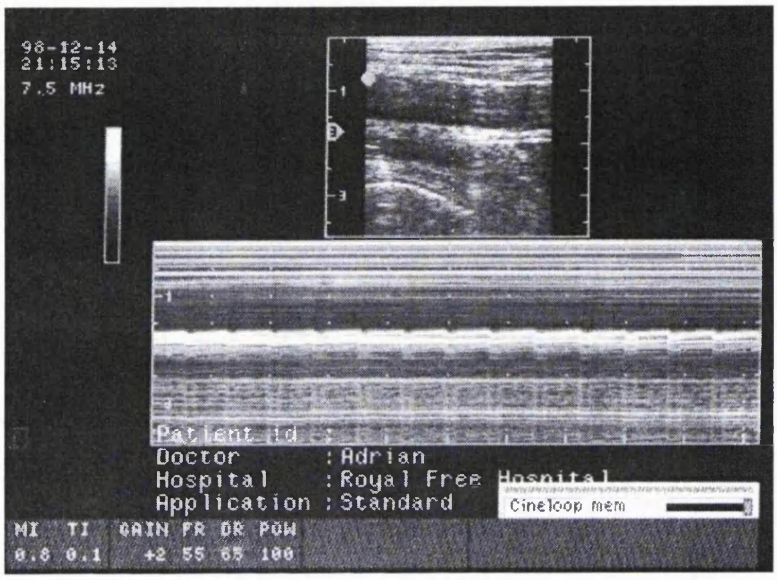

Fig. 2.2

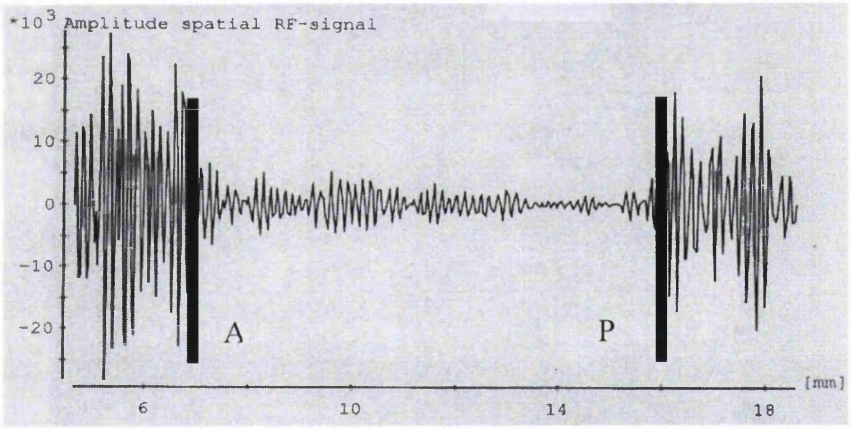

Fig. 2.3

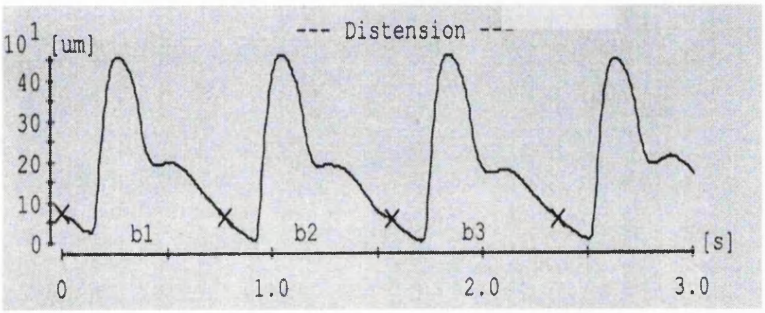

Opposite:

Fig. 2.4. Sites of compliance sampling.

Fig 2.4.

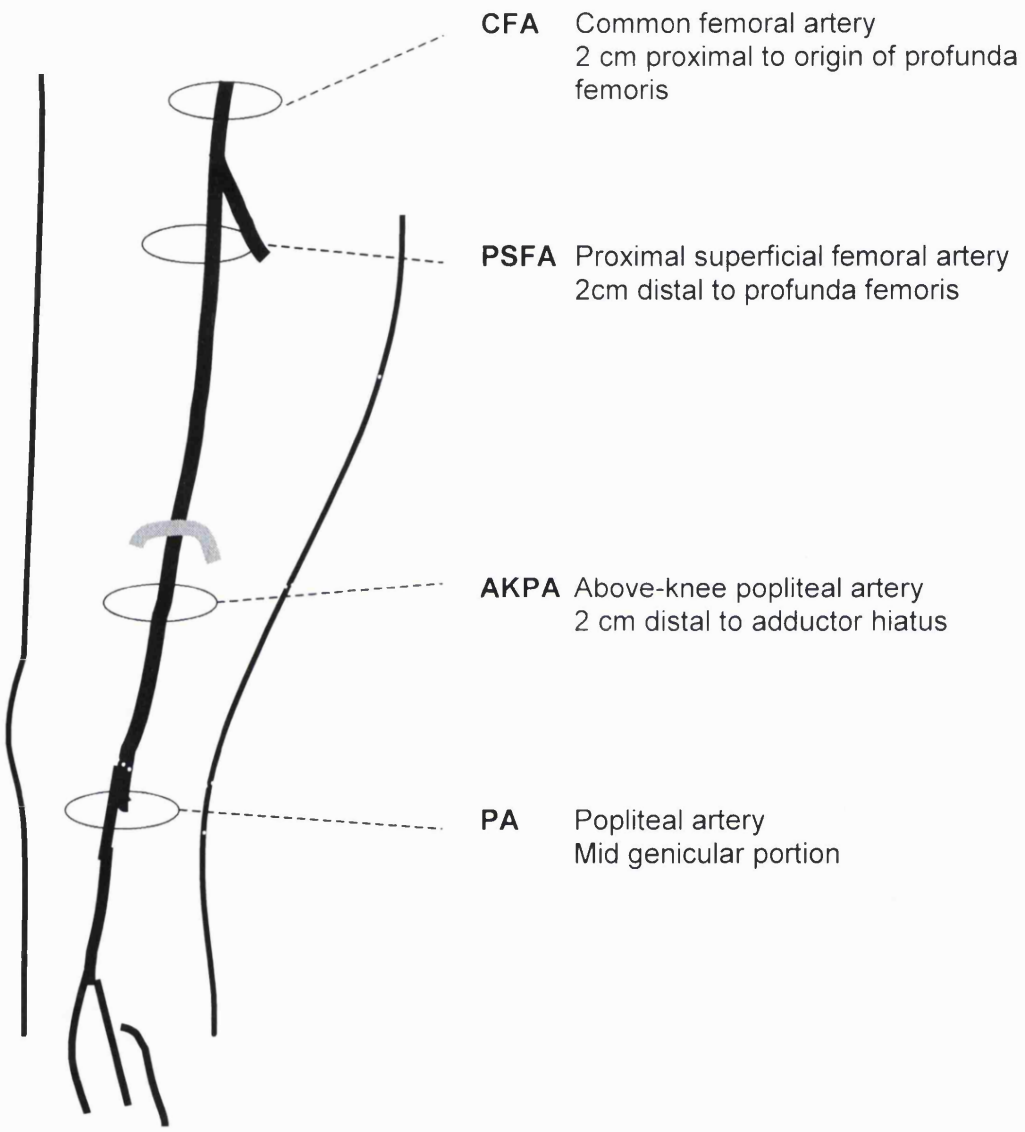
CFA Common femoral artery
2 cm proximal to origin of profunda femoris
PSFA Proximal superficial femoral artery
2cm distal to profunda femoris
AKPA Above-knee popliteal artery
2 cm distal to adductor hiatus
PA Popliteal artery
Mid genicular portion

In two group 1 limbs the presence of calcified atherosclerotic non-stenosing plaque prevented accurate imaging of the AKPA and the PA respectively. Calculated variables that lay more than three standard deviations (SD) away from the group mean were regarded as spurious and excluded from data analysis; a single result pertaining to excess AKPA stiffness in a Group 1 patient was treated as such.

A personal computer running a statistical software package (Prism 2.01, Graphpad Software, San Diego, USA) was used to compare inter-group differences in subject characteristics (age, height, body-mass index, and mean arterial blood pressure) with the Mann-Whitney test. Inter-group differences in vessel diameter, diametrical compliance and stiffness index were similarly sought. Differences in diametrical compliance and stiffness index between individual vessel wall sites were assessed by Kruskal-Wallis analysis of variance and localised using Dunn's post-test. Inter-group comparisons of luminal diameter, diametrical compliance and stiffness index were undertaken with respect to group 1 versus group 2, and group 3 versus group 2.

2.2.5. Measurement of observer variation and error

Two sonographers participated in this study (Mr Giudiceandrea and Mr Tai). Therefore, in 5 of the Group 2 subjects dual measurements were undertaken by both operators on the AKPA, which had been noted to be the most technically demanding segment of the vessel to image. Thus the same segments were imaged sequentially by both sonographers on the same occasion. For each patient, three separate registrations were made of vessel wall movement and blood pressure, where each registration consisted of three cardiac cycles. Compliance, stiffness and diameter data from the three registrations was averaged to give a single mean result for these variables as observed by an individual sonographer. Similarly, these variables were also calculated from vessel wall movement data and simultaneously obtained blood pressure as observed by the second sonographer. Observer variability was calculated for

these measurements of vessel wall diameter, compliance and stiffness index (β) as the error of a single estimation e [256] where

$$e = \sqrt{\Sigma d^2 / 2n} \qquad [2.2]$$

d being the difference between paired measurements and n the total number of paired observations (n=5).

Additionally, the coefficient of variation CV [257] was determined, where

CV = Interobserver error x 100 / pooled mean values [2.3]

and

interobserver error = SD mean difference / $\sqrt{2}$. [2.4]

2.3. Results.

Groups 1 and 2 were comparable with respect to age, weight, height, and systolic, diastolic and mean blood pressures (table 2.1). There were no significant differences were observed between the two groups with regard to these subject characteristics.

Vessel wall luminal diameter is given in table 2.2. Systolic luminal diameter was observed to be greater in group 2 subjects versus group 1 subjects for all vessel segments, reaching significance at the CFA, PSFA and PA sites. Group 2 systolic luminal diameter was also observed to be greater than was the case for group 3 subjects in each of the four segments studied, although these differences were not statistically significant.

The diametrical compliance (% $mmHg^{-1}$ x 10^{-2}) and stiffness (β) data for all three groups are summarised in table 2.3 and depicted graphically in figure 2.5. When compared to group 2, group 1 subjects exhibited a general trend toward lowered arterial compliance and excess stiffness, which reached significance at the CFA and AKPA segments. When compared to group 3, group 2 participants did not demonstrate any significant differences in compliance and stiffness index values for the proximal regions of the femoropopliteal vessel, although the popliteal segment proved significantly stiffer and less distensible in the older cohort.

Compliance and stiffness were found to markedly vary according to the site of measurement along the length of the femoropopliteal vessel. Analysis of variance in each group revealed significant inter-site variation in both compliance ($P<0.01$, $P<0.0001$ and $P<0.001$ for respectively) and stiffness ($P<0.01$, $P<0.0001$ and $P<0.0001$ for groups 1, 2 and 3 respectively). The CFA was consistently observed to be the most compliant, and with the exception of the popliteal artery in group 3, the least stiff vessel segment. The AKPA

exhibited least distensibility and comparison of compliance and stiffness values for the CFA versus AKPA revealed statistically significant differences in vessel wall properties across all three groups (table 2.4). The AKPA also exhibited significantly lower compliance and greater stiffness than the PSFA in group 1 and the PA in group 3.

Measurements of inter-observer variability for paired observations undertaken on the AKPA in 5 subjects are summarised in table 2.5. Inter-observer discrepancies were small for measured vessel luminal diameter and stiffness index and moderate for diametrical compliance.

Opposite:

Fig. 2.5. Scatter-plots of compliance (**Fig. 2.5.1.**) and stiffness index (**Fig. 2.5.2.**), with bar representing mean, for specific segments of the femoropopliteal artery (CFA ■, PSFA □, AKPA •, and PA O) in study groups 1, 2 and 3.

Fig 2.5.1.

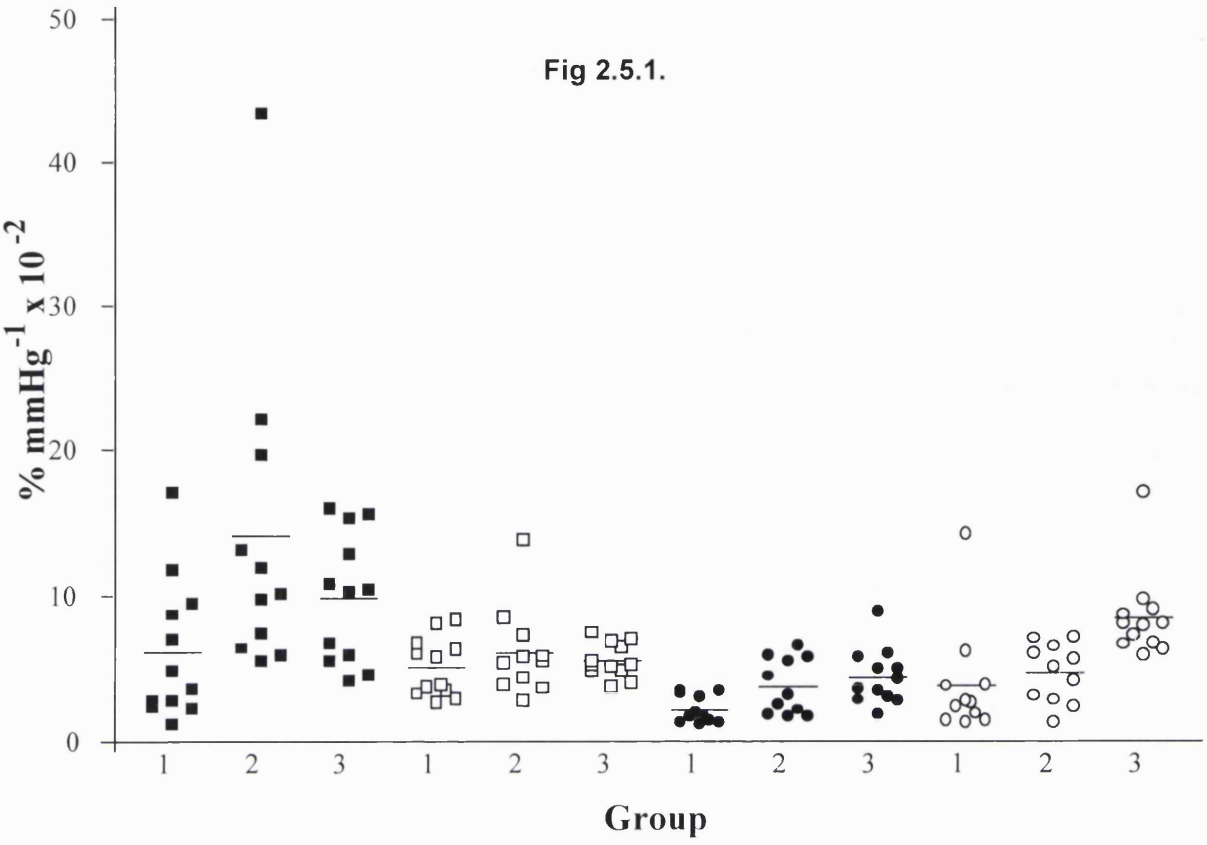

Fig 2.5.2.

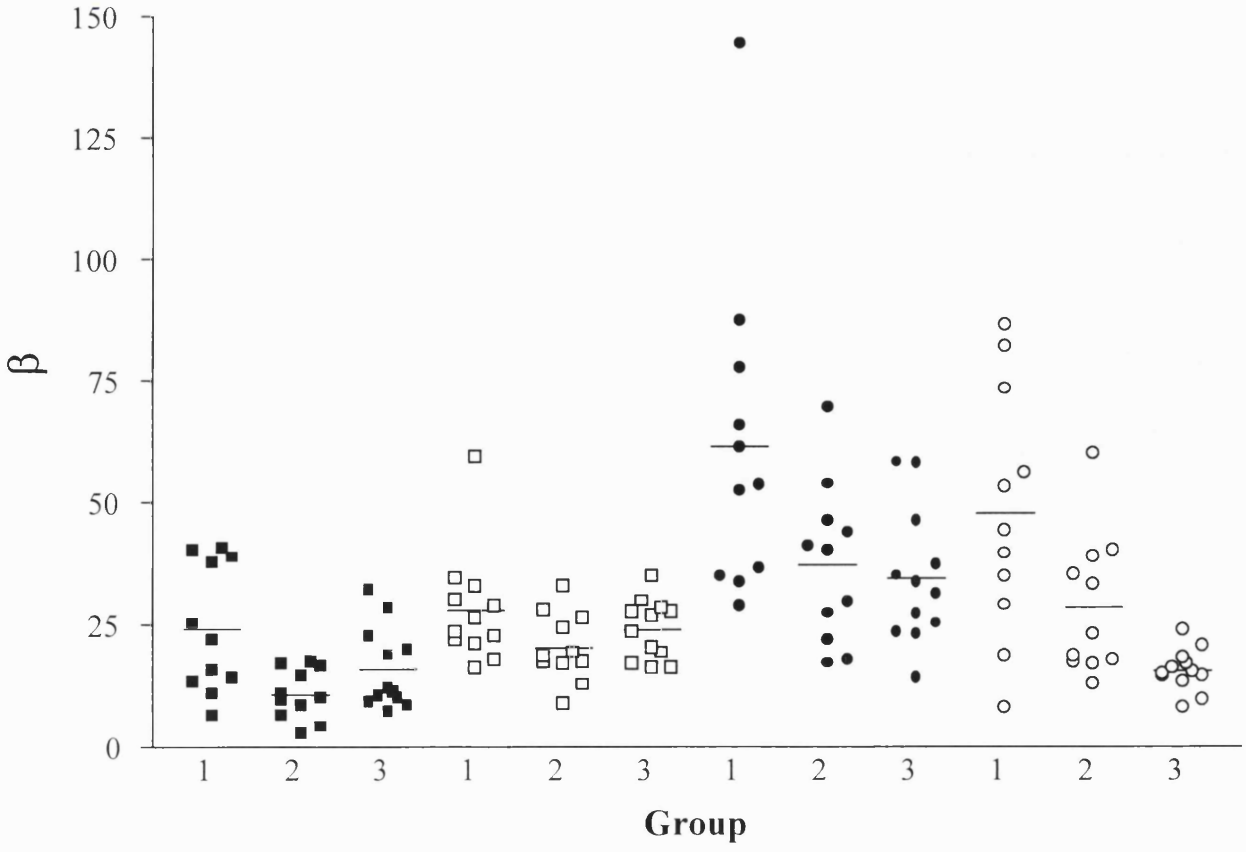

Table 2.1. Subject characteristics for study groups 1, 2 and 3 ; mean ± SD.

	Group 1	Group 2	Group 3
N	11	11	12
Age (Years)	74.7 ± 5.7	69.4 ± 10	28.8 ± 4.2
Height (cm)	166 ± 9.2	163 ± 10	172 ± 10.4
Weight (Kg)	67.2 ± 13.1	67 ± 14.5	71.2 ± 10.4
Body-Mass Index* (Kg/M^2)	24.3 ± 3.6	25.1 ± 3.4	24.1 ± 2.8
MABP (mmHg)	87.7 ± 9.7	92.3 ± 10.9	77.4 ± 7.1
Systolic BP (mmHg)	136 ± 17	139 ± 17.7	110 ± 8.8
Diastolic BP (mmHg)	66 ± 7.6	69 ± 9.1	61 ± 6.6
Sex ratio (M:F)	5:6	5:6	6:6
*Vasoactive medications***:*			
Beta blockers	3	2	-
Ca^{2+} channel blockers	1	1	-
ACE inhibitors	2	1	-
Nitrates	1	1	-

*where BMI = weight/$height^2$.
**Numbers of subjects receiving cardiovascular medication. ACE = angiotensin converting enzyme inhibitors. Nitrates = Nitric Oxide donor medications .

Table 2.2. Average vessel luminal systolic and diastolic diameter (mm) for study groups 1, 2 and 3 ;mean ± SD. P values refer to statistical comparison of systolic diameters . P < 0.05 represented as * and P <0.01 as **.

Diameter						P Values	
	Group 1		*Group 2*		*Group 3*	*Grps 1 v 2*	*Grps 2 v 3*
	Sys	Dia	Sys	Dia	Sys Dia		
CFA	7.2 ± 1.8	6.8 ± 1.8	9.3 ± 1.2	8.7 ± 1.6	8.3 ± 1.8 7.9 ± 1.7	**	NS
PSFA	6.4 ± 1.8	6.2 ± 1.7	7.8 ± 1.2	7.5 ± 1.2	7.2 ± 1.5 7.0 ± 1.4	*	NS
AKPA	6.1 ± 2.4	6.0 ± 2.3	6.5 ± 0.9	6.4 ± 1.0	6.3 ± 0.8 6.1 ± 0.8	NS	NS
PA	5.5 ± 1.9	5.4 ± 1.9	7.3 ± 1.3	7.1 ± 1.3	6.1 ± 1.1 5.9 ± 1.1	*	NS

Table 2.3. Mean (± SD) femoropopliteal arterial diametrical compliance and stiffness.

Compliance (% $mmHg^{-1} \times 10^{-2}$)				P Values	
	Group 1	*Group 2*	*Group 3*	*Groups 1 v 2*	*Groups 2 v 3*
CFA	6.2 ± 4.8	14.1 ± 11.1	9.9 ± 4.4	*	NS
PSFA	5.1 ± 2	6.1 ± 3	5.6 ± 1.2	NS	NS
AKPA	2.2 ± 0.9	3.8 ± 1.9	4.4 ± 1.9	*	NS
PA	3.9 ± 3.8	4.7 ± 2	8.5 ± 2.9	NS	**

Stiffness index (β)				P values	
	Group 1	*Group 2*	*Group 3*	*Groups 1 v 2*	*Groups 2 v 3*
CFA	24.1 ± 13.1	10.7 ± 5.12	15.9 ± 8.2	*	NS
PSFA	27.9 ± 11.4	20.3 ± 7	23.9 ± 6.1	NS	NS
AKPA	61.4 ± 33.4	37.1 ± 16.3	34.5 ± 13.7	*	NS
PA	47.8 ± 25.4	28.6 ± 14.4	15.5 ± 4.2	NS	**

Petersen's Elastic Modulus (x 10^6dyne cm^{-2})			
	Group 1	*Group 2*	*Group 3*
CFA	3.8 ± 2.9	1.4 ± 0.7	1.7 ± 0.8
PSFA	3.0 ± 1.2	2.6 ± 1.0	2.5 ± 0.5
AKPA	7.2 ± 2.8	4.5 ± 2.3	3.5 ± 1.5
PA	5.5 ± 3.0	3.6 ± 2.4	1.7 ± 0.4

P values <0.05 represented as * and P <0.01 as **. For the purposes of comparison with other published data, compliance values are also expressed as Ep in dynes/cm^2 .

Table 2.4. Results of statistical comparisons of compliance and stiffness index made within groups between individual vessel segments in study groups 1,2 and 3. P values <0.05 represented as *, P<0.01 as **, and P<0.001 as ***.

COMPLIANCE:

SEGMENT		*PSFA*			*AKPA*			*PA*		
	GROUP	**1**	**2**	**3**	**1**	**2**	**3**	**1**	**2**	**3**
CFA	1	NS	-	-	*	-	-	NS	-	-
	2	-	NS	-	-	***	-	-	**	-
	3	-	-	NS	-	-	**	-	-	NS
PSFA	1	-	-	-	**	-	-	NS	-	-
	2	-	-	-	-	NS	-	-	NS	-
	3	-	-	-	-	-	NS	-	-	NS
AKPA	1	-	-	-	-	-	-	NS	-	-
	2	-	-	-	-	-	-	-	NS	-
	3	-	-	-	-	-	-	-	-	***

STIFFNESS:

SEGMENT		*PSFA*			*AKPA*			*PA*		
	GROUP	**1**	**2**	**3**	**1**	**2**	**3**	**1**	**2**	**3**
CFA	1	NS	-	-	**	-	-	NS	-	-
	2	-	NS	-	-	***	-	-	**	-
	3	-	-	NS	-	-	**	-	-	NS
PSFA	1	-	-	-	*	-	-	NS	-	-
	2	-	-	-	-	NS	-	-	NS	-
	3	-	-	-	-	-	NS	-	-	NS
AKPA	1	-	-	-	-	-	-	NS	-	-
	2	-	-	-	-	-	-	-	NS	-
	3	-	-	-	-	-	-	-	-	***

Table 2.5. Comparison of mean observations of vessel luminal diameter, stiffness and compliance undertaken at the AKPA in 5 control patients by two observers (where *e* is the error of a single estimation of the measured or calculated variable; CV the coefficient of variation of that variable).

VARIABLE	OBSERVER I		OBSERVER II
Luminal Diameter (mm)			
Mean	6.4		6.1
SD	1		0.8
e		± 0.4	
CV		4.2%	
Stiffness (β)			
Mean	39.5		38.4
SD	13.2		8.61
e		± 3.2	
CV		5.9%	
C (%mmHg^{-1} × 10^{-2})			
Mean	3		2.7
SD	1.5		1
e		± 0.4	
CV		11.8%	

2.4. Discussion.

2.4.1. Measurement of compliance

Phase-locked echo-tracking was used to determine vessel wall motion in response to cyclical change in blood pressure. Firstly a B (brightness) mode image is obtained of the arterial segment under investigation, whereby depth resolution is achieved by analysis of high-frequency sound waves (radiofrequency signals) generated from a linear-array probe; the time delay between emission of a short burst and the reception of an echo signal representing the depth of origin of the signal. When switched to M (motion) mode, with the line of interest set perpendicular to the artery, the amplitude of the radiofrequency (rf) signal is displayed as a function of time. Although it is possible to estimate from the screen the change of vessel wall position with time, measurement of fine motion is precluded due to inadequate screen resolution. Instead, the rf signal is stored over a large number of M-lines throughout a specified number of cardiac cycles. Once the required number of beats has been recorded, review of the first M-line allows automatic identification of the wall-lumen transition, the assignment of gates to these points of the rf signal, and the positioning of sample volumes at the walls. Doppler processing of the rf signal at the gated positions enables calculation of the degree of change in the spatial position of the vessel walls and integration of this data updates a displacement waveform. Simultaneously, the position of the sample volumes is updated according to wall motion data so as to ensure that the echo signals captured always originate from the same source (*i.e.* wall-lumen interface) irrespective of wall excursion [258,259].

There are other accepted techniques available to measure vascular compliance including those that utilise laser-light, electrical force transducers, magnetic resonance imaging, digital X-Ray angiography and measurement of pulse-wave velocity [260]. Ultrasound wall tracking was used in this study as it is non-invasive, safe and has an extensive record of clinical application, having been used for determining vessel distensibility in the common femoral artery [247,248,250] aorta [254,261], and carotid artery [247,248,262-264]. It is a reliable tool; the inter-

observer variability (CV) of 4.3% for measured femoral artery diameter is comparable to other published series [265,266].

A justifiable criticism of the study protocol is that no attempt was made to assess the intra-observer variability in observations of pulsatile change, diametrical compliance and stiffness. It was considered that the the prime source of measurement error would result from the different abilities of the two observers in accurately visualising the correct arterial segment, properly aligning the linear array at right angles to the axis of flow, and minimizing probe movement during vessel wall motion capture. During our initial, informal trials with the walltracking system it was noted that the degree of agreement between observers measuring diameter and compliance measurements in the same individual at one sitting was less than that for consecutive measurements made by a single observer on the same individual. This is the experience of other workers using wall-tracking equipment [265,266], and thus it was decided to concentrate attention on inter-observer variation since it was thought that this would be the main contributor to observer error in the methodology employed. Nontheless, it is acknowledged that this assumption remains unproven and that proper measurements of intra-observer error would have been valuable.

During those same initial trials, it was consistently found that of all the segments studied, the above-knee popliteal artery was the most difficult region to image. In order to make sure that the artery was appropriately identified, verification of flow was frequently necessary by means of colour flow duplex Doppler imaging. This action was not needed when visualizing the other segments of the femoro-popliteal segment as high quality B and M-mode images were readily obtainable due to the superficial nature of those vessel regions. Logically, it follows that observer variability would be highest in this segment due to the additional technical difficulties involved. For this reason, and for additional practical considerations, it was decided to restrict measurements of observer variability to the AKPA.

Interestingly, inter-observer variability was higher for stiffness index (CV 5.9%) than vessel diameter (CV 4.2%) and higher still for diametrical compliance (11.8%). A possible explanation for this finding lies in the fact that compliance measurements are also dependent upon measuring blood pressure. Measured blood pressure varies from minute-to-minute, and thus from observation-to-observation. Consequently, this additional variability would be reflected in discrepancies between compliance data generated by the first observer against that determined by the second. Arterial wall stiffness is a calculation of distensibility whose formula minimizes the influence of the systolic-diastolic pressure differential (a denominator in the formula used to calculate compliance) by logarithmic treatment of pressure factors. Thus the finding that the variability of stiffness observations is lower than that for compliance. Similarly, when arterial wall breadth was measured, variability is even lower, as the measurements are simply estimates of vessel diameter and not calculations of distensibility occurring in the context of an acknowledged, described blood pressure change.

Other sources of error [260] can include failure of the wall-tracking system to accurately discriminate between the vessel wall and lumen, and the erroneousness insonation of the vessel wall at oblique angles of attack (thereby falsely elevating vessel diameter). Additionally, if there is a twisting or side-to-side component of the pulsatile motion exhibited by the vessel then the wall displacement profile generated may not be accurate. These errors are compounded when trying to assess small vessels. The original intention of this study was to measure the compliance of the infra-genicular vessels additional to femoropopliteal artery . Unfortunately, accurate visualisation of these arteries and thus capture of vessel wall-motion was difficult and initial results (not presented) were unfeasibly erroneous. It was therefore decided to limit this investigation to the femoropopliteal segment as described.

2.4.2. Patient selection

We utilised non-invasive measurements of brachial blood pressure [248,265] to calculate common femoral artery distensibility. A theoretical source of error when comparing measurements in patients with PVD against healthy controls is that significant stenoses between central and peripheral arteries in diseased patients may nullify the legitimacy of utilising brachial blood pressure as an estimate of femoropopliteal blood pressure. Selecting PVD patients who had undergone successful PTA (as judged by post PTA check angiography and ABPI equal to or greater than 1.0 at time of investigation) ensured that such bias was minimal. Groups 1 and 2 were otherwise well matched for other possible determinants of vascular distensibility including sex, age, body mass and blood pressure.

On the advice of the Chairman of the Royal Free Hospital Research Ethics Committee, it was deemed unnecessary to apply for specific ethical approval for the studies detailed. The rationale for this was that measurement of compliance is not reported to be associated with physical or psychological morbidity. Thus written approval was not specifically sought. Nontheless, studies were undertaken in accordance with Royal Free Hospital Dept of Surgery standing protocols on good ethical research practice. Informed consent was obtained from participants and all data obtained was anonymised and treated confidentially

2.4.3. Peripheral vascular disease and vessel distensibility

The femoropopliteal artery was observed to be less compliant and stiffer in the PVD cohort than the age-matched control group ; differences were significant at the CFA and AKPA for both compliance and stiffness index. Lower compliance indicates that PVD arterial segments exhibited less functional reserve in accommodating changes in intra-luminal pressure; greater vascular stiffness suggests that these arteries are distinctly less distensible - at any physiological pressure - than normal aged vessel. This is in agreement with primate models of atherosclerosis [267] and other reports of the effect of atherosclerosis on arterial

distensibility in the carotid artery [263], and in the aortas of atheroma-prone heart-transplant recipients [268] and patients with cerebrovascular disease [269] . Atherosclerosis appears to affect blood vessel stiffness by changing the intrinsic material properties of artery wall, causing elastolysis, collagen deposition and medial degeneration [251] . However, it is acknowledged that atherosclerosis has also been observed to increase [38] or to have no effect [252,270] upon the elastic behaviour of arteries. In an *in vitro* study of stress and strain in human external iliac segments retrieved from necropsy [271], Petersen's elastic modulus (Ep) was measured at 8.5 ± 3.3 dynes cm^{-2} in healthy arteries and 9.5 ± 2.4 dynes cm^{-2} in atherosclerotic vessels – a statistically insignificant difference. Direct comparison of our results with other *in vivo* studies investigating the compliance of the femoral artery [247-250] is hampered by the many different terms used to describe arterial elasticity that different investigators have utilised to measure arterial distensibility.

2.4.4. Alternative interpretations of inter-group differences in distensibility

It is acknowledged that comparisons between the PVD subjects and their age-matched controls may be confounded by the unquantified effect of angioplasty upon localised vascular distensibility. In 3 patients (2 common femoral artery and 1 superficial femoral artery) the case notes record that angioplasty was undertaken at a site later subject - by study protocol - to compliance assessment. Balloon angioplasty may have an effect analogous to the balloon injury model used to study smooth muscle cell (SMC) proliferation *in-vivo* [272], when SMC proliferation is observed following the degranulation of platelets adherent to endothelium-denuded arterial lumen. This may partially account for decreased local vascular distensibility in the region of the angioplasty site but does not explain the pattern of pan-arterial stiffening that the subjects of the PVD group exhibited.

Several other reasons may explain the differences observed between the group 1 subjects and their age-sex matched group 2 controls. Notably, the vessels in the PVD group were

smaller in diameter at all sites along the femoropopliteal artery compared to those vessels in group 2. The law of Laplace describes an inverse relationship between vessel wall thickness and wall stress [273]; if the observed narrowing were due to increased wall thickness in the PVD cohort then this also would explain the reduced compliance and increased stiffness of the femoropopliteal artery in this cohort. It is reasonable to suggest this as an explanation since arteries affected by peripheral vascular disease are subject to thickened walls arising from the dual processes of intimal-medial thickening and atheroma formation [42]. However, since wall thickness was not measured it is not possible to validate this interpretation of the data. Arterial diameter is also partly-determined by smooth muscle tone, which itself is dependent upon sympathetic activity and local humoural factors such as endothelium derived relaxing factor (nitric oxide) [250,251] ; differential influence of these factors between the groups may also account for the observed disparity in luminal diameter and hence vessel distensibility between the two groups.

2.4.5. Comparison of old healthy (group 2) and young healthy (group 3) subjects.

Interestingly a consistent trend was noted for vessels from group 3 to be of narrower diameter than those from group 2, although statistical comparison revealed there to be no significant difference with regard to vessel diameter, compliance or stiffness. An exception to this trend was the popliteal segment in group 2, which was notably less distensible. These results are consistent with previously published work [247-249], showing that age itself has little effect upon lower-limb vascular distensibility and that lower-limb arteries tend towards greater diameter with age. Benetos *et al* [247] studied CFA distensibility in 78 subjects (52 with mild-to-moderate hypertension) from 23 -71 years of age and found a non-significant increase in vessel diameter with age but no change in distensibility. Similarly, data from Laogun and Gosling [249] who measured vessel pulse-wave velocity in the limbs of 600 healthy volunteers up to the age of 65 did not demonstrate any decrease in ilio-femoral compliance from 20 years of age

onwards. Van Merode [248] and colleagues studied the relative distension (i.e. percentage change in vessel luminal diameter during each cardiac cycle) of the CFA and its immediately bifurcating branches in two cohorts of 10 young (20-30 yrs) and 10 older (50-60 yrs) healthy volunteers. They noted that the relative distension of both proximal deep and superficial femoral artery was not altered by age, although they recorded decreased relative distension in at the CFA in the older group; the investigators also noted the younger vessels to be of narrower bore. These observations might be explained by interpreting the change in diameter as an adaptive response to threatened decrease in wall distensibility brought on by ageing. It is increasingly accepted [69,70,250,273] that arteries are capable of varying luminal diameter as a mechanism to preserve vascular compliance and functional efficiency in storing pulsatile energy. As discussed in chapter 1, this effect is probably modulated via endothelial-dependent detection of change in wall shear force with resultant release of NO and adrenergic inhibition of smooth muscle tone. However, the relationship between enhanced diameter and preservation of compliance in older healthy controls was not consistently observed in this study, as the popliteal segment of older control subjects was significantly less compliant and more stiff than in younger controls, despite a trend toward greater diameter. This raises the possibility that the more distal parts of the lower-limb arterial system are prone to age-related loss of vascular compliance whilst more proximal pathways are protected. Thus, arterial dilatation occurring as an adaptive response to ageing may eventually be reversed by the sclerosing peripheral vascular disease in susceptible subjects.

2.4.6. The pattern of femoropopliteal compliance.

Compliance and stiffness varied along the femoropopliteal segment in both groups. Notably, in all groups the CFA was more distensible compared to distal segments – significantly so versus AKPA in group 1, AKPA and PA in group 2, and the AKPA in group 3. The marked disparity between the compliances of CFA and AKPA may be a reflection of the greater

muscularity, diminished bore and increased wall thickness-to-vessel diameter ratio that is observed in distal arteries [273]. These factors may account for the reduced AKPA elasticity, especially when combined with a possible tethering effect produced by the artery's site within the adductor canal. It is interesting to note that in all groups, the AKPA was consistently the least distensible region, and that this region is notorious as a prime site for the development of atherosclerotic lesions [16,17]. In group 1 the heterogeneity of compliance and stiffness between individual sites was not as pronounced as for group 2, suggesting that a particular feature of lower-limb vascular disease is the differential influence it has upon vessel stiffness in different areas of the femoropopliteal artery.

2.4.7. Implications for the design of a compliant vascular graft

These studies indicate that the compliance of the femoropopliteal artery is variable, and that arterial compliance is principally dependent upon two factors: a history of lower-limb vascular disease and the anatomic location of the vessel segment. In order to minimise compliance mismatch a graft should match the artery it is to replace. The logical conclusion is that such prostheses should reproduce the biomechanical qualities of diseased vessels, which in this study exhibited significantly different compliance characteristics from normal vessels. Unfortunately, diseased-matched grafts may not have the perfusion efficiency associated with grafts that reproduce the compliance properties of normal, disease free vessels. The solution to this dilemma is currently unknown [96], but is likely that either option would result in prostheses that more accurately reproduce the *in vivo* arterial elasticity than currently available grafts.

Chapter 3.

An assessment of the *in vitro* compliance characteristics of the Chronoflex CPU graft versus other vascular conduits commonly used for infrainguinal reconstruction.

3.1. Introduction

Preliminary measurements have suggested that the new Chronoflex CPU graft can potentially provide a greater degree of graft-artery compliance match than either PTFE or Dacron prostheses [243]. In chapter 2 it was determined that the *in vivo* vascular compliance of the femoropopliteal segment is around 2.2 - 6.2 %mm Hg^{-1} $x10^{-2}$ in diseased arteries and 3.8 - 14.1 %mm Hg^{-1} $x10^{-2}$ in healthy, aged vessels. The aim of the experiments undertaken in this chapter was to assess the extent to which the new Chronoflex CPU graft reproduces the elastic behaviour of such vessels. The compliance qualities of vascular grafts may be observed *in vivo* following implantation within the arterial circulation. However, an *in vitro* approach, using a flow circuit model of arterial flow allows a fuller characterisation of behaviour since flow and pressure variables may be altered, under full control, as required. Thus, a flow circuit was used to study - over a range of mean pressures - the *in vitro* dynamic compliance and stiffness properties of the new prosthesis. The study included an assessment of the compliance characteristics of other vascular conduits commonly used for lower-limb bypass surgery. It was hypothesised that the compliance of the new graft would match that of human lower-limb artery to a significantly greater degree than either ePTFE or Dacron grafts.

3.2. Methods and materials

3.2.1. The flow circuit.

A flow circuit (figure 3.1.) specifically designed to accurately reproduce the haemodynamic characteristics of pulsatile arterial blood flow in the lower limb was fabricated [246]. This was then used to perfuse segments of the vascular grafts and human vessels under study. The flow model comprised a variable-speed electromagnetic centrifugal pump (Bio Medicus Inc., Minnetonka, USA), flexible plastic tubing and fluid reservoir. An electronic governable flow waveform conditioner (FWC), consisting of an electronically controlled solenoid gate was sited in series with the circuit and used to generate arterial flow waveforms with a systolic : diastolic period of 1:2 . An inline solenoid valve was used to condition the flow waveform. A controller unit, (essentially an Astable circuit with variable mark-to-space ratio and frequency), provided a square wave of +0-5 Volts. This opened the valve via the solenoid resulting in the transmission of the prevalve pressure as a pulse, which produced the desired flow waveform. Instantaneous flow rate was measured using a 6mm tubular flow probe connected to a Transonic Medical Flowmeter (TMF) system (HT207, Transonic Medical System Inc., USA) . Pressure measurements within the circuit were made using a Millar-tip pressure catheter (Millar Instruments, Inc., Houston, Texas, USA). The perfusion solution was made using a mixture of 8% low molecular weight Dextran (Molecular Weight 77 000 Dalton, Sigma-Aldrich Co Ltd, Poole, Dorset, UK) added to a solution of M199 (Life Technologies, Paisley, Scotland), 20% foetal bovine serum, 7.5% sodium bicarbonate (Sigma-Aldrich Co Ltd, Poole, Dorset, UK), 200 mm L-glutamine (Gibco BRL, Life Technologies Ltd, Inchinnan Business park, Paisley, UK), penicillin 10000 U/ml and streptomycin 10 mg/ml and buffered at pH 7.20 . The viscosity of this medium - 0.035 g/cm/s (poise) or 0.0035kg/m/s (SI units) - has previously been determined to approach that of whole human blood using a cone plate viscometer

Opposite:

Fig. 3.1. Schematic of flow circuit.

Fig. 3.1.

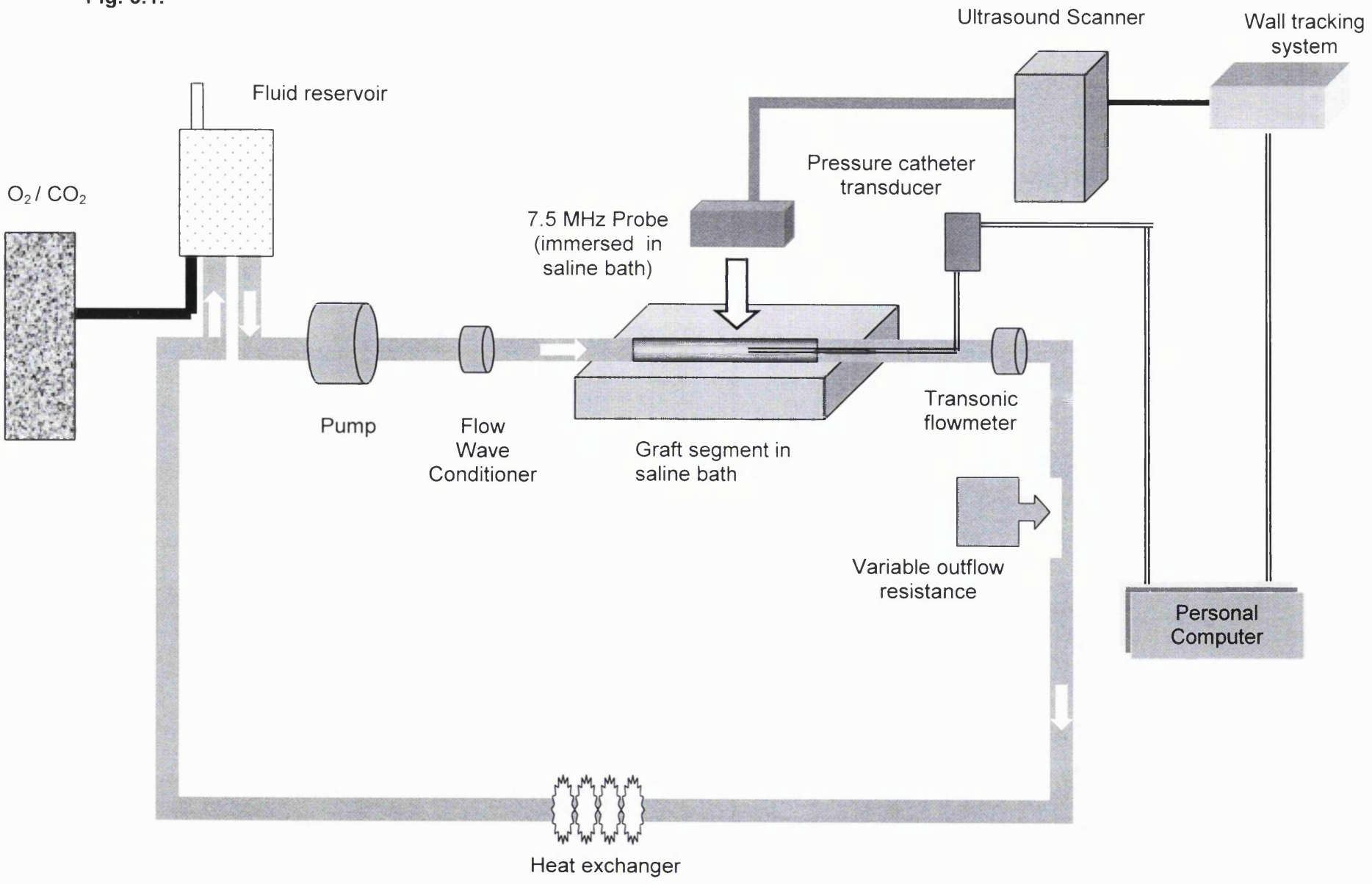
Ultrasound Scanner
Wall tracking system
Fluid reservoir
O_2 / CO_2
Pressure catheter transducer
7.5 MHz Probe (immersed in saline bath)
Pump
Flow Wave Conditioner
Graft segment in saline bath
Transonic flowmeter
Variable outflow resistance
Personal Computer
Heat exchanger

(Low-Shear 30 Contraves, Switzerland). A gas mixture of 95% oxygen and 5% carbon dioxide was bubbled through the fluid reservoir and the perfusate was maintained at 37°C via a heat exchanger (Portex, Hythe, Kent, UK). The pCO_2, pO_2 and pH were checked with an automatic blood gas analyser (BG electrolyte systems, Instrumentation Laboratory Company, Lexington, MA USA). Pressure was varied by increasing the level of the fluid reservoir above the graft segment and by varying the diameter of an outflow resistance sited distally to the grafts. The haemodynamic variables of the perfusion circuit are given in table 3.1.

3.2.2. Grafts and vessels

Four centimetre test segments of 5 mm diameter Chronoflex CPU grafts (Cardiotech International Ltd, Brymbo, Wrexham), 5 mm PTFE grafts (Impra Inc, Crawley, W. Sussex), 5 mm uncrimped knitted Dacron grafts (Sulzer Vascutek Ltd, Linchinnan, Renfrewshire) and human external iliac artery segments retrieved from organ donors were studied. Segments of proximal human saphenous vein salvaged from patients undergoing Trendelenberg's procedure were also investigated but only those vessel segments deemed free of varicose change were retained for study. All human vessels were obtained in accordance with local ethical committee standing orders regarding experimental use of discarded human tissues, stored in Ringer's lactate solution at 4°C and studied within 24 hours of harvest. All prosthetic grafts were washed and degassed with 70% ethanol and, to ensure minimal transmural leakage of perfusate and loss of intraluminal pressure, grafts were subject to a pre-clotting procedure. This was carried out by forcing 10mls of freshly obtained whole human blood through graft interstices; once the blood had clotted a further 10 mls of fresh blood was perfused through the graft and the process repeated until no further transmural leakage of blood observed. Grafts were then washed in normal saline. Prosthetic graft and vessel segments were mounted in series with the flow circuit using a specially constructed perfusion rig that allowed mounting of up to 6 specimens simultaneously (figure 3.2.) . Segments were

subject to longitudinal stretch in order to reproduce the likely *in vivo* conformation [273] : thus human artery and vein were stretched by 30%, and Chronoflex CPU and Dacron by 10%; the inelastic nature of PTFE prevented longitudinal expansion. The perfusion rig and graft/vessel specimens were then placed in a bath containing normal saline maintained at 37° C and exposed to flow.

3.2.3. Measurement of vessel wall movement

Real time B-Mode and M-Mode images of test segments were obtained via a duplex colour flow ultrasound system (Pie 350, Pie Medical Systems, Maastricht, Netherlands) with signal output to a high-resolution echo-locked wall tracking system (Wall Track Version 2, Pie Medical Systems, Maastricht, Netherlands) as described in chapter 2. The 7.5 MHz linear array probe was immersed in the bath and positioned directly over the segment under investigation, and the end-diastolic and end-systolic intraluminal diameters automatically determined over the pulsatile cycle (figure 3.3). In order to reduce variability in measurements due to positional change of the linear array, it was held in place using a specially machined supporting frame. Measurements were made using a constant pulse pressure over a range of mean pressures. For each mean pressure and test segment, three measurements of wall movement were made, and the experiment was repeated six times. For each mean pressure, the compliance (C) and stiffness (β) values were calculated according to equations [1.3] and [1.4] for saphenous vein, Chronoflex CPU, PTFE and Dacron and compared to those of artery using one-way analysis of variance (ANOVA) with Bonferroni post-test.

Opposite:

Fig. 3.2. Perfusion rig, saline bath and travelling mount for ultrasound probe

Fig. 3.2.

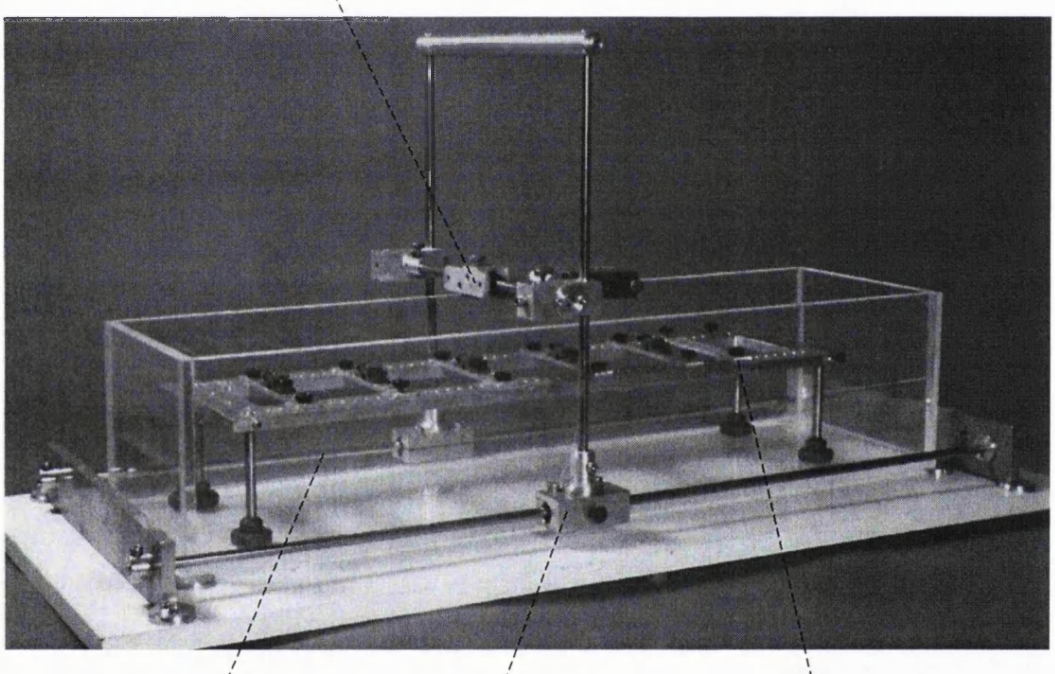
Cradle for 7.5 Mhz ultrasound probe
Perspex bath
Ballbearing mounting and cradle track
Stainless steel perfusion rig equipped with adjustable mounts for graft segments

Opposite:

Fig. 3.3. **Fig. 3.3.1)** B and M-Mode images of saphenous vein mounted within flow circuit. Note intra-luminal pressure catheter.

Fig. 3.3.2.) Resultant RF signal generated by anterior and posterior walls of imaged vein.

Fig. 3.3.3.) Distension-time curve generated by wall tracking system.

Fig. 3.3.1.

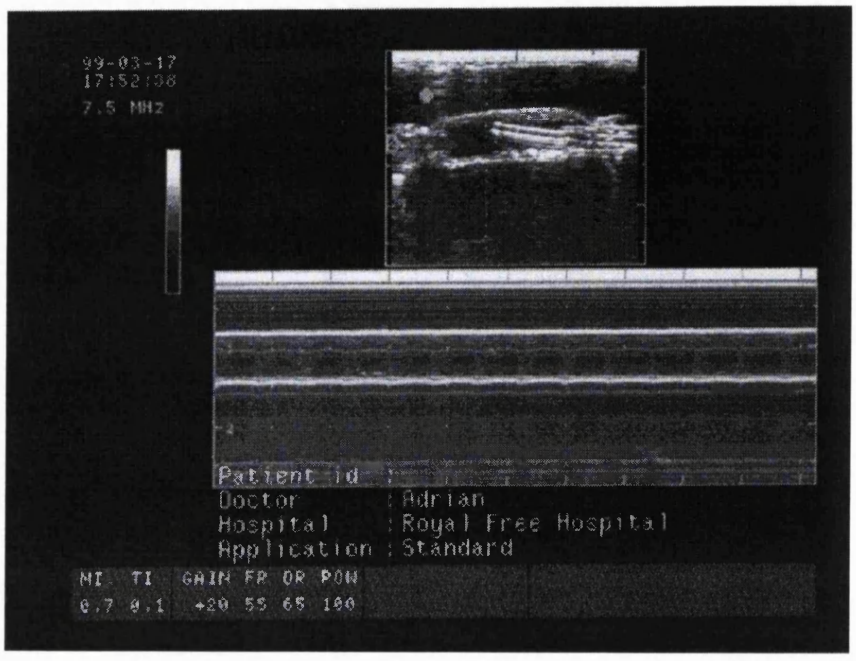

Fig. 3.3.2.

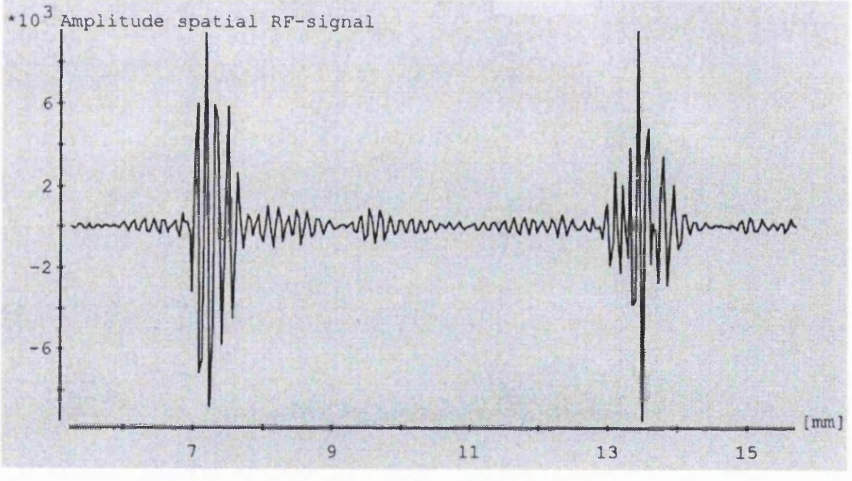

Fig. 3.3.3.

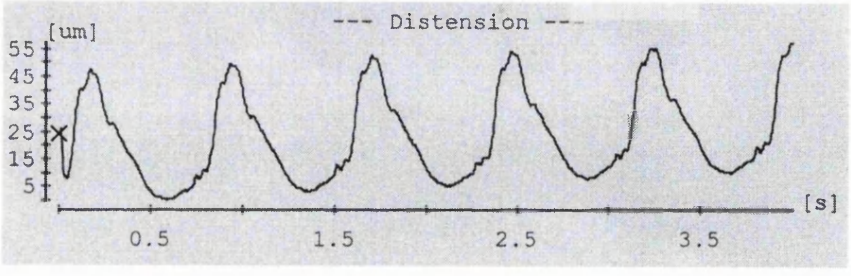

3.2.4. Evaluation of reproducibility.

Although the inter-observer error for luminal diameter, compliance and stiffness data associated with *in vivo* measurements was determined in chapter 1, reproducibility in the *in vitro* environment was unknown. This was investigated by taking dual estimations of luminal diameter change (each the average of three separate measurements) in 5 of the arterial segments. This was undertaken at two mean pressures – 30 and 100mmHg. Variability was calculated for measurements of vessel wall diameter, compliance and stiffness index (β) as the error of a single estimation e and the coefficient of variation CV using equations [2.2] and [2.3] respectively

3.3. Results

The results of the reproducibility study are given in table 3.2, which shows that intra-observer variability was minimal when measuring luminal diameter, compliance and stiffness. A summary of the diameter, compliance and stiffness index values for prosthetic and vessel segments is provided in table 3.3. Figure 3.4. depicts the variation of compliance and stiffness index with respect to incrementally increased mean pressure for prostheses and vessel segments. Arterial and venous compliance was observed to behave non-linearly in response to elevation of mean perfusion pressure.

ANOVA comparison revealed highly significant variance in compliance and stiffness exhibited by PTFE, Dacron, Chronoflex CPU, vein and artery (P values of <0.001 for each mean pressure studied, from 30 through to 100mmHg). Table 3.4 summarises the outcome of subsequent Bonferroni post-testing that compares, for each mean pressure, the compliance and stiffness index values of saphenous vein, Chronoflex CPU, Dacron and PTFE grafts to artery. There were no significant differences between the compliance values of Chronoflex CPU and artery at mean pressures 30 to 60mmHg, or between the stiffness index results from mean pressures 30 to 90mmHg. Comparing Dacron and PTFE to artery, significantly higher stiffness and lower compliance was observed at mean pressures 30 through 90mmHg and 30 through 100mmHg respectively, although Dacron grafts did not differ significantly from artery in either compliance or stiffness at the mean pressure of 100mmHg. Comparison of the elastic properties of saphenous vein to artery revealed no significant differences between the two vessel types at 30 and 100mmHg in terms of either compliance or stiffness, although there were clearly significant disparities in compliance from 40 through 90mmHg and in stiffness at 50, 60 and 80mmHg.

Opposite:

Fig. 3.4. **Fig. 3.4.1.)** Compliance-Mean Pressure curves for vessels and grafts. Curves for anisotropic vessels (artery, vein) generated using non-linear regression (single phase exponential decay model); curves for isotropic prostheses generated using linear regression.

Fig. 3.4.2.) Stiffness-Mean Pressure curves for vessels and grafts. All curves generated using linear regression model.

Fig. 3.4.1.

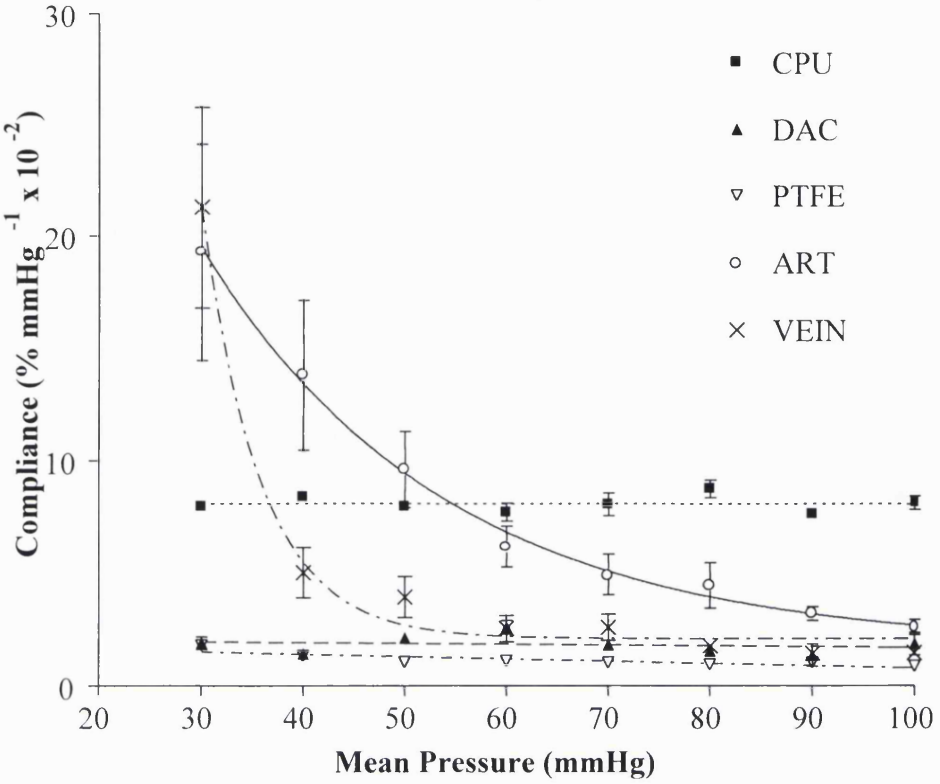

Fig. 3.4.2.

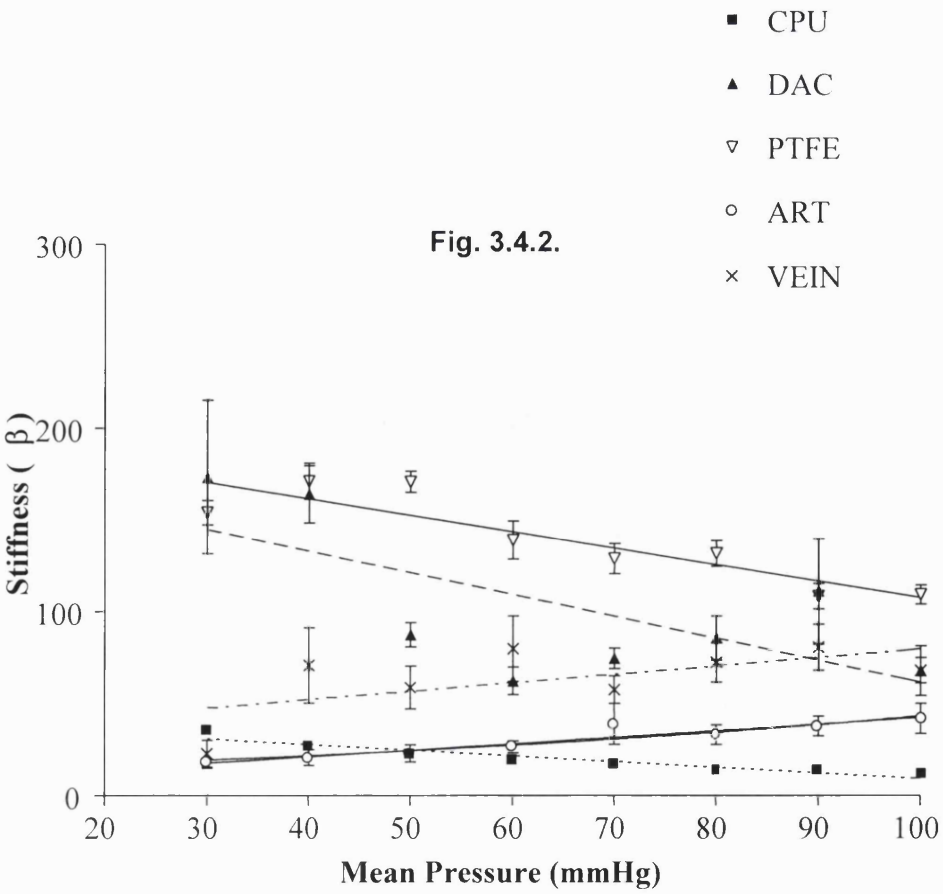

Table 3.1. Typical flow circuit haemodynamic values (mean ±SD).

Physical Parameter	Variable
Mean Pressure (mmHg)	30-100 increased by 10mmHg increments
Pulse Pressure (mmHg)	60.5 ± 0.8
Frequency of pulsatile cycle (hz)	1
Flow rate mls/min	132 ± 24
Perfusate Temperature (°C)	37
Perfusate viscosity (poise)	0.035

Table 3.2. Reproducibility of luminal diameter, stiffness and compliance measurements (where *e* is the error of a single estimation of the measured or calculated variable; CV the coefficient of variation of that variable).

Mean Pressure 30mmHg

Variable	Observation I		Observation II
Luminal Diameter (mm)			
Mean	5.4		5.38
SD	1.05		1.11
e		± 0.06	
CV		1.1 %	
Stiffness (β)			
Mean	19.2		19.0
SD	4.99		4.73
e		± 0.44	
CV		2.57%	
C (%mmHg^{-1} x 10^{-2})			
Mean	15.1		15.1
SD	2.95		2.82
e		± 0.38	
CV		2.79%	

Mean Pressure 100mmHg

Variable	Observation I		Observation II
Luminal Diameter (mm)			
Mean	6.19		6.17
SD	0.91		0.95
e		± 0.05	
CV		0.78 %	
Stiffness (β)			
Mean	29.7		28.9
SD	2.55		1.59
e		± 1.19	
CV		4.5%	
C (%mmHg^{-1} x 10^{-2})			
Mean	3.28		3.3
SD	0.14		0.17
e		± 0.1	
CV		2.82%	

Table 3.3. Mean (SD) Systolic diameter, compliance (C) and stiffness (β) values: averaged over the entire mean pressure range and observed at 30 and 100 mmHg.

	Artery	Vein	Chronoflex CPU	Dacron	PTFE
Diameter (mm)					
Averaged	6.8 ± 0.3	4.9 ± 0.2	6.1 ± 0.8	5.4 ± 0.2	5.4 ± 0.1
30mmHg	6.3 ± 1.2	4.8 ± 1.5	5.9 ± 0.2	5.5 ± 0.3	5.3 ± 0.1
100mmHg	7.1 ± 1.1	5.1 ± 1.8	6.9 ± 0.4	5.6 ± 0.1	5.4 ± 0.2
C (% $mmHg^{-1}$ x 10^{-2})					
Averaged	8.0 ± 5.9	5.0 ± 6.7	8.1 ± 0.4	1.8 ± 1.2	1.2 ± 0.3
30mmHg	19.3 ± 11.9	21± 11	8.0 ± 0.4	1.9 ± 0.7	1.8 ± 0.2
100mmHg	2.6 ± 0.8	1.5 ± 0.4	8.1 ± 0.7	1.87 ± 1.2	0.9 ± 0.1
β					
Averaged	29.9 ± 9	63.7 ± 18.6	20 ± 8.0	103.1 ± 43.1	139 ± 24.8
30mmHg	17.8 ± 7.3	22.0 ± 18.0	35.6 ± 2.2	173.2 ± 102.4	154 ± 16.4
100mmHg	41.8 ± 20	67.9 ± 16.7	11.9 ± 1	67.8 ± 32.3	109 ± 5.2

Table 3.4. Outcome of ANOVA comparison of compliance (C) and stiffness values (β) of PTFE, Dacron, vein and Chronoflex CPU against artery with Bonferroni analysis (P values >0.05 = ns, <0.05,<0.01 and <0.001 as *,** and *** respectively).

Pressure (mmHg)		PTFE		Dacron		Vein		Chronoflex CPU	
Mean	Systolic/Diastolic	C	β	C	β	C	β	C	β
30	70/10	***	***	***	***	ns	ns	ns	ns
40	80/20	***	***	***	***	**	ns	ns	ns
50	90/30	***	***	***	***	**	*	ns	ns
60	100/40	***	***	***	**	***	**	ns	ns
70	110/50	***	***	***	**	*	ns	***	ns
80	120/60	***	***	**	***	**	*	***	ns
90	130/70	***	**	***	**	**	ns	***	ns
100	140/80	**	***	ns	ns	ns	ns	***	*

3.4. Discussion

As stated in Chapter 1, arteries are not merely passive conduits, conducting blood from one part of the circulation to another. Their elastic structure allows the energy-efficient transmission of pulsatile blood-flow together with simultaneous damping of excessive pressure fluctuations and the matching of the impedance characteristics of the proximal arterial tree to distal branches [85-87]. Ideally, prosthetic vascular grafts should simulate these biophysical qualities [41]. The aim of this chapter was to quantify the extent to which the compliance of the new Chronoflex CPU graft matches those of human muscular artery in comparison to ePTFE, Dacron and human saphenous vein.

3.4.1. Methodological considerations

The elastic behaviour of a vessel can be determined statically by measuring incremental change in vessel diameter during step-wise inflation of an intraluminal balloon, but this approach does not allow for the contribution that vessel or graft wall viscosity (i.e. inertia) makes upon the *in vivo* elastic response [85]. The amount of radial movement (strain) that a vessel wall exhibits in response to a change in intra-luminal pressure (stress) is not only dependent upon the magnitude of the pressure change but also the rate at which the pressure is applied *i.e.* wall behaviour is viscoelastic [86]. Thus, in order to fully characterise likely *in vivo* graft or vessel viscoelastic behaviour, a dynamic approach was required. This is the reason why a pulsatile flow circuit, capable of supporting biological tissues, was designed to allow cyclical application of wall stress and the reproduction and manipulation of physiological flow parameters. This *in vitro* approach allowed rigorous control of the physical forces that the grafts or vessels were exposed to in order to allow valid comparison of different vessels and graft types.

As in chapter 2, the ultrasound echo-locked wall tracking system was used to record change in graft or vessel diameter over each pulsatile cycle. It was noted that variability was less than that observed *in vivo* ; this may be due to a number of factors. Firstly, the perfusion rig allowed uniform stretch of the vessels and prevented non-radial movement. Secondly, errors due to probe movement were precluded by locking the probe into position above each segment. Finally, the perfusion pressures for each recording were uniformly applied and did not differ from vessel to vessel. Thus the *in vitro* variability reflects the error or variability of the wall-tracking system in locating the vessel walls.

Both the anterior and posterior walls of the subject graft must be imaged for ultrasound wall tracking to be successful. It was initially noted that whilst Chronoflex CPU, Dacron and artery were readily imaged in this respect, ePTFE grafts were difficult to fully visualise. This was due to the intensely echogenic nature of ePTFE; the anterior wall was seen but the posterior wall was hidden in the "shadow" caused by reflection of ultrasound energy from the anterior graft surface. Degassing the graft in 70% ethanol noticeably improved translucency of the grafts, thereby implicating the presence of microscopic air bubbles in the graft wall as the likely source of the echogenicity. For purposes of consistency, all prosthetic grafts were similarly treated with alcohol prior to perfusion, although it did not further enhance visualisation of Chronoflex CPU and Dacron grafts.

It was anticipated that the Dacron grafts would require pre-clotting. However, the wetted ePTFE and Chronoflex CPU grafts also required preclotting in order to avoid leakage of perfusate and loss of intraluminal pressure. Normally, these grafts do not require preclotting when used *in vivo* as the graft interstices are quickly sealed with fibrin and other elements of whole blood upon restoration of blood flow. Such elements were not present in the perfusate that was used, leading to excessive trans-mural egress of circulating fluid. In the initial attempts to solve this problem a solution of bovine collagen was air-dried onto each graft type in order to prevent leakage, but this rendered the grafts abnormally stiff and was eventually

abandoned in favour of the pre-clotting technique. Theoretically, a fibrin mesh may possibly contribute to the structural strength of a preclotted graft and thereby alter the elastic behaviour, but the specific effect of pre-clotting upon the mechanical properties of these grafts was not studied.

Freshly harvested organ donor external iliac artery segments were used in this study as they were readily available. It would have been preferable to use more distal arterial segments arising from the femoropopliteal or infragenicular arteries but the harvesting protocol prevented excision of vessels not accessible by abdominal laparotomy.

Another criticism of the *in vitro* approach is the limited applicability it has to the *in vivo* situation. *In vitro* studies may overestimate *in vivo* arterial elasticity as the latter is influenced by the degree to which adjacent connective tissues tether arterial wall excursion [85]. Furthermore, *in vivo* vessels experience a variable amount of smooth muscle tone secondary to sympathetic and humoural influences [250].

3.4.2. Anisotropy and isotropy

It was decided to measure the elastic behaviour of the grafts and vessels over a range of mean pressures. This is because arterial tissue is a heterogeneous, non-hookean (*i.e.* does not exhibit a linear pressure-distension curve) material whose compliance behaviour is strongly pressure-dependent [85,89]. At low pressures the load is predominantly borne by highly distensible elastin fibres but at high pressures it is transferred to the poorly elastic collagen fibres [273,274]. Vein is also non-hookean but unlike artery, load is transferred to the collagen fibres at lower stress (pressure) because venous walls contain less elastin and smooth muscle. Consequently vein is incompliant when exposed to the higher mean pressures associated with arterial circulation. The stretch behaviour of arteries and veins is anisotropic *i.e.* the extent of distension is dependent upon the degree of pre-stretch (the operating mean blood pressure) prior to the application of the stress (the pulse-pressure). Generally, non-

biological prosthetic grafts do not exhibit this behaviour and there is little or no change in degree of circumferential stretch (compliance) as mean pressure changes, at least over the physiological range [89].

3.4.3. Comparison of the compliance of prosthetic grafts against artery

When averaged over the entire pressure range, the mean compliances of Chronoflex CPU and artery appeared similar (8.1 ± 0.4 and 8.0 ± 5.9 % $mmHg^{-1}$ x 10^{-2} respectively). There was no significant difference between artery and stiffness at mean pressures 30-60 mmHg but elevation of the pressure above this range caused disparity in compliance behaviour as arterial distensibility diminished : at 100 mmHg the compliances were 8.1 ± 0.7 for Chronoflex CPU and 2.6 ± 0.8 % $mmHg^{-1}$ x 10^{-2} for artery ($P < 0.001$). Thus the new graft appears "over-compliant" compared to artery in this pressure range, principally because of the homogenous, uni-elastic quality of the honeycombed urethane.

However, it can be argued -from a theoretical viewpoint- that this pattern of compliance might be advantageous. Firstly, if only partial matching is possible, then it may be preferential to match for the lower pressures found in the low-flow, low-pressure environment of the diseased infrageniculate arterial tree, rather than the higher pressures associated with less diseased and more proximal regions. Secondly, following implantation, porous prosthetic grafts become invaded by connective tissue elements that can fix the graft wall thereby diminishing the compliance that initially existed [88,218]. Thus it may be necessary to engineer a degree of "over-compliance" into the graft in order to buffer subsequent tissue-induced stiffening.

As expected, PTFE was considerably stiffer and less compliant than artery over the whole pressure range. The knitted Dacron grafts were similarly inelastic although the diminishment of arterial distensibility at higher mean pressures meant that their respective compliance and stiffness indices were not statistically different at 100mmHg.

3.4.4. Comparison of in vitro and in vivo results

In chapter 2 it was observed that popliteal arterial compliance (mean ± SD) in patients with PVD (group 1) and age-sex matched controls (group 2) was 3.9 ± 3.8 and 4.7 ± 2 %mmHg^{-1} x 10^{-2} respectively, measured at mean blood pressures of 88 and 92 mmHg respectively . With the proviso given above *apropos* the applicability of *in vitro* data, these values can be compared to the compliance data obtained in this study for a similar mean pressure of 90mmHg, where Dacron and ePTFE had compliance values of 1.4 ± 1 and 1 ± 0.3 %mmHg^{-1} x 10^{-2} respectively whilst Chronoflex CPU was more compliant at 7.6 ± 0.2 % mmHg^{-1} x 10^{-2}. Interestingly, the *in vitro* compliance of the external iliac artery segments was 3.2 ± 0.85 % mmHg^{-1} x 10^{-2} – similar to the *in vivo* popliteal compliance values given above, though different from the *in vivo* common femoral artery values of 6.2 ± 4.8 and 14.1 ± 11.1 %mmHg^{-1} x 10^{-2} observed in elderly PVD (group 1) and age-sex match control subjects (group 2) respectively. This suggests that utilising external iliac artery segments *in vitro* as a model for the *in vivo* behaviour of the popliteal segment may be valid, at least at a mean pressure of 90mmHg.

3.4.5. Utility of stiffness index (β) for in vitro measurements

Stiffness index β was originally formulated in order to allow valid comparison of distensibility between vessels exposed to differing mean blood pressure [254,255], as comparison of compliance is only allowed when mean pressures are equivalent. Thus its maximum utility lies in the *in vivo* arena where comparison between subjects is desired. In this study, measurements of graft or vessel distensibility were undertaken for the same mean pressure over a pressure range of 30 –100 mmHg and therefore comparison of compliance values is valid. The difference in pressure-dependency between compliance

and stiffness index (β) explains the observation that the stiffness values of artery and Chronoflex CPU exhibit similarity over a more extensive pressure range ($P>0.05$ from 30-90mmHg) than was the case for the relevant compliance values.

In summary, it was demonstrated that the new CPU vascular prostheses provides a greater degree of graft-arterial compliance and stiffness match than is the case with either ePTFE or Dacron, although under *in vitro* conditions the match is only partial and limited to the lower pressure range.

Chapter 4.

An *in vitro* assessment of optimal seeding density, incubation time, response to pulsatile shear stress and viability of endothelial cells seeded on to Chronoflex CPU grafts.

4.1. Introduction

It was stated in chapter 1 that single stage endothelial cell seeding of prosthetic vascular grafts, as proposed by Herring and colleagues [151], may potentially reduce the thrombogenicity of lower-limb prostheses. However, whilst single stage seeding has been found to be applicable and practical, clinical trials have failed to show that it confers enhanced graft patency [166,172]. This is in contrast to two-stage seeding which improves graft patency [171,173] but is relatively inapplicable because of the necessity for trained personnel and cell culture facilities. The aim of single stage seeding is to establish a stable monolayer within hours, rather than weeks, of the seeding process; but only 1-14% [193-195] of cells seeded directly onto the unmodified graft lumen remain adherent following exposure to bloodflow. Investigators have thus concentrated on enhancing the resistance of seeded cells to arterial shear-stress, either by modifying the graft luminal surface with adhesive residues such as fibronectin [195-199] or by pre-conditioning the seeded graft with a period of *in vitro* perfusion, prior to implantation [197,205,206]. CPU grafts made from Chronoflex possess a porous, honeycombed luminal surface that may be favourable for cell attachment, and an initial study has shown that endothelial cells exhibit greater resistance to pulsatile flow when seeded on to Chronoflex CPU grafts as compared to standard ePTFE grafts [246]. The attraction of an endothelial cell-seeded Chronoflex CPU graft is that it would offer the dual benefits of antithrombogenicity and an enhanced compliance profile.

Grafts which retain EC are likely to be less thrombogenic than those that do not. Two key determinants of the number of cells likely to stick to a given graft surface are incubation time (the period for which the cells are left on the graft following seeding prior to graft implantation) and seeding density (the number of cells delivered to the graft per unit surface area). There are no studies that have sought to determine the correct seeding density or incubation time necessary for maximal cell adhesion when seeding on to polyurethane grafts. Therefore, the

principal purpose of the study in this chapter was to determine, with respect to CPU, the influence of seeding density and incubation time upon subsequent resistance to a shear-related displacement force. Additionally, the effects of Chronoflex CPU-incubation upon the metabolism of seeded endothelial cells the resistance of seeded cells to a quantified pulsatile shear stress was investigated.

4.2. Methods and materials

4.2.1. Influence of seeding density on cell adhesion.

4.2.1.1. Culture of endothelial cells.

Human umbilical vein endothelial cells (HUVEC) were harvested from human umbilical vein as described by Jaffe [275]. All procedures were carried out using aseptic techniques in a flow hood. The bulk of the cell culture was undertaken by Mr N.Tai and Dr H. Salacinski. Human umbilical cords were obtained from the labour suite of the Royal Free Hospital, Hampstead and stored in a collecting medium consisting of 40 mls 20% basic medium, 10mls foetal bovine serum (Gibco, Paisley, Scotland UK), 0.05ml Fungizone (Sigma-Aldrich, Poole, Dorset, UK) and 0.2ml Gentamycin (Sigma-Aldrich). The basic medium was obtained from a stock solution made up from 500mls M199 medium (Gibco), 15mls 7.5% sodium bicarbonate solution and 5mls penicillin/streptomycin solution consisting of penicillin 10000U/ml and streptomycin 10mg/ml (Gibco). Cords were collected within 24 hours of delivery and used if free of clamp marks or needle holes. Both ends of the umbilical vein were identified and cannulated with 4cm lengths of sterile nasogastric tubing and then secured with sterile silk ties. The cord was flushed several times with warm phosphate-buffered saline (PBS; in-house stock) to remove all clotted blood prior to instillation of 25mls of warm, filtered collagenase solution consisting of 12.5mg collagenase A (Boehringer Mannheim, Lewes, E.Sussex UK) suspended in 25mls basic medium. Both ends of the vein were clamped and the cord incubated at 37°C for 10 minutes. The cord was massaged gently prior to flushing the collagenase/cell suspension into a 50ml centrifuge tube. The collagenase was neutralised by the addition of an equal volume of complete medium obtained from stock made up of 157mls basic medium, 40mls 20% foetal bovine serum and 3.6mls, 200mM L-glutamine solution (Gibco). The cell suspension was centrifuged at 300G for 7 minutes after which the supernatant medium was removed, the cell pellet resuspended in 5mls of warmed complete medium, transferred to a $25cm^2$ tissue culture flask and incubated at 37°C/5%CO_2 . Twelve-

to-twenty-four hours later, the flasks were gently washed with 8mls PBS to remove red blood cells and fed with 5mls complete medium. The flasks were viewed daily under high power transilluminated microscopy and the presence of endothelial cells verified by confirmation of their characteristic cobblestone morphology. Once a confluent monolayer was achieved cultures were passaged onto a 75cm^2 flask by discarding the old medium, washing the cells with 8mls warm PBS and adding 3mls 10% trypsin solution (Gibco). The flask was incubated for 3 minutes prior to gentle tapping in order to loosen all the cells and the addition of 7mls complete medium. The cell suspension was spun at 300G for 7 minutes before discarding the supernatant, resuspension of the cell pellet in 8mls complete medium, pipetting into a gelatin coated 75cm^2 flask and the addition of 100μl endothelial growth supplement (Gibco). Cultures were passaged every 2-3 days at a ratio of 1:2 and fed every other day.

4.2.1.2. Cell radiolabelling with radioisotope

Cell numbers were amplified in tissue culture until the third passage. Following trypsinisation and resuspension in M199 medium, a cell count was obtained and the cells radiolabelled using a modification of the method of Sharefkin *et al* [276]. 1.8MBq of ^{111}indium chloride (Amersham International, Amersham, Bucks UK) per 10^6 cells was added to the cell suspension which was then incubated at 37°C for a period of 15 minutes. Additionally, a control centrifuge tube containing the same volume of M199 and same amount of activity was also incubated for 15 minutes. The cell suspension was washed with complete medium and centrifuged at 300g for 7 minutes. 50μl of supernatant from both control and cell-laden centrifuge tubes was taken and kept for subsequent gamma counting. The washing procedure was then twice repeated. The resultant cell pellet was resuspended in complete medium and diluted to achieve the concentrations necessary to achieve a range of seeding densities, from 2 –24 x 10 ^{5} cells /cm^2.

Percentage labelling efficiency PLE (%) was calculated as:

$$AC \ / \ (AC + AS) \times 100 \qquad [4.1]$$

where AC = activity in cell-laden supernatant and AS = activity in control supernatant.

4.2.1.3. Seeding chambers and washing protocol

The required volumes of cell suspension were pipetted onto 0.5cm^2 segments of Chronoflex CPU graft material mounted within modified cryogenic vials (2.0 ml; Nalgene, Nalge Company, Rochester, NY, USA) as described by Budd *et al* [277]. Each 'seeding chamber' (figure 4.1.) was then topped up with complete medium if the final seeding volume was less than 1ml, placed in a multiwell tissue culture plate (Berton Dickinson Labware, New Jersey, USA), and incubated for 6 hours at 37°C. Following completion of the incubation period, the seeding chambers were then placed in a gamma counter and their activity measured. Grafts were then washed i.e. culture medium was removed from the seeding chamber, 400 μl of fresh culture medium was instilled and removed, and the graft rinsed with a further 400μl of medium prior to a further addition of culture medium to the seeding chamber. Washings and seeding chambers were then gamma counted. The washing / counting process was then repeated twice, such that by the end of the procedure each graft segment was subject to three washes. The experiment was repeated four times for cell densities ranging from 2-12 x 10 ^{5} cells /cm^2 and three times for cell densities ranging from 14 - 24 x 10 ^{5} cells /cm^2 . Using a technique described by Anderson *et al* [278] the influence of initial cell seeding density upon cell attachment was determined. Graft radioactivity was attributed to the number of cells remaining adherent CA (cm^{-2}) following each wash , where:

$$CA \ (cm^{-2}) = CR \ (\%) \times CS \ (cm^{-2}) \qquad [4.2]$$

Where CS is the seeding density (cells seeded cm^{-2}) and CR is the percentage of cells remaining on the graft surface following each wash, and is calculated as

$$CR = \frac{\text{post-wash radioactivity}}{\text{pre-wash radioactivity}} \times 100 \quad [4.3]$$

The activity in the seeding chamber was corrected for spontaneous leakage of ^{111} indium by the method of Stansby *et al* [279]. In a parallel experiment HUVEC were labelled with ^{111} indium, washed and resuspended in 2mls of complete medium. Following incubation for 6 hours the suspension was spun at 300G for seven minutes and the supernatant removed. Cells were resuspended and then a gamma count was obtained of both cell suspension and supernatant. The experiment was repeated four times and a correction factor (CF) was calculated as follows:

$$CF = \frac{\text{mean counts (cell suspension)} + \text{mean counts (supernatant)}}{\text{mean counts (cell suspension)}} \quad [4.4]$$

Curves of cell seeding density and post-wash activity were plotted and analysed using a statistics software package (Prism 2.01, Graphpad Software, San Diego, CA, USA).

4.2.1.4. Control experiments

To ensure that activity from graft segments was related to attached, labelled cells and not merely graft-bound ^{111} indium, a control series consisting of seeding chambers "seeded" with 1ml acellular culture medium containing 0.9 MBq Indium activity per well (equivalent to activity from cells seeded at $10x10^5$ / cm^2 at 100% labelling efficiency) was similarly washed and counted.

In a parallel experiment, PTFE grafts (Impra Inc., Crawley, W. Sussex UK) were seeded with radiolabelled HUVECs at densities ranging from 2-8 x 10^5 cells cm^{-2} and subjected to

Opposite:

Fig. 4.1. Seeding chambers and 24 well culture plate.

Fig. 4.1.

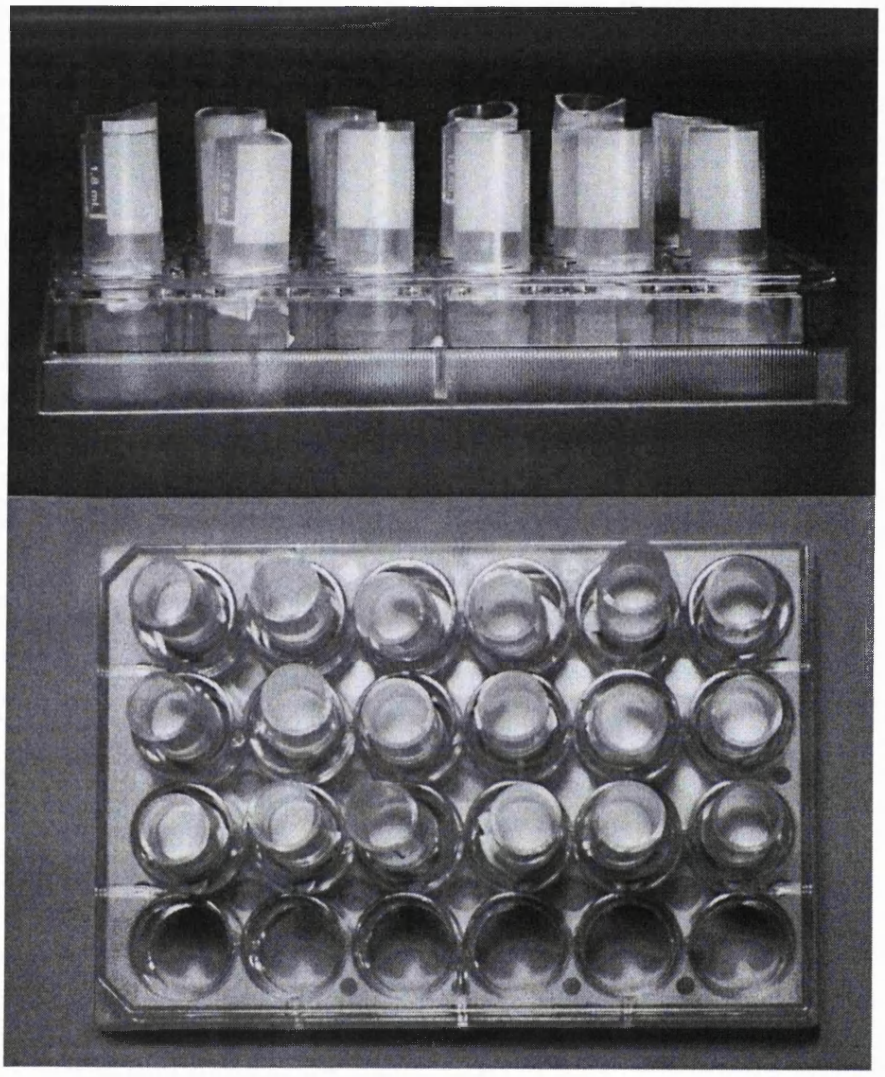

the washing and counting procedures as described for Chronoflex CPU in order to allow comparison of seeding efficiencies between the new graft and PTFE.

4.2.1.5. Scanning electron microscopy (SEM) study

In the SEM study, Chronoflex CPU segments mounted within seeding chambers were seeded with unlabelled HUVECS at densities ranging from 2-24 x 10^5 cells/cm^2. Following 6 hours of incubation, the graft segments were washed three times and prepared for SEM. Seeded graft surfaces were fixed in 1.5% glutaraldehyde, made up from 20 mls of 20% paraformaldehyde (Merck Ltd., Lutterworth, Leics., UK) added to 16 mls 25% glutaraldehyde (TAAB, Laboratories Equipment Ltd., Aldermaston, Reading, UK) and 59 mls PBS, for a minimum of 2 hours. The grafts were then washed with several changes of PBS and postfixed using 1% osmium tetroxide (Merck Ltd) and 1.5% potassium ferricyanide (Merck Ltd) for $1^1/_2$ hours. The specimens were then washed with distilled water and dehydrated in a graded acetone series 30%, 50%, 70%, 90% and 100% (high purification liquid chromatography grade 2) for 15 minutes and then allowed to air dry. The specimens were stuck onto aluminium stubs with double sided sticky tabs (TAAB) and then coated with gold using an SC500 (EMScope) sputter coater. The stubs were then examined and photographed using a Philips 501 SEM. The micrographs were examined for density of cell coverage and morphological evidence of cell adhesion.

4.2.2. Effect of incubation time on cell adhesion

HUVECs were radiolabelled with ^{111} indium chloride, counted and aliquoted at a uniform seeding density onto Chronoflex CPU segments mounted within seeding chambers as described previously. Seeding chambers, containing 1ml of complete medium laden with HUVECs at a density of 10 x 10^5 cells/cm^2, were then incubated at 37°C 95%O_2 /5%CO_2 for a variable incubation period of 30 minutes, 1, 2, 4 and 6 hours. Following incubation, the graft

segments were subjected to three washing procedures prior to gamma counting the washings and the graft segment. The experiment was repeated six times and percentage cell adhesion post-washing for each time period was calculated. A correction factor to account for cumulative loss of label at each time point was determined. Differences between incubation times of % cell adherence were sought by one way analysis of variance and localised using the Bonferroni test.

An SEM study was performed on CPU segments seeded, incubated and washed as described above. The micrographs were examined for density of cell coverage and morphological evidence of cell adhesion.

4.2.3. Effect of in vitro perfusion on cell adhesion

As described in the previous chapter, a mock circulation was used to simulate the flow, pressures and pulsatility of lower-limb arterial flow. Additionally a Nuclear Medicine Image Processing System (NMIP) was used to determine ongoing cell retention during graft perfusion. This consisted of a gamma camera (Nuclear Diagnostics Ltd, Northfleet, Kent UK) positioned beneath the perfused graft segments (figure 4.2.). Flow velocity was measured using a single channel 20 MHz pulsed Doppler velocimeter (MDV-20, Millar Instruments, Inc., USA) connected to a Doppler tipped-catheter placed inside the graft. Perfusion pressure (mean and pulse), flow rate and flow velocity were continuously monitored and adjusted accordingly by varying pump speed, reservoir level and circuit output resistance to maintain haemodynamic values consistent with arterial perfusion.

Opposite:

Fig. 4.2. Diagram of flow model.

Fig. 4.2.

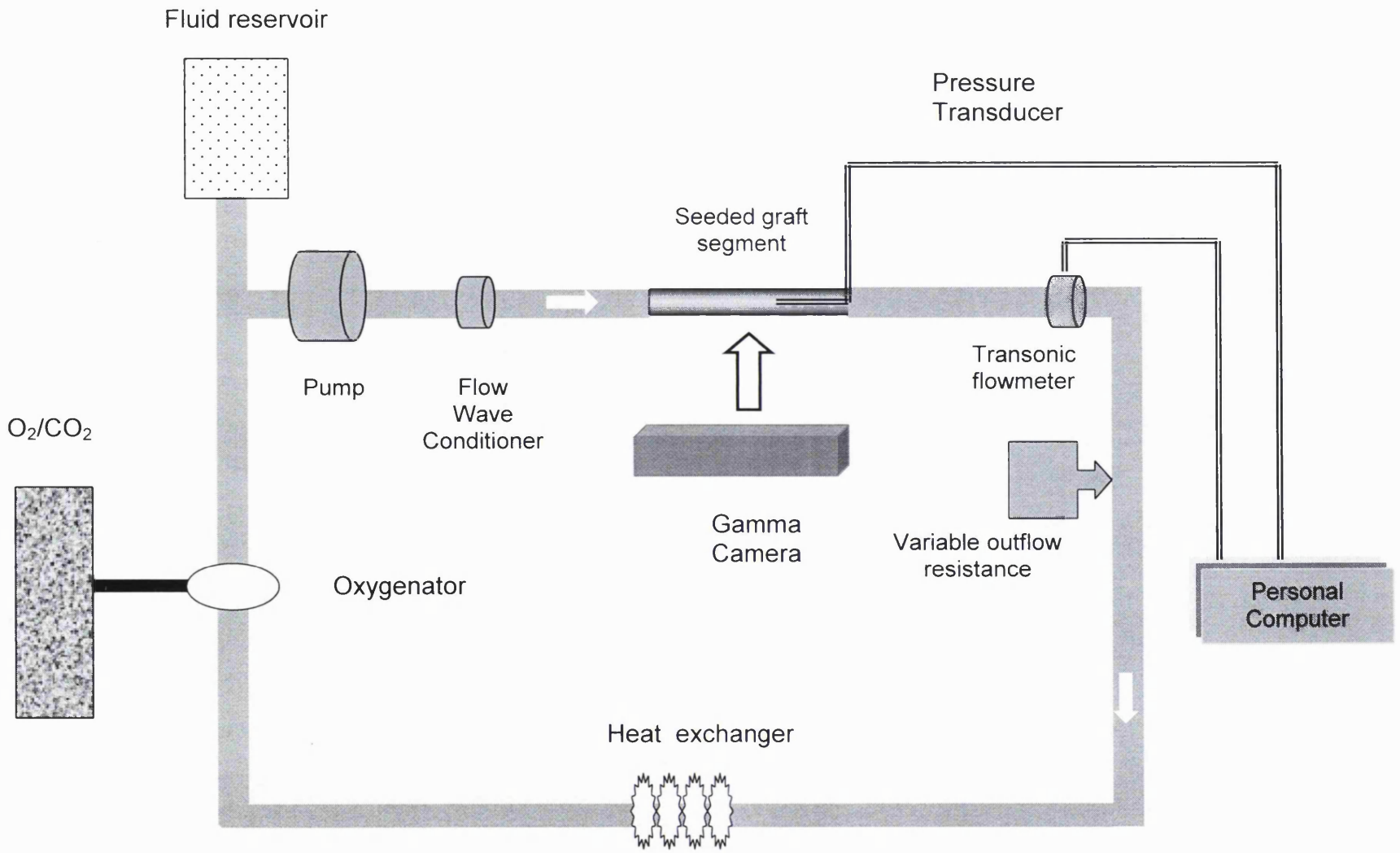
Fluid reservoir
Pressure
Transducer
Seeded graft
segment
Pump
Flow
Wave
Conditioner
Transonic
flowmeter
O_2/CO_2
Gamma
Camera
Variable outflow
resistance
Oxygenator
Personal
Computer
Heat exchanger

4.2.3.1. Calculation of shear-stress

Wall shear stress (τ, measured in Nm^{-2} = 10 dyne cm^{-2}) was calculated from the Wormersley formula for oscillating flow [280]:

$$\tau_w = \frac{\alpha}{\sqrt{2}} \mu \frac{U}{R} \qquad [4.5]$$

were: μ is fluid viscosity (kg/m/s) ; U is volumetic velocity (m/s), R is the graft radius (m) and α is the Wormersley parameter (a non dimensional parameter which characterises pulsatility).

The Wormersley parameter is calculated as

$$\alpha = R\sqrt{\frac{\omega}{\nu}} \qquad [4.6]$$

where: R is graft radius (m); ω is angular velocity (s^{-1}) and ν is kinematic viscosity . Angular velocity is derived as:

$$\omega = 2\pi f \qquad [4.7]$$

where f is the frequency (Hz) of the third harmonic of the sine-wave period of the pulsatile cycle, (i.e. $\sqrt{3}$ X frequency of sine wave). Kinematic viscosity is defined as:

$$\nu = \mu / \rho \qquad [4.8]$$

where ρ is the density in kgm^3. The density of the perfusate was $1000Kgm^3$ (similar to that of human blood at 1020 Kgm^3)

4.2.3.2. Reynolds number and inlet length

Calculated shear stress values are only valid if the flow in the region of the seeded cells is non-turbulent *i.e.* the velocity profile is parabolic. To ensure this was the case two steps were

taken. Firstly, the Reynolds number (*Re*; a dimensionless value) for the pre-determined flow and haemodynamic variables was calculated, as a Reynolds number less than 2300 is associated with laminar flow [281].

$$Re = V d \; / \; \nu \qquad [4.9]$$

where V is flow velocity and d is luminal diameter.

Secondly, the inlet length L was calculated. This is defined as the length of straight graft that allows reformation of parabolic flow after turbulence caused by the passage of perfusate across the joint between flow tubing and graft [282].

$$L = \frac{2 \rho k V r}{\mu} \qquad [4.10]$$

where k is a derived constant (0.08 for pulsatile flow [281]).

4.2.3.3. Preparation and seeding of grafts

The inlet length according to equation [17] was determined to be 5.5cm. Therefore 10cm segments of intact CPU graft were prepared, of which a 2cm portion distal to the proximal 6 cm (inlet length) was deemed the seeding zone.

HUVECs were trypsinised and radiolabelled as previously described. The chosen seeding density was informed by results obtained from the experiments described in section *4.2.1.* Cells were resuspended in complete medium (volume 1.57 mls) .and injected into the lumen of the graft seeding zone, which was isolated from the adjacent graft by means of rubber syringe plungers obtained from 1.0ml disposable syringes (Sherwood Medical, N.Ireland, UK). Grafts were then incubated at 37°C and 5%CO_2 in complete medium for the pre-determined optimum incubation period (obtained from experiments described in section *4.2.2.*) prior to removal of the syringe plungers, drainage of excess medium, mounting into the flow circuit and exposure to flow.

Initial experiments were conducted on cells seeded onto unmodified graft material. However, as was described in chapter 3, excess transmural leakage of perfusate from the graft was encountered with consequent loss of circulatory pressure. This was addressed by subjecting grafts to a pre-clotting procedure prior to seeding and perfusion such that graft interstices were filled with fibrin. The pre-clotting procedure consisted of clamping each graft distally prior to forcing 10mls of fresh blood into the graft lumen and thence through the graft wall. This was repeated twice such that by the third occasion minimal egression of blood through the walls of the graft was noted. Normal saline solution was then run into each graft lumen prior to seeding in order to remove excess clot.

4.2.3.4. Assessment of cell adherence during arterial flow

Cell adherence during graft perfusion was monitored by measuring changes in graft radioactivity with respect to time. The section of plastic tubing containing the vascular grafts was laid down on the gamma camera and dynamic scintigraphic imaging was performed using a 40 cm field of view. An on-line graphics workstation (Sun Microsystems, California USA) recorded all images within 64 by 64 matrices. Initially, images were obtained prior to initiation of flow at time 0. Following initiation of flow to 30 minutes perfusion time images were acquired every 5 minutes with acquisition every 15 minutes thereafter until the conclusion of the experiment following 6 hours of perfusion . Scintigraphic images were analysed to generate time activity curves. Cell attachment (CA) was calculated as:

$$CA = \frac{GCPM\ t_n - BCPM\ t_n}{GCPM\ t_{n=0}} \qquad [4.11]$$

Where GCPM and BCPM is activity in counts per minute over the graft and background respectively at time n ; $n=0$ is prior to exposure to flow.

Time activity curves were corrected for spontaneous leakage of indium by employing the correction factors generated for static leakage in section 4.2.1.3. Grafts were perfused over a 6 hour study period and the experiment was repeated six times. Longer periods of perfusion were associated with contamination of the perfusate and thus excluded from the study.

4.2.4. Cell viability

Vitality of HUVECs was measured using a colorimetric dye assay of the redox state of their incubating culture medium (AlamarBlue, Serotec Ltd, Kidlington, Oxford, UK). Over a 24 hour period incubation period, assessment was made of a) HUVEC seeded Chronoflex CPU graft segments, following incubation in complete medium at 5% CO_2 / 95% O_2 for 6 hours and washing b) HUVEC seeded 24 well polystyrene culture plates following incubation in complete medium at 5% CO_2 / 95% O_2 for 6 hours and washing c) sham-seeded and incubated graft segments d) sham-seeded and incubated 24 well polystyrene culture plates. All seeding was carried out at 10 x 10^5 cells/cm^2. At 4, 8, 12 and 24 hours samples of the supernatant were removed and AlamarBlue was aseptically added. Absorbance was measured in an Labsystems Multiscan MS UV visible spectrophotometer at a wavelength of 570 nm and 600nm). Additionally, cells seeded onto transparent culture wells were visually assessed under high power-microscopy in order to ensure that the positive control HUVECs appeared viable. The experiment was repeated six times with statistical differences sought by one way analysis of variance and Bonferroni post-test.

4.3. Results.

Mean ± SD radiolabelling efficiency was 45 ± 11 % (n=6). Unbound indium attached to the graft segments accounted for less than 6.2 ± 2.1% of activity attributed to attached seeded cells (n=6). A total of 86.3 x 10^6 cells were used in these experiments and because of the cell numbers required, it was not practical to restrict each experiment to cell batches arising from the culture of a single cord. Table 4.1. gives the results of the leakage experiments.

4.3.1. Influence of seeding density on cell adhesion

The adherence - pre and post washings - of HUVECs seeded at progressively higher concentrations on Chronoflex CPU is depicted graphically in figure 4.3.1. Prior to washing of graft segments, a linear relationship was observed between density of cells seeded and activity present in the seeding chambers ($Y = 4.23x - 3528$; $R^2 = 0.9896$; $P<0.0010$). With each wash the relationship became progressively less linear such that following 3 washing procedures a non-linear dose-response curve is evident (table 4.2.). Figure 4.3.2. shows that Chronoflex CPU graft segments reached a saturation density of 9.65 ± 1.2 x 10^5 cells /cm^2 for an initial seeding density of 18 x 10^5 cells /cm^2 (cell retention 53.6 ± 12.5 %) . Percentage cell retention following each wash for individual seeding densities is given in table 4.3. When PTFE and CPU graft segments were seeded with equal densities of HUVECs over the range 2 – 8 x 10^5 cells/cm^2 the pooled mean percentage of cells adherent following three washes was 9.00 ± 7.71 and 32.3 ± 11.3 respectively ($P<0.0001$). Similarly, in SEM micrographs of CPU graft segments seeded with progressively higher densities of cells and washed three times, an initial seeding density of 18 x 10^5 cells /cm^2 resulted in confluent monolayers (fig 4.4.); lower seeding densities resulted in subconfluent appearance.

Table 4.1. Leakage of 111-indium (Mean ± SD), expressed as % of initial cell-bound activity

Time (mins)	Loss (%)
30	10.9 ± 3.4
60	17.3 ± 4.9
120	19.3 ± 4.1
240	20.9 ± 5.5
360	21.9 ± 2.8

Table 4.2. R^2 values for data series depicted in figure 4.3.1.

Data Series	Regression	*R^2 Values*
Pre-Wash	Linear	0.99
Post Wash 1	Non-linear	0.99
Post wash 2	Non-linear	0.99
Post Wash 3	Non-linear	0.99

Opposite:

Fig. 4.3. **Fig. 4.3.1.)** Plot of activity (counts per minute, mean ± standard deviation) in seeding chambers against initial seeding density (cells/cm^2) before and following 1-3 washes of seeded Chronoflex CPU segments; with non-linear regression curves.

Fig. 4.3.2.) Bar chart of cells seeded versus cells adherent (mean ± standard deviation) following completion of washing procedures.

Fig. 4.3.1.

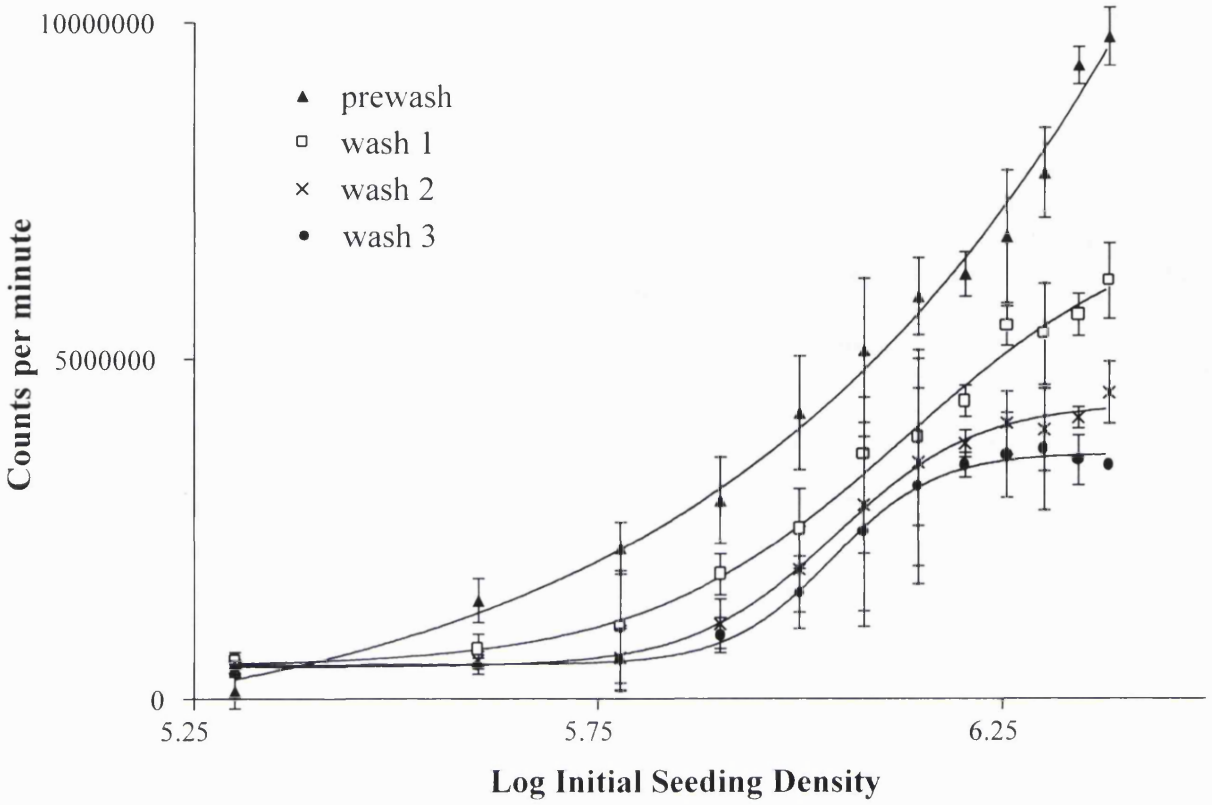

Fig. 4.3.2.

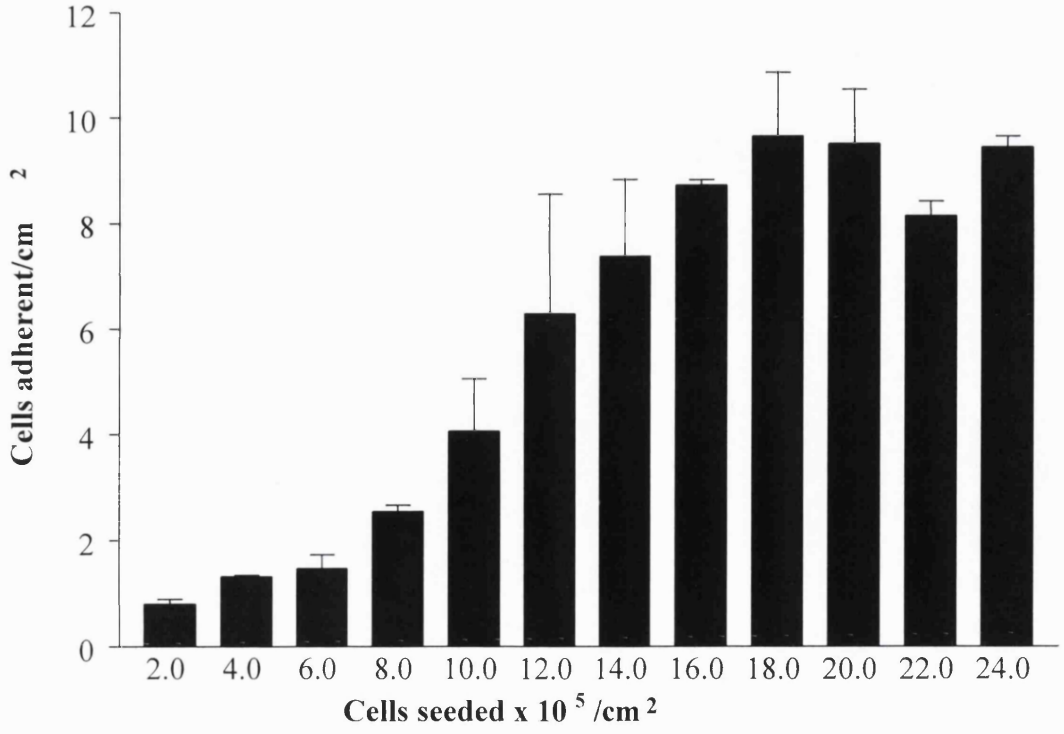

Opposite:

Fig. 4.4. Typical SEMs (Magnification x 220) of unseeded control Chronoflex CPU segment **(Fig. 4.4.1.)** and CPU seeded with HUVECs at 4 x 10^5 **(Fig. 4.4.2.)** 6 x 10^5 **(Fig. 4.4.3.)** 10 x 10^5 **(Fig. 4.4.4.)** 14 x 10^5 **(Fig. 4.4.5.)** and 18 x 10^5 cells cm^2 **(Fig. 4.4.6.)**; low-power view (x 55) at 18 x10^5 **(Fig. 4.4.7.)** and edge of seeded portion of CPU graft (x 28) at 18x 10^5 **(Fig. 4.4.8.)** .

Fig. 4.4.1.

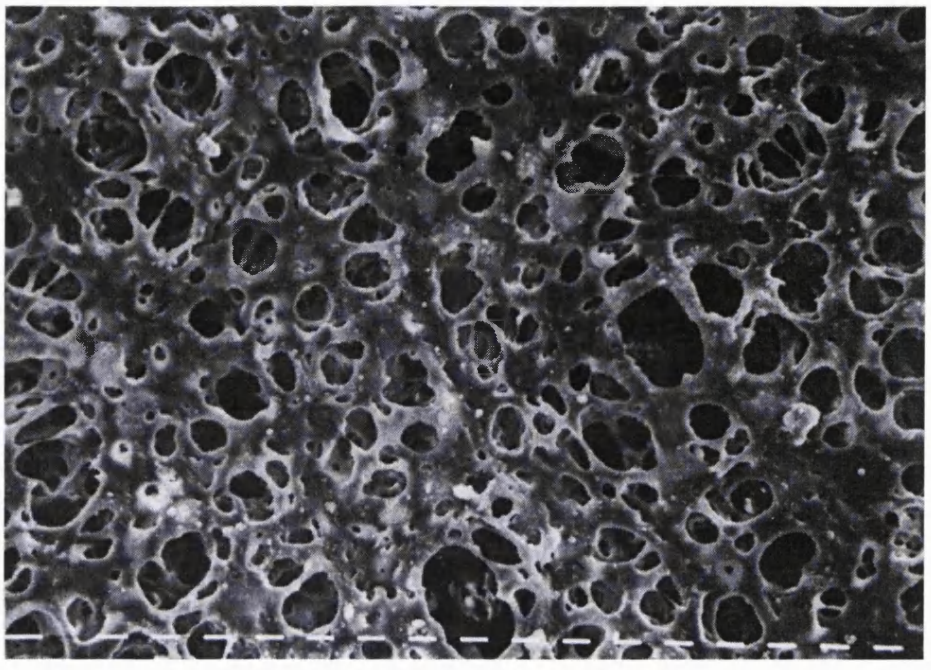

Fig. 4.4.2.

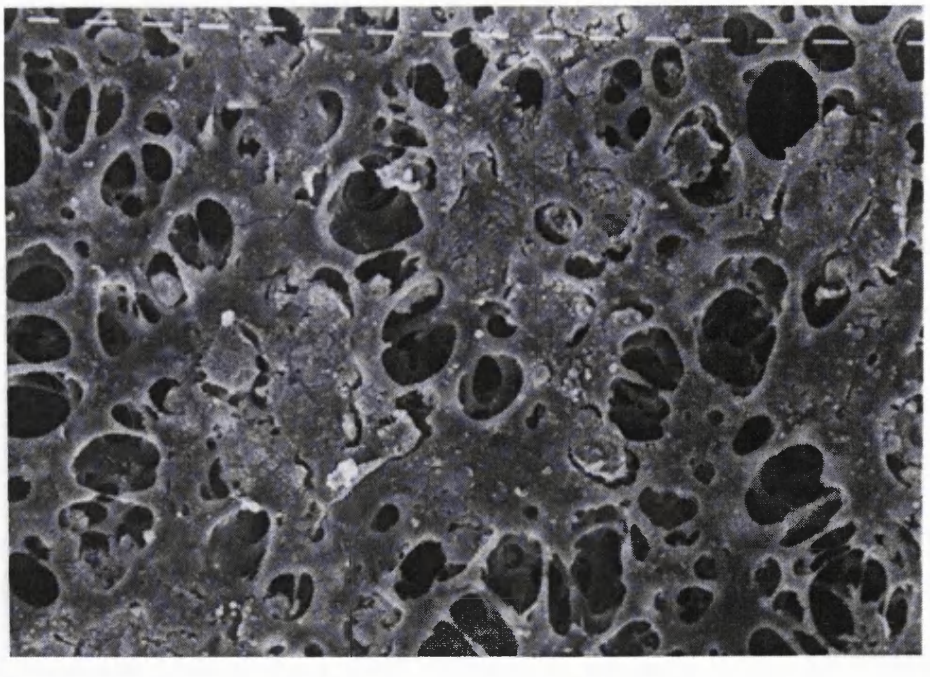

Fig. 4.4.3.

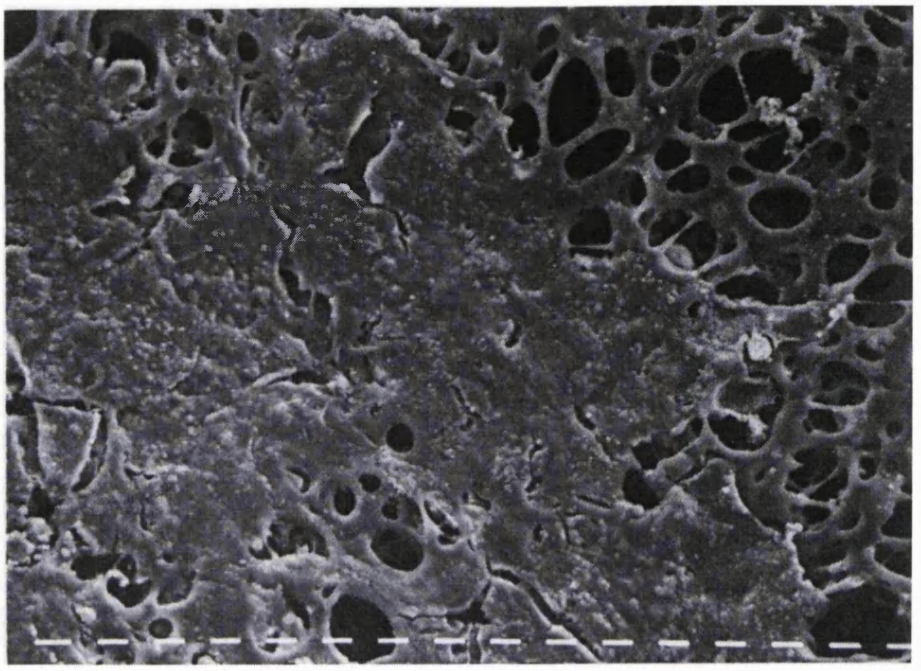

Fig. 4.4.4.

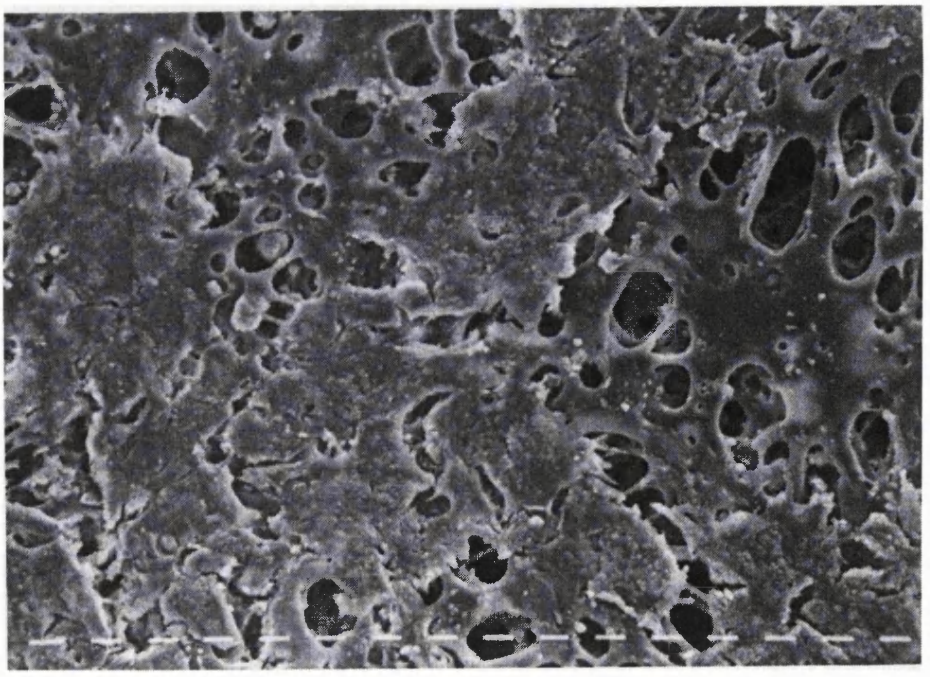

Fig. 4.4.5

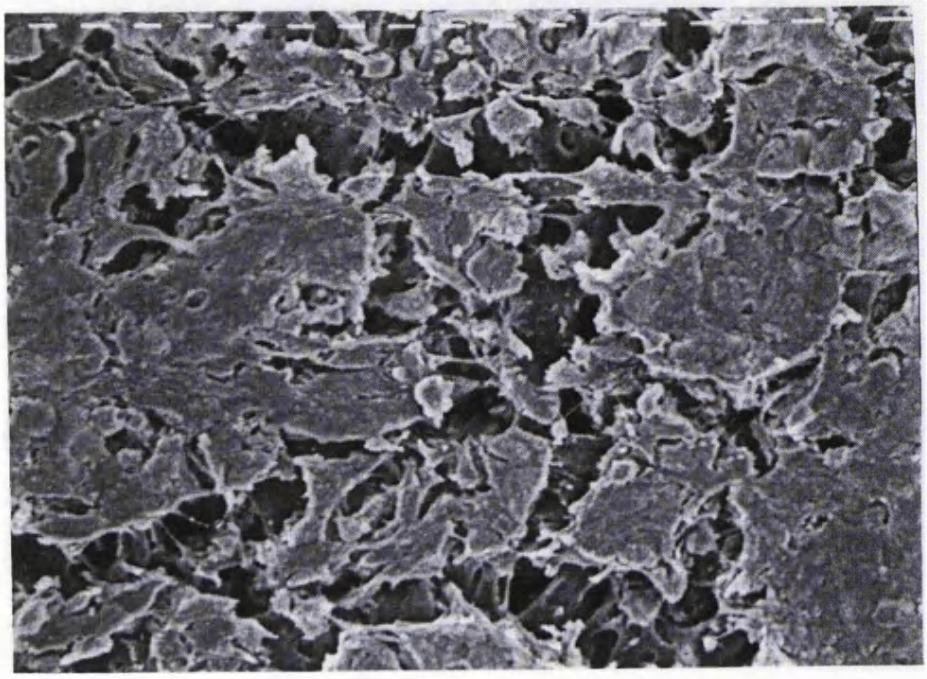

Fig 4.4.6.

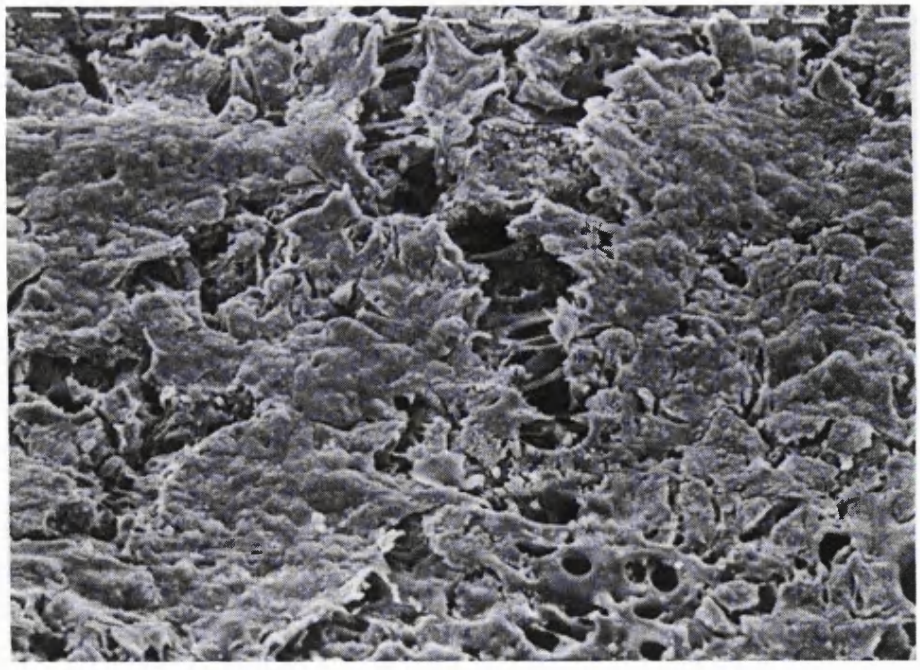

Fig. 4.4.7.

Fig. 4.4.8.

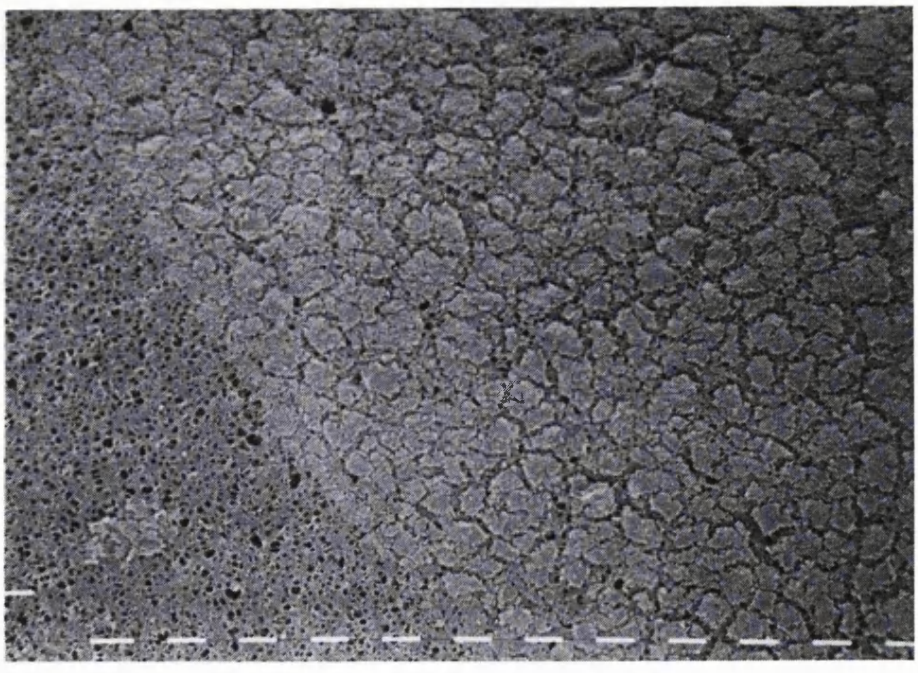

Table 4.3. Cell retention after 1, 2 and 3 washes for graft segments seeded from 2- 24 x 10^5 cells/cm^2

Initial Seeding Density	**Mean (SD) Cell retention (%)**		
(x 10^5 cells/cm^2)	post wash 1	post wash 2	post wash 3
CPU			
2	50.0 ± 10.9	41.8 ± 11.3	40.0 ± 11.6
4	49.5 ± 4.41	39.2 ± 1.7	33.0 ± 2.14
6	45.2 ± 32.1	25.7 ± 18.4	24.5 ± 17.8
8	65.5 ± 19.3	37.5 ± 8.00	31.8 ± 4.50
10	64.1 ± 31.9	49.3 ± 28.9	40.6 ± 24.3
12	74.5 ± 40.0	60.5 ± 40.9	52.4 ± 36.0
14	65.3 ± 15.8	58.7 ± 20.9	52.7 ± 19.7
16	69.9 ± 1.55	60.0 ± 1.20	54.5 ± 1.2
18	79.5 ± 14.0	60.6 ± 12.0	53.6 ± 12.5
20	66.0 ± 9.7	51.2 ± 8.13	47.5 ± 10.9
22	60.4 ± 2.4	44.5 ± 0.44	37.0 ± 3.4
24	63.0 ± 7.24	45.9 ± 3.9	39.3 ± 2.2
PTFE			
2	12.1 ± 1.8	12.1 ± 1.8	6.45 ± 1.87
4	20.9 ± 9.5	20.9 ± 10.0	14.9 ± 14.3
6	18.2 ± 4.3	18.2 ± 4.1	7.8 ± 3.5
8	19.4 ± 2.6	7.83 ± 3.48	5.08 ± 3.04

4.3.2. Effect of incubation time on cell adhesion.

Significant differences in activity (retained cells) were observed amongst Chronoflex CPU segments incubated for different periods (ANOVA $P<0.05$), with 53.6 ± 16.8 % of initially seeded cells adherent following 4 hours of incubation compared to 29.6 ± 9.43 % for 30 minutes incubation ($P<0.05$) (figure 4.5.) . There were no significant differences in adherence between grafts incubated for 4 versus 6 hours. SEM's of seeded segments (Fig 4.6) revealed adherent, flattened and abundant cells in segments incubated for longer (i.e 4-6 hours) durations. Graft material incubated for shorter periods bore either scanty numbers of cells or cells that were rounded and poorly opposed to the graft.

4.3.3. Effect of in vitro perfusion on cell adhesion

The haemodynamic parameters as calculated for this flow circuit are given in Table 4.4.

The effect of pulsatile flow on seeded grafts is shown in figure 4.7.

Opposite:

Fig. 4.5. Bar chart of activity (mean ± SD) remaining on graft segments (%) following washing procedure.

Fig. 4.5.

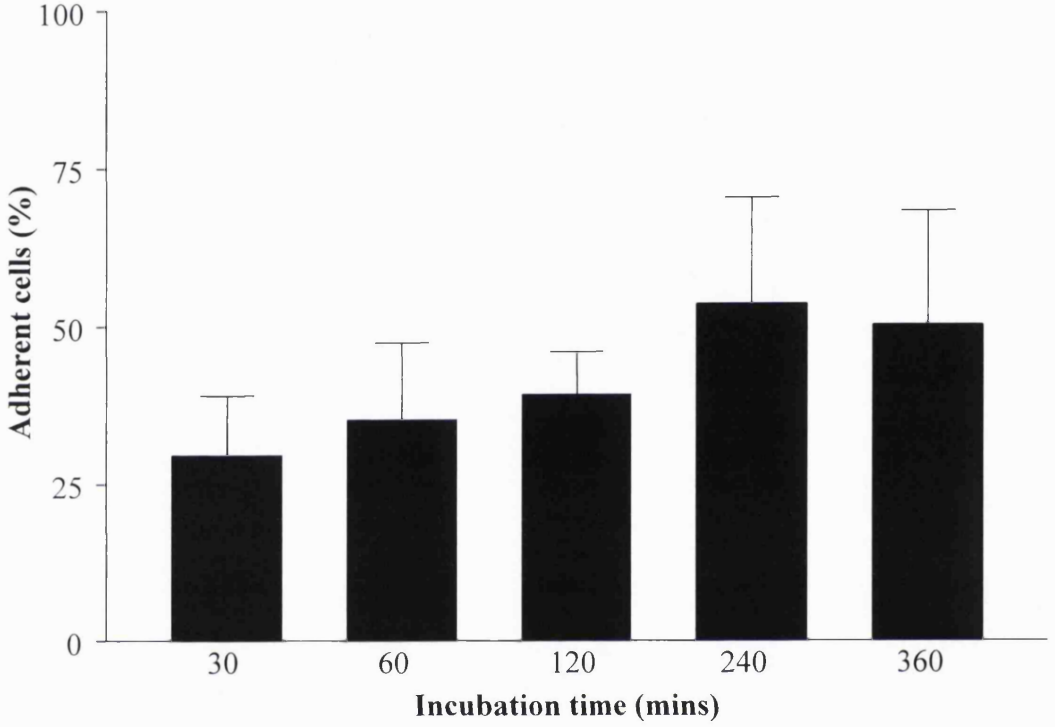
100
75
50
25
0
Adherent cells (%)
30
60
120
240
360
Incubation time (mins)

Opposite:

Fig. 4.6. Typical SEMs of graft segments (magnification x 220) incubated for 30 minutes **(Fig. 4.6.1.)** , 1 hour **(Fig. 4.6.2.)** , 2 hours **(Fig. 4.6.3.)**, 4 hours **(Fig. 4.6.4.)** and 6 hours **(Fig. 4.6.5.)**.

Fig. 4.6.1.

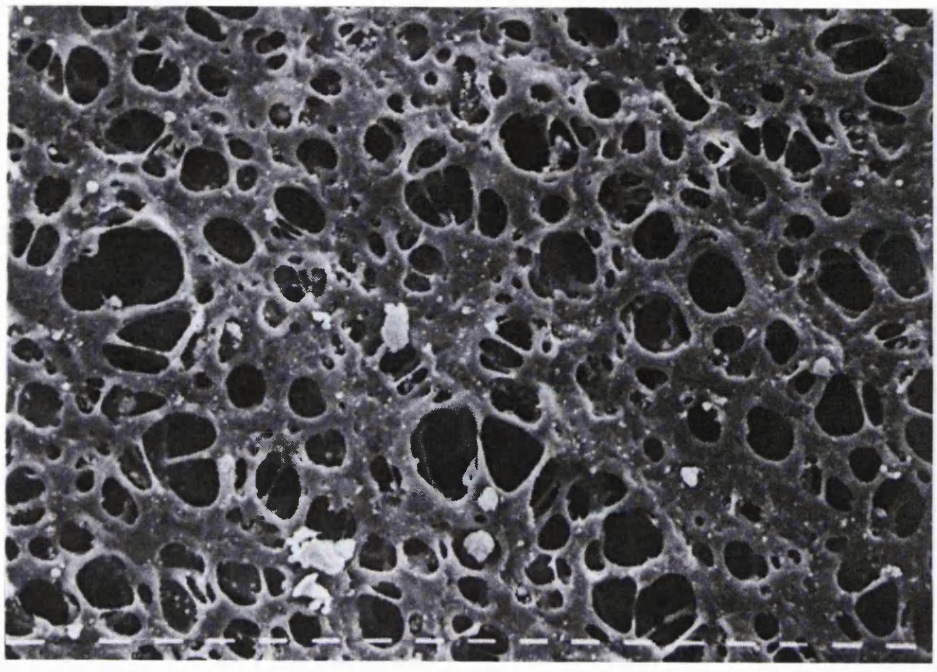

Fig. 4.6.2.

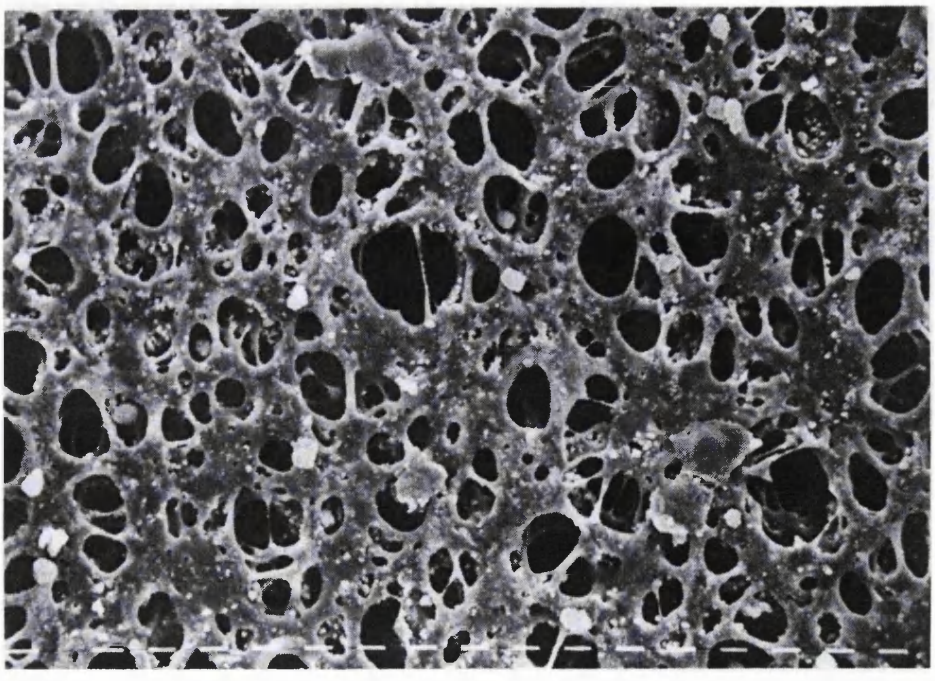

Fig 4.6.3.

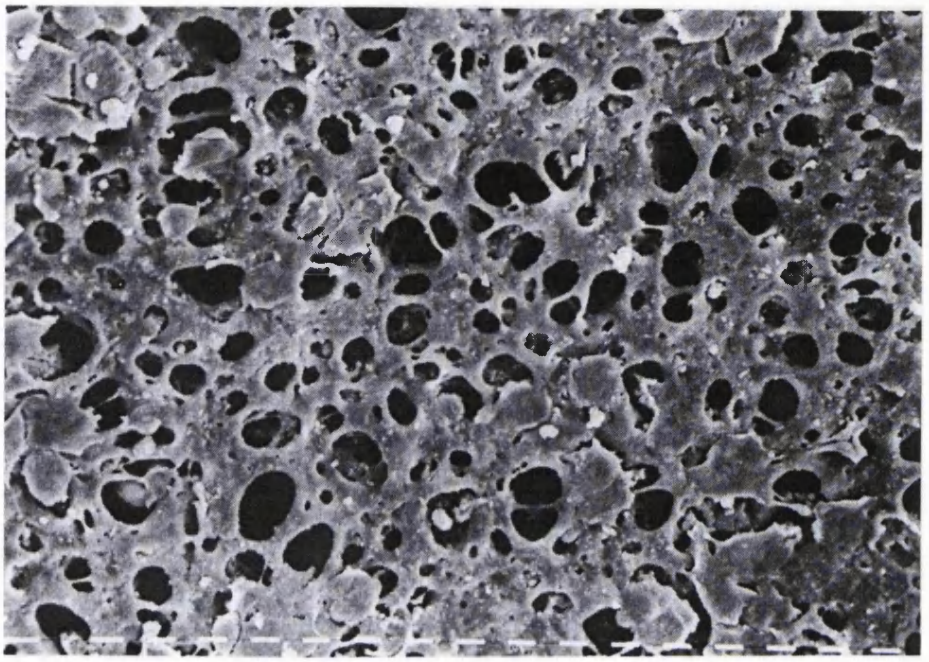

Fig 4.6.4.

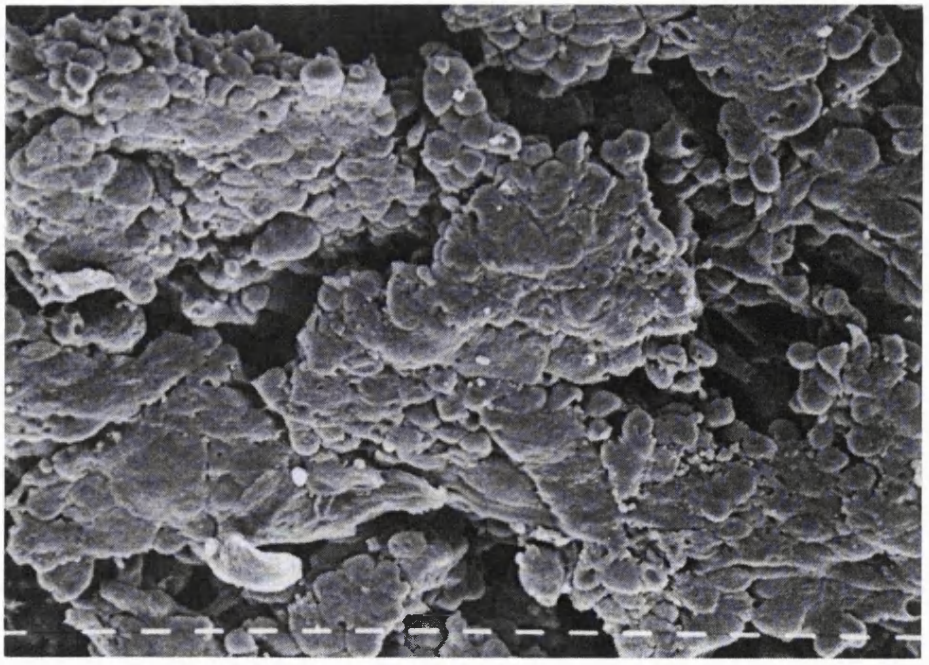

Opposite:

Fig. 4.7. Retention of endothelial cells seeded onto Chronoflex CPU grafts at optimal density and incubation period and exposed to pulsatile flow. At time zero counts were taken from the graft segments post seeding and incubation after the initial inoculating volume has been allowed to drain out. Thus at time zero all activity is attributed to adherent cells and prior to cell loss following flow is 100%.

Fig 4.6.5.

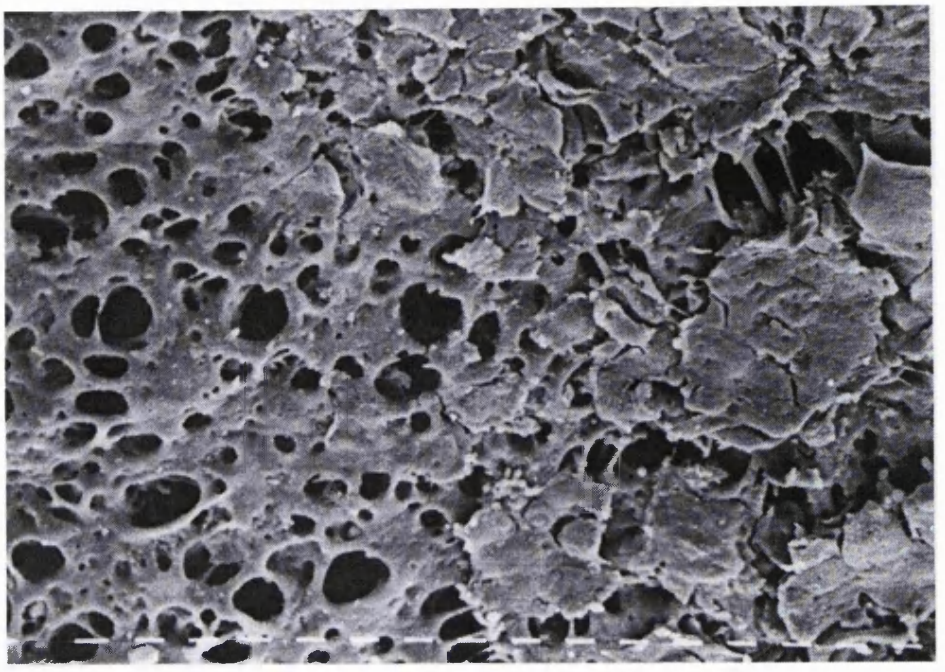

Fig 4.7.

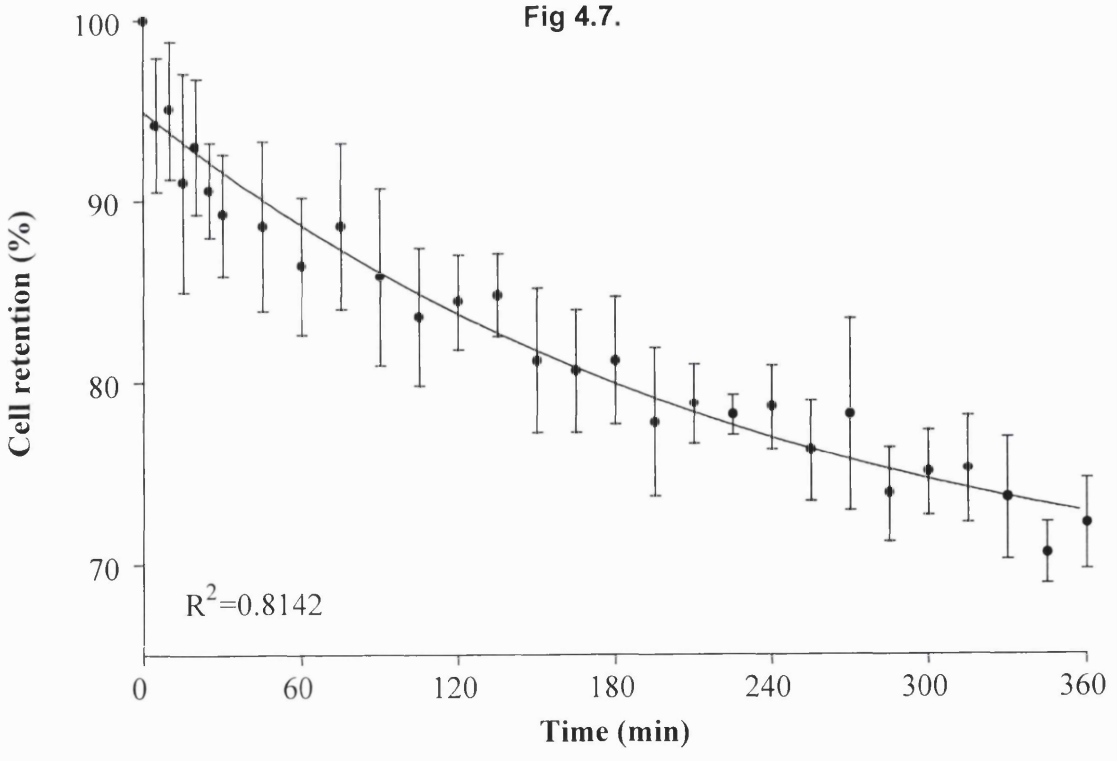

Table 4.4. Summary of flow circuit haemodynamic parameters.

Variable	Mean ± SD
Frequency of pulsatile cycle (Hz)	1
Temperature °C	37 ±1.1
Mean flow ± SD (ml/min)	209 ± 12
Pressure (mmHg)	120/90
PH	7.3 ± 0.05
PO_2(kPa)	21 ± 1
PCO_2(kPa) of solution	4.2 ± 0.3
Viscosity of solution (poise)	0.035 ± 0.2
Inlet length (cm)	5.5
Peak Reynolds number	516 ± 24
Mean shear stress (dyn/cm^2)	7.51 ± 0.3
Peak shear stress (dyn/cm^2)	24.4 ± 0.7
Wormersley parameter	2.74
Mean velocity ± SD (cm/sec)	23.5 ± 1.0

4.3.4. Cell viability

The AlamarBlue assay of cell viability (Fig 4.7.) exposed significant differences in absorbance of incubating cell media between unseeded versus seeded graft segments at 4 hours ($P<0.05$) and at 8, 12 and 24 hours ($P<0.001$); seeded wells and unseeded wells also exhibited similar differences in absorbance at 4 hours ($P<0.01$) and at 8, 12 and 24 hours ($P< 0.001$). Comparing the absorbances of seeded Chronoflex CPU segments and seeded culture wells, no statistical differences were present at 4 and 8 hours of incubation. At 12 hours the mean absorbance of effluent from CPU seeded segments and seeded culture wells was 174 ± 14.0 and 216 ± 40.6 arbitrary units (AU) respectively ($P<0.05$) and at 24 hours was 274 ± 36.2 and 214 ± 31.2 AU respectively ($P<0.01$). Quantitative analysis of the SEM photo-micrographs show seeded HUVECs to exhibit cell flattening, spreading and surface specialisations such as slender microvilli, folds and corrugations.

Opposite:

Fig. 4.8. Bar chart of absorbance (mean ± SD) for control and seeded graft segments and culture wells.

Fig 4.8.

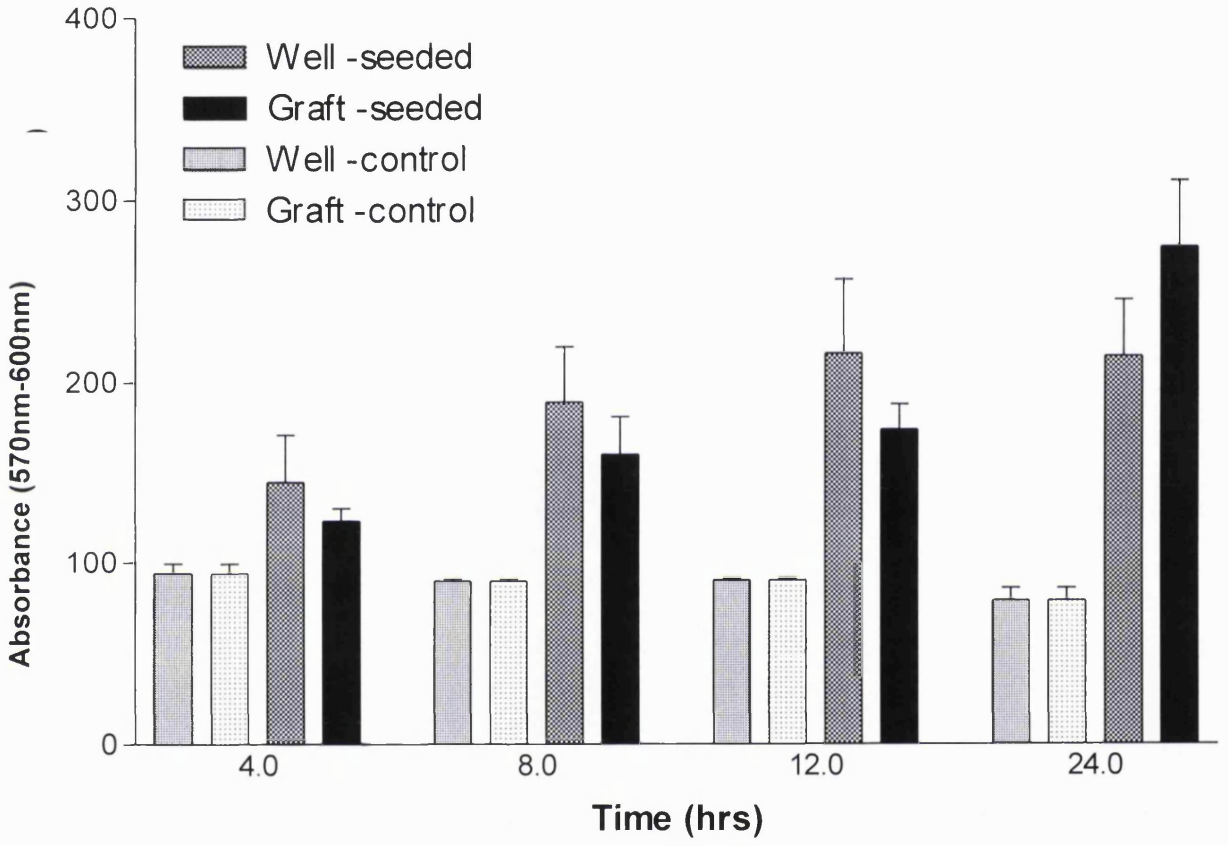
400
300
200
100
0
Absorbance (570nm-600nm)
Well -seeded
Graft -seeded
Well -control
Graft -control
4.0
8.0
12.0
24.0
Time (hrs)

4.4. Discussion

The common goal of all single-stage endothelial cell seeding techniques is to establish as many viable cells as possible on the intimal surface of a prosthetic vascular graft, within the shortest feasible time-period. Although the conditions necessary to achieve this objective in PTFE and Dacron grafts have been the subject of comprehensive investigation[194,283,284] seeded polyurethane grafts have received comparatively little attention. Furthermore, much of this limited research has been directed at two-stage [205,206,284,285] rather than single stage [287-289] seeding protocols. The purpose of this study was to advance understanding of the conditions required to achieve efficient endothelial cell seeding of this new material, to study the viability of cells once seeded onto Chronoflex CPU, and to determine the pattern of cell loss under conditions of arterial flow.

4.4.1. Seeding density

In previous comparative studies we have seeded Chronoflex CPU at densities of 1-3 x 10^5 cells / cm^2, based on data drawn from seeding studies carried out on PTFE [175,194,278]. Chronoflex CPU differs from PTFE in chemistry and structure and the aim was to independently ascertain the optimum seeding density for this graft. Segments were seeded with progressively higher amounts of cells, incubated and then washed three times in order to ensure that all poorly adherent cells were removed, and in the case of supraconfluent seeding densities, were not heaped upon each other prior to final gamma counting or SEM [194]. Both SEM and radiolabelling data revealed that seeding HUVECs on Chronoflex CPU at densities beyond 18 x 10^5 cells /cm^2 did not result in increased cell adherence, with Chronoflex CPU saturating at a seeding density of 9.65 x 10^5 cells/cm^2. This seeding density is two-to-three times higher than has been reported from similar studies conducted on PTFE. Using DNA fluorescence, indium labelling and SEMs to quantify cell attachment, Harker's group [175, 278] found PTFE to saturate at 3.6 x 10^5 cells/cm^2 whilst Kent *et al* [194], have reported saturation at

1-2 x 10^5 cells/cm^2 using a tritium-labelling protocol. However, these studies were performed on grafts coated with either fibronectin or collagen; and it was acknowledged that such coatings serve to seal graft interstices and create a flat surface for cells to attach to [278]. It is known that uncoated, porous Dacron grafts have a greater effective surface area available for cell seeding than smooth surface substitutes [62], and it is likely that the greater surface area of the porous, uncoated segments used in these experiments accounts for the disparity in saturation densities. There has been no other work carried out on the cell saturation qualities of honeycombed CPU, and it remains to be seen whether coating CPU with fibronectin, collagen or other extra-cellular matrix proteins would increase cell retention. In the present study and previous work from this laboratory, uncoated Chronoflex CPU appears to retain at least three times as many cells than uncoated PTFE when seeded at equivalent densities and exposed to a shear-related force [289] (that is, a standardised washing procedure). Modification of the seeding surface may abolish the advantageous surface architecture of the graft, reducing cell adhesion, lowering the saturation density of the graft and thus reducing the total number of endothelial cells that the graft could support. However, it is noted that maximal cell retention for Chronoflex CPU following three washes was comparatively low at 54.5 ± 1.2 % (seeded at 16 x 10^5 cells / cm^2). Augmenting the graft lumen might improve seeding efficiency such that fewer cells have to be seeded in order to achieve the same saturation density.

4.4.2. Incubation time

It was found that maximal cell attachment was observed following 4 hours incubation when 53.6 ± 16.8 % of initially deployed cells resisted three washes - twice as many cells as was the case for segments incubated for the shortest time period under study. Thus, duration of incubation influences the resistance of CPU seeded cells to subsequent shear, as has been described for cells seeded upon glass slides [290], PTFE [194,277,278,289,290-292] and Dacron [278,291,292] grafts. Cells require time to come into proximity with the graft surface, and thence

for the initiation of receptor-dependent cytoskeletal change and cell spreading to take place [290] . There is a lack of consensus about the optimum length of time to allow these attachment processes to occur, with various investigators concluding that maximal cell retention occurs with 15 [278], 45 [290], 60 [277], or 90 [194] minutes of seeding. In a finding analogous to the SEM evidence presented in this study, Curti and colleagues observed the ultrastructural morphology of PTFE seeded cells to be spread, smooth and flattened by four hours incubation [292] but concluded that optimal seeding conditions will vary substantially according to graft type and treatment. Indeed, Suguwara *et al* demonstrated that the incubation periods for maximal cell retention in Dacron and ePTFE grafts were substantially different at 8 and 24 hours respectively [293].

There have been comparatively few studies on what constitutes the optimum incubation period for endothelial cell seeded CPU grafts. In our initial studies on a first-generation poly(ether) polyurethane [289] , it was determined that maximal cell retention occurred with an incubation time of 60 minutes; and thus this incubation period was utilised in a subsequent study concerning cell loss from seeded grafts made from Chronoflex CPU and PTFE exposed to pulsatile flow. However, in the original investigation the longest incubation period studied was 90 minutes and no data was available on the effect of longer incubation periods. Ballerman and colleagues used an incubation period of 4 hours for cell-seeded spun PU grafts prior to exposure to pre-conditioning, sub-arterial flow but had not experimentally validated this time as the best one [205,206] .

Unfortunately, it may not be possible to integrate a four-hour incubation period into a single-stage protocol. This is because, once the additional time necessary for procurement, extraction, purification and deployment of the endothelial cells is considered, such a long incubation period unjustifiably lengthens the time required to perform a revascularisation/seeding procedure. However, modification of the luminal surface can shorten the time to maximal adherence. Lin *et al* have developed a method for covalently

bonding the arginine-glycine-D-aspartate (RGD) cell binding residue to carboxylated polyurethanes, and have found the numbers of cells bound to RGD treated polyurethane-coated slides following a 4 hour incubation period to increase five-to-ten fold [288] . It remains to be seen if comparable results can be produced by similar treatments of CPU grafts made from Chronoflex.

4.4.3. Effect of pulsatile flow

The seeding chamber method, a standard technique in endothelial cell seeding experiments [277,293,294] is practical and facilitates the simultaneous assessment of multiple seeded graft segments. The method readily allows the efficient investigation of determinants of cell adhesion such as seeding density and incubation time, but the shear stresses generated by the washing procedure and experienced by the EC have never been quantified and are likely to be different from the stresses caused by pulsatile flow in arteries or on intact vascular grafts.

Therefore, it was important to test the seeding parameters defined as optimal (according to the seeding chamber experiments) under dynamic flow conditions. Thus, the effect of pulsatile flow on grafts seeded at 16×10^5 cells / cm^2 and incubated for 4 hours was studied. Allowing for leakage of isotope from the HUVECs, 72.2 ± 2.5 % of initially adherent cells were still adherent to the graft at the end of the perfusion period. This data closely matches that from the previous study of fibronectin-coated CPU seeded at 2.5×10^5 cells / cm^2 when, following 6 hours of perfusion cell retention was 73 ± 8% [246] . However, although a non-linear single phase exponential decay curve could be fitted to the data points ($R^2 = 0.81$), a plateau was not reached during the 6 hour perfusion period and longer periods of perfusion will be required to determine at what point cell loss effectively ceases. In this study longer periods of perfusion were associated with microbial

colonisation despite an antibiotic-charged perfusate; microbial filters were also tried but found to lower the flow-rate of the circuit to an unacceptable degree.

The flow circuit itself was specifically designed to accurately simulate the conditions of perfusion found in the human peripheral arterial circulation. Many previously described flow systems have been deficient in this respect: producing sub-arterial shear stress [175,195,278,295,296] with flat, non-tubular graft segments[175,195,278,295,296] for inadequate periods with insufficiently viscous fluids such as haemacel [295], tissue culture medium [175,194,297] and M199 [296]. Arterial shear stress varies from 2-20 dynes/cm^2 in linear segments of the arterial tree to 30-100 dynes/cm^2 in the region of flow dividers and sharp angulations. Peak shear stress in this circuit was calculated at 24.4± 0.7 dynes/cm^2 i.e. within the physiological range and well below the critical Yield stress of 400 dynes/cm^2 (identified by Fry as the threshold stress above which morphological signs of injury become apparent in endothelial cells [280]). Laminar flow was assured by ensuring that haemodynamic variables resulted in a Reynolds number less than 2300 (i.e. 516 ± 24) and by siting the seeded cells more than 5.5cm (the inlet length) downstream from disturbances in flow caused by the join between graft and circuit tubing.

It should be noted that the flow circuit used in these experiments differed in an important respect from that used in the experiments described in chapter 3. In order to maximise cell viability over the time course of the study, it was decided to incorporate a hollow-fibre oxygenator, placed in series with the flow circuit, facilitating efficient oxygenation of the perfusate. When initial trials were conducted with this apparatus in the chapter 3 studies, it proved impossible to maintain a uniform pulse pressure across the range of pressures necessary to allow full characterisation of the grafts' compliance properties. This was presumuably due to the additional resistance to flow that the oxygenator generated. Consequently the hollow-fibre oxygenator was not used and gases were simply bubbled through the fluid reservoir at a rate sufficient to give adequate oxygenation and

carbonation. In the latter seeding experiments, the mean circulatory pressure was not varied and thus the restrictions preventing use of the oxygenator did not apply.

Unfortunately, it was not possible to test seeded grafts without pre-clotting them first. The porosity of the grafts allowed excess transmural leakage of circulatory fluid with subsequent loss of perfusion pressure, thereby making maintenance of the desired range of haemodynamic conditions for the duration of the experiment impossible. Consequently it was decided to test grafts, which had been preclotted and were thus leak proof. Therefore, a limitation of these results is that they reflect the adherence of cells to Chronoflex CPU whose luminal surface has been modified.

4.4.4. Viability of seeded cells

To determine if CPU was toxic to HUVECs, a colorimetric dye analysis of the culture medium of cells seeded and incubated on Chronoflex CPU graft segments was undertaken. The AlamarBlue assay reflects the redox potential of the cells under study, as its constituent resazurin is reduced by functional cell membranes to resarufin with attendant change in colour from blue to pink [298]. The assay is a variant of the long-established resazurin reduction test, which has been used for 50 years to assess milk for yeast and bacterial contamination [324,325]. Over the past 10 years the test has gained in popularity in assessing mammalian cell viability, and has been used to measure the viability of endothelial cells seeded on polyurethane materials [299],and to assess the proliferation of lymphocytes [326], *S.Aureus* [327], fibroblasts [328], and nerve cells [329]. The test has been quantified against other well-characterised viability/proliferation assays such as ^{3}H-thymidine incorporation and MTT (3-(4,5-dimethylthiazol-2-yl)-2,5-diphenyl tetrazolium bromide spectroscopy [326,328,330]. Unlike such assays, the alamar Blue assay has been found to be simple to use, cost-effective, does not involve the use of radioisotopes, does not require extraction techniques, does not result in

termination of cell culture, and does not react chemically with polyurethane [299]. As such, it was chosen as the priniciple means of quantifying EC viability in these experiments.

Using this assay it was noted that at 4 and 8 hours post-seeding and washing there was a trend toward greater bioreduction in the culture-well seeded cells compared to the Chronoflex CPU seeded cells, with a significant difference at 12 hours. However, at 24 hours the trend had reversed, with seeded CPU segments exhibiting significantly greater bioreduction activity than seeded culture wells. Thus the initial metabolic/reproductive activity in cells seeded onto CPU lags behind that of control cells, although by 24 hours the CPU cultures have superseded the polystyrene cultures, reversing the temporary deficit. SEM micrographs of seeded endothelial cells demonstrated morphological normality.

In conclusion, it was found that uncoated CPU grafts made of honeycombed Chronoflex saturate at 9.65×10^5 cells / cm^2 and for maximal cell retention should be seeded at 16-18 x 10^5 cells/ cm^2 and incubated for 4 hours. Over 70% of the initially adherent cells seeded under these conditions onto pre-clotted Chronoflex CPU grafts remain attached following exposure to arterial flow and shear stress. Chronoflex itself does not appear to have any sustained effect on endothelial cell viability, and grafts made from this material appear to hold considerable promise for single stage seeding applications. Augmentation with endothelial matrix proteins may be required to enhance cell retention and reduce the optimum incubation period.

Chapter 5.

An *in vitro* assessment of the resistance of the Chonoflex CPU graft to degradative oxidative and hydrolytic stress

5.1. Introduction

It is of prime importance that a vascular prosthesis be biostable; that is, resistant to excessive structural deterioration during the lifespan of the recipient patient. Grafts which are insufficiently durable may become aneurysmal - as has been reported with glutaraldehyde-treated umbilical vein grafts [49] - thereby necessitating replacement in order to avoid catastrophic failure. Grafts made from ePTFE or Dacron (both of which are highly ordered, bio-resistant crystalline materials) retain their mechanical strength *in vivo* [47,255], although progressive knot slippage [46] and slow hydrolysis of susceptible ester-linkages [255] occurring over decades may lead to subtle change in the stability of Dacron. The biostability of ePTFE and Dacron is an important reason for the pre-eminence of such grafts in arterial reconstruction, despite the fact that their compliance is poor, thrombogenic potential high and healing response inadequate.

Vascular grafts made from polyurethane exhibit enhanced compliance but are biodegradable if the polymeric structure contains a high proportion of ester or ether-linkages [224,226,227]; and *in vivo* chemical or structural deterioration has been reported in poly(ether) grafts such as those made from Biomer [219] and Mitrathane [235] , and in poly(ester-carbonate) conduits such as the Vascugraft [238] prostheses. This has led to the development of polyurethanes that have been strategically modified in order to reduce susceptibility to biodegradation. Chronoflex AR/LT is a polyurethane where the soft segment domain is dominated by carbonate groups (Figure 5.1) and thus the proportion of ether linkages is substantially lower than is the case with poly(ether) polyurethanes [241]. In an initial study, Chronoflex CPU grafts survived 250 days of *in vitro* exposure to an oxidising system, whereas the same system resulted in catastrophic failure in poly(ether) urethane control grafts. Additionally, no changes in graft tensile strength or chemical composition were observed following 20 months *in vivo* implantation [245]. Similar durability has been reported in grafts made from Corethane, which also utilises a high proportion of carbonate linkages to impart bioresistance [300].

Opposite:

Fig. 5.1. Chemical structure of Chronoflex.

Opposite:

Fig. 5.1. Chemical structure of Chronoflex.

Figure 5.1.

Structure Of ChronoFlex AR/LT GP

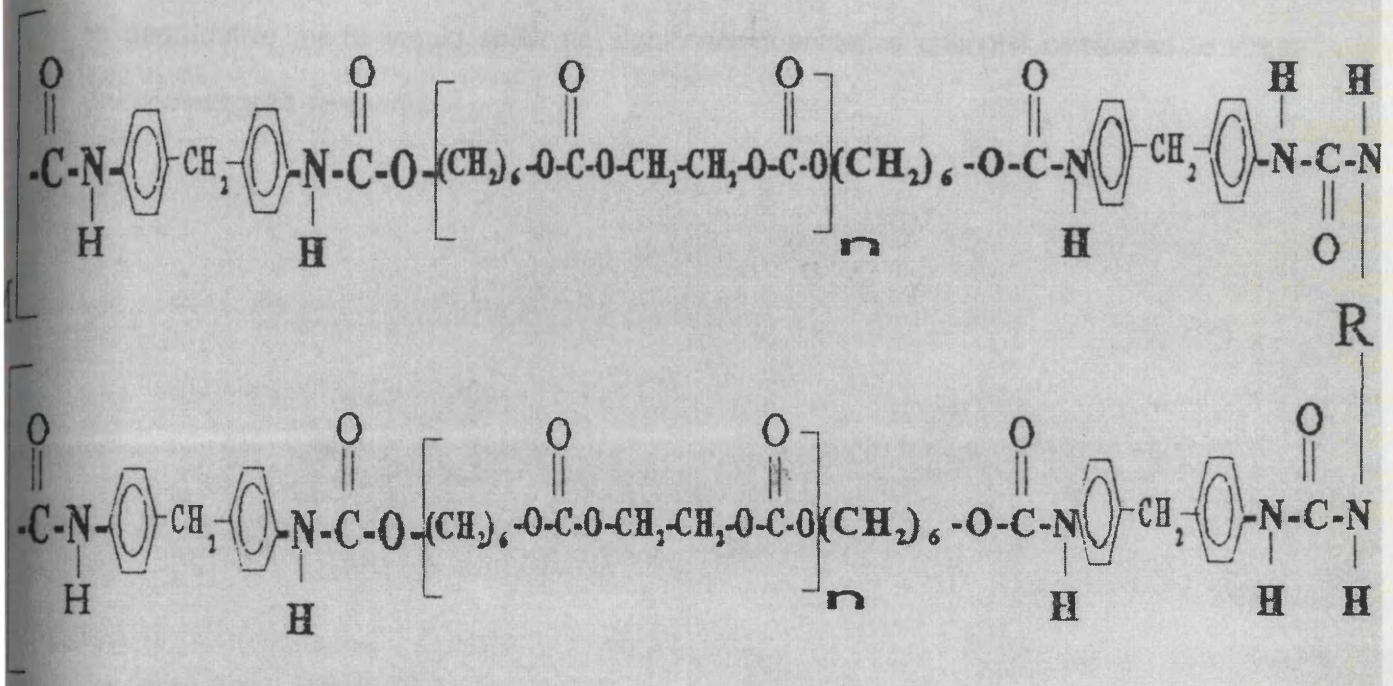

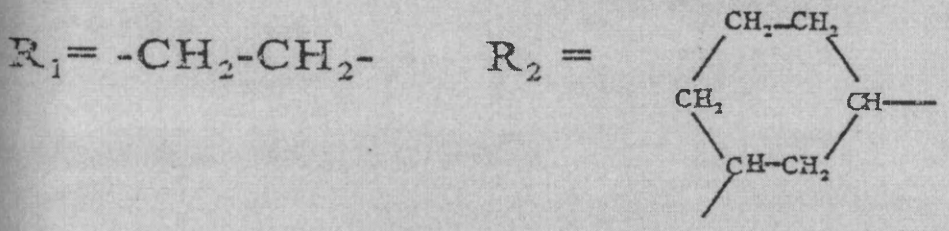

Where R may be either R_1 = Ethylene Diamine
or R_2 = 1,3 Diamino-Cyclohexane

In this chapter the experimental aim was to confirm the ability of Chronoflex CPU grafts to resist degradative forces by assessing the effect of several different solutions on the polymer with outcome measured in terms of graft appearance on scanning electron microscopy and compliance characteristics. It was hypothesised that Chronoflex CPU graft segments exposed to degradative media would show no significant quantitative changes compared to virgin, unexposed graft segments.

5.2. Methods and materials

5.2.1. Graft materials.

Poly(carbonate) and poly(ether) urethanes were supplied by Cardiotech International Inc, Wrexham, UK.

5.2.2. Ageing of graft specimens.

The polymers' susceptibility to chemical degradation was investigated by incubating graft specimens in a variety of chemically aggressive solutions [301] at 37°C. Samples were also incubated in distilled water under the same conditions to act as a negative control.

5.2.2.1. Plasma protein fractions.

The procedure for plasma fractionation with polyethylene glycol (PEG) was adapted from the method described by Hao *et al* [301]. A beaker containing 100ml citrated human plasma (derived from fresh frozen plasma obtained from the Blood Transfusion Department, Royal Free Hospital) was placed in a cold room. PEG (Mw 3350 Sigma-Ultra grade, Sigma Chemical Co. Ltd., Poole, Dorset, UK) was added slowly to plasma in the amount of 10g/100 ml. After 60 min stirring, the 10% PEG precipitate, designated fraction I, was removed by centrifuging the solution for 30 min at 2000 rpm. An additional 10g of PEG was then added to the supernatant followed by centrifugation to obtain fraction II (the 10-20% PEG precipitate). This process was then repeated to obtain a third precipitate and plasma fraction. The precipitates were reconstituted to the original volume of plasma (100 ml) with phosphate-buffered saline (PBS). Hao has approximated the distribution of plasma proteins throughout the fractions (table 5.1.). Specimens were immersed in plasma protein fraction solutions at 37°C for 70 days on a shaker platform; and solutions were changed once weekly. At the completion of the experiment, the polymer specimens were rinsed in distilled water, dried in air, and stored prior to assessment.

5.2.2.2. Effect of lysosomal enzymes.

Solutions of cholesterol esterase (CE) were prepared by dissolving CE powder (Sigma Chemical, 0.05 M phosphate buffered solution at pH 7.0, 1U ml^{-1}), which was then sterile filtered using a 0.22 μm filter [226]. Solutions of phospholipase A_2 (PLA) (porcine pancreatic PLA, Sigma Chemical Co) were prepared in buffer solution (50 mM Tris, pH 8.0 containing 6.8 mM $CaCl_2$) at a concentration of 0.18 U ml^{-1} (where 1 U is defined as the hydrolysis of 1 μM min^{-1} phosphatidylcholine at pH 8.0 at 37°C) [302]. Solutions were replaced on a weekly basis. Specimens were immersed in PLA/ CE solutions at 37°C for a total of 70 days in a shaker platform prior to rinsing, drying and storage.

5.2.2.3. Effect of chemical oxidation and peroxidation.

As described by Zhao [300] and Meijs [303] suitable oxidising systems can be made by combining hydrogen peroxide (Fluka Chemicals, Buchs, Germany,) cobalt chloride (Sigma) and t-butyl peroxide (Sigma). Therefore, solutions were made up of (i) 1.63 M H_2O_2 and 0.10 M $CoCl_2 \cdot 6H_2O$. ($H_2O_2/CoCl_2$) to induce formation of hydroxyl radicals, (ii) 1.63 M terminal - butyl hydroperoxide and 0.10 M $CoCl_2 \cdot 6H_2O$ (t-but/$CoCl_2$) to induce peroxidation i.e. generation of alkyl and hydroxyl radicals (iii) 1.63 M t-butyl hydroperoxide, 0.10 M $CoCl_2 \cdot 6H_2O$ and 0.10 M glutathione, (Glut/t-but/$CoCl_2$) in order to induce thiyl radicals. Solutions were replaced once a week. At the end of the 70 day treatment period, samples were washed and dried in air, ready for assessment.

5.2.3. Assessment of materials

5.2.3.1. Scanning electron microscopy (SEM)

SEM examination was performed by Robert Carson (Cardiotech) at the EM unit, Department of Biological Sciences, The University of Manchester Medical School, using a Cambridge Stereoscan 360 SEM. The micrographs were examined for features indicating ESC such as fissuring, interlocking cracking and crazing of the graft material.

5.2.3.2. Compliance measurements

The flow circuit (as described in Chapter 3) was utilised to measure the compliance of graft segments, although unlike previously the perfusate was not oxygenated because biological tissues were not utilised. Additionally, each graft segment was subject to the usual preclotting procedure (as described in chapter 3) . Measurements of graft wall motion were made using the Walltracking ultrasound system, using a constant pulse pressure (60 mmHg) at two mean pressures – 50 and 100 mmHg. For each mean pressure and graft segment, three measurements of wall movement were made, and the experiment was repeated six times. At both mean pressures, the compliance (C) values were calculated according to equation [1.3]. The β stiffness index was not calculated, as the utility of this index in *in vitro* studies - where comparisons of elasticity are made at the same blood pressure - is limited (as was discussed in chapter 3). Statistically significant differences in the compliance values of grafts incubated in different media were sought by ANOVA and localised using the Bonferroni test.

Table 5.1. Majority distribution of selected plasma proteins (Reference 301)

Fraction	Plasma Proteins
I	IgG, Fibrinogen, C-3 component, Plasminogen, B-lipoprotein
II	IgA, alpha-2-macroglobulin, prothrombin, haptoglobin
III	Albumin, alpha-1-acid glycoprotein, C1 esterase inhibitor, alpha lipoprotein

5.3. Results

Typical SEMs of the graft segments are provided in figure 5.2. Environmental surface cracking (ESC) was visible on all poly (ether) grafts treated with plasma fractions I-III, t-but/$CoCl_2$ and Glut/t-but/$CoCl_2$. ESC was visible on the Chronoflex CPU graft segments exposed to t-but/$CoCl_2$ (table 5.2.).

The results of compliance measurements made on the grafts are depicted in figures 5.3 and 5.4. It was not possible to mount all segments because some grafts did not survive the pre-clotting procedure prior to perfusion *i.e.* the pressure necessary to force fresh blood through the graft interstices resulted in rupture of the segment. This phenomenon occurred exclusively in segments treated with media noted to cause ESC on SEM examination.

Overall, there were significant differences in the compliance values obtained for Chronoflex CPU grafts incubated in different media ($P<0.0001$ for measurements made at both mean pressures). Chronoflex CPU grafts treated with the glutathione/t-butyl peroxide/cobalt chloride mixture exhibited significantly greater compliance than grafts incubated in distilled water (i.e. 15.0 ± 7.44 vs $7.97 \pm 2.01\%$ $mmHg^{-1} \times 10^{-2}$, $P< 0.05$ at 50mmHg and 28.0 ± 8.1 vs 6.89 ± 2.14 % $mmHg^{-1} \times 10^{-2}$, $P <0.001$ at 100mmHg). Other media had no significant effects on graft compliance although measurements were not possible in grafts exposed to t-butyl peroxide /$CoCl_2$.

Poly(ether) grafts exposed to plasma fractions I-IV, Glutathione/ t-butyl peroxide /$CoCl_2$ and t-butyl peroxide/$CoCl_2$ did not survive the preclotting process intact. There were significant differences in compliance amongst the remaining grafts ($P<0.0001$ for both mean pressures). Grafts exposed to the t-butyl peroxide/$CoCl_2$ mixture had significantly greater compliance than water incubated controls (9.84 ± 2.13 vs 5.66 ± 0.85, $P<0.001$ at 50 mmHg and 8.58 ± 0.77 vs 4.36 ± 1.11, $P<0.001$ at 100 mmHg). Other media had no significant effects on graft compliance.

Opposite:

Fig. 5.2. SEMs of poly(ether) grafts (Mag x 250) outer surface. **Fig. 5.2.1)** normal porous structure; **Figs. 5.2.2 and 5.2.3.)** Typical features of environmental surface cracking of specimen after 70 days incubation in plasma fraction II. Note pitting and scoring of surface with coalescence of pores to form irregular cracks. **Fig 5.2.4.** Equivalent view of post-incubation Chronoflex CPU graft . **Fig 5.2.5.** and **5.2.6.** Comparison of Chronoflex CPU graft and poly(ether) grafts after incubation in glutathione/t-butyl peroxide/cobolt chloride.

Opposite:

Fig. 5.2. SEMs of poly(ether) grafts (Mag x 250) outer surface. **Fig. 5.2.1)** normal porous structure; **Figs. 5.2.2 and 5.2.3.)** Typical features of environmental surface cracking of specimen after 70 days incubation in plasma fraction II. Note pitting and scoring of surface with coalescence of pores to form irregular cracks. **Fig 5.2.4.** Equivalent view of post-incubation Chronoflex CPU graft . **Fig 5.2.5.** and **5.2.6.** Comparison of Chronoflex CPU graft and poly(ether) grafts after incubation in glutathione/t-butyl peroxide/cobolt chloride.

Fig. 5.2.1

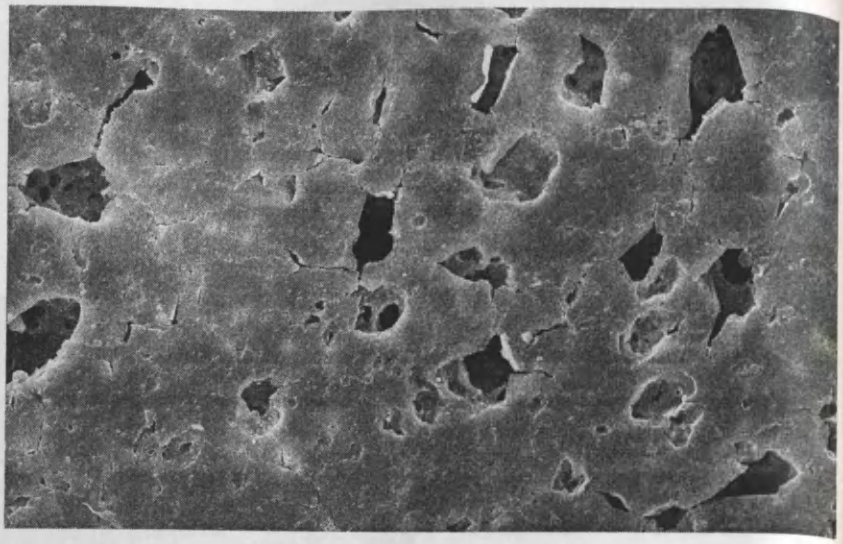

Fig 5.2.2.

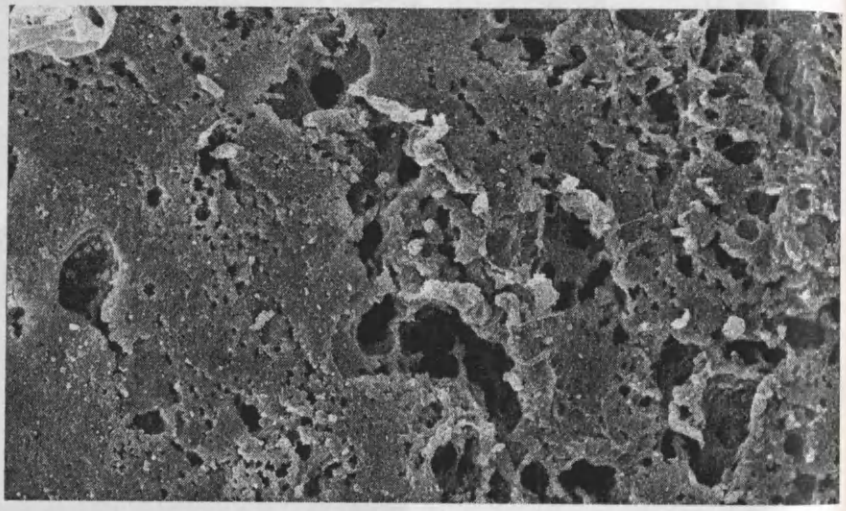

Fig 5.2.3.

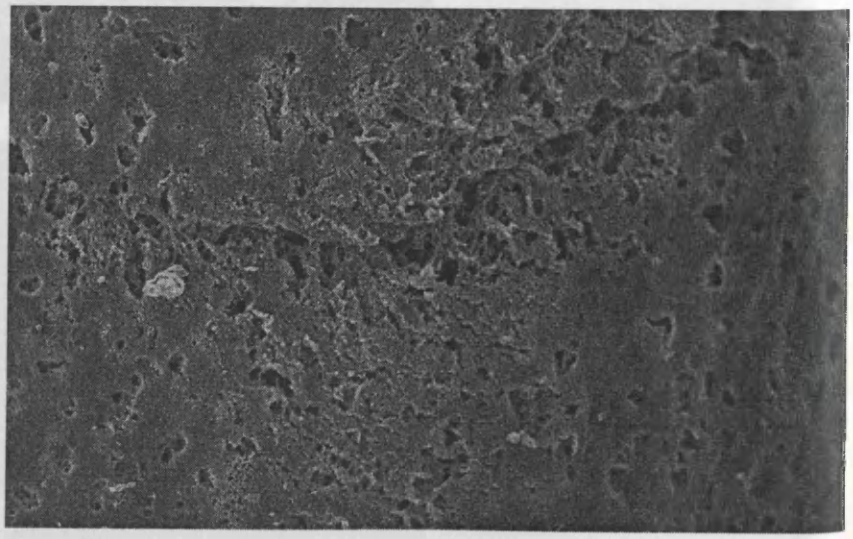

Fig 5.2.4.

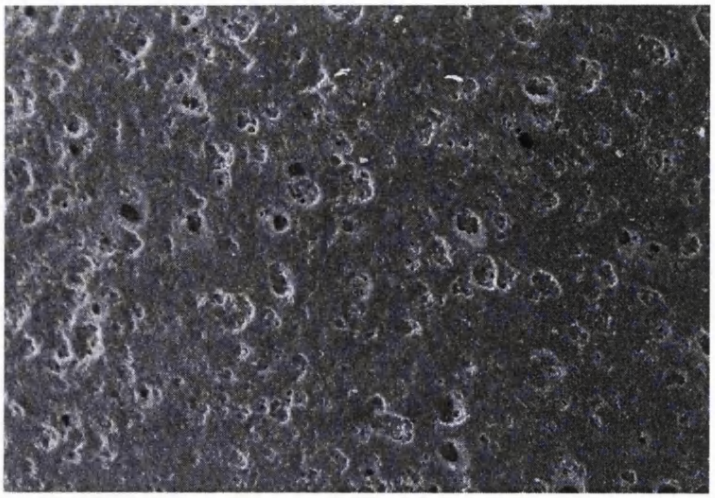

Fig 5.2.5.

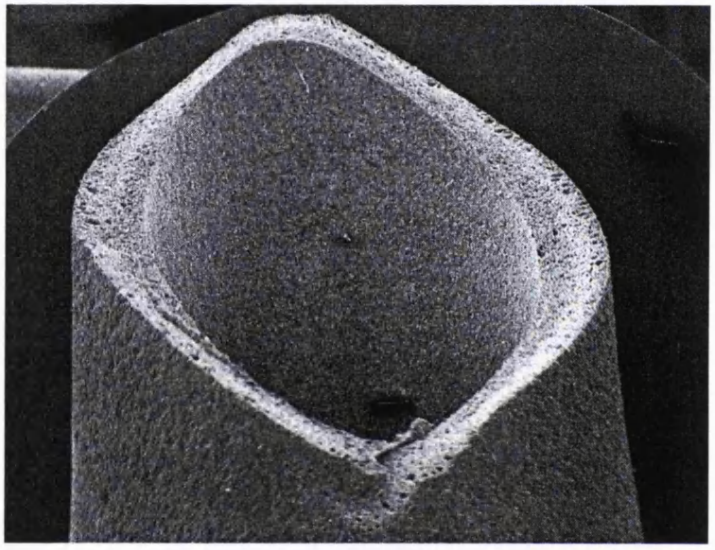

Fig 5.2.6.

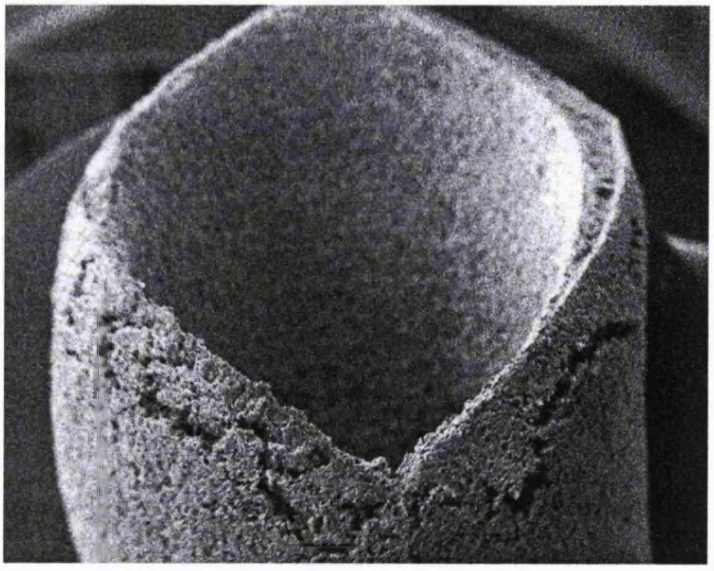

Opposite:

Fig. 5.3. Bar charts depicting (mean ± SD) compliance of Chronoflex CPU grafts, measured at mean pressures of 50 and 100 mmHg, following 70 days immersion in degradative media. Abbreviations: PF1-3, plasma fractions 1-3; CE, cholesterol esterase;PLA, phospholipase A2; G/B/Co, glutathione/t-butyl peroxide/cobolt chloride; H2O2/Co, hydrogen peroxide/cobolt chloride.

Figure 5.3.

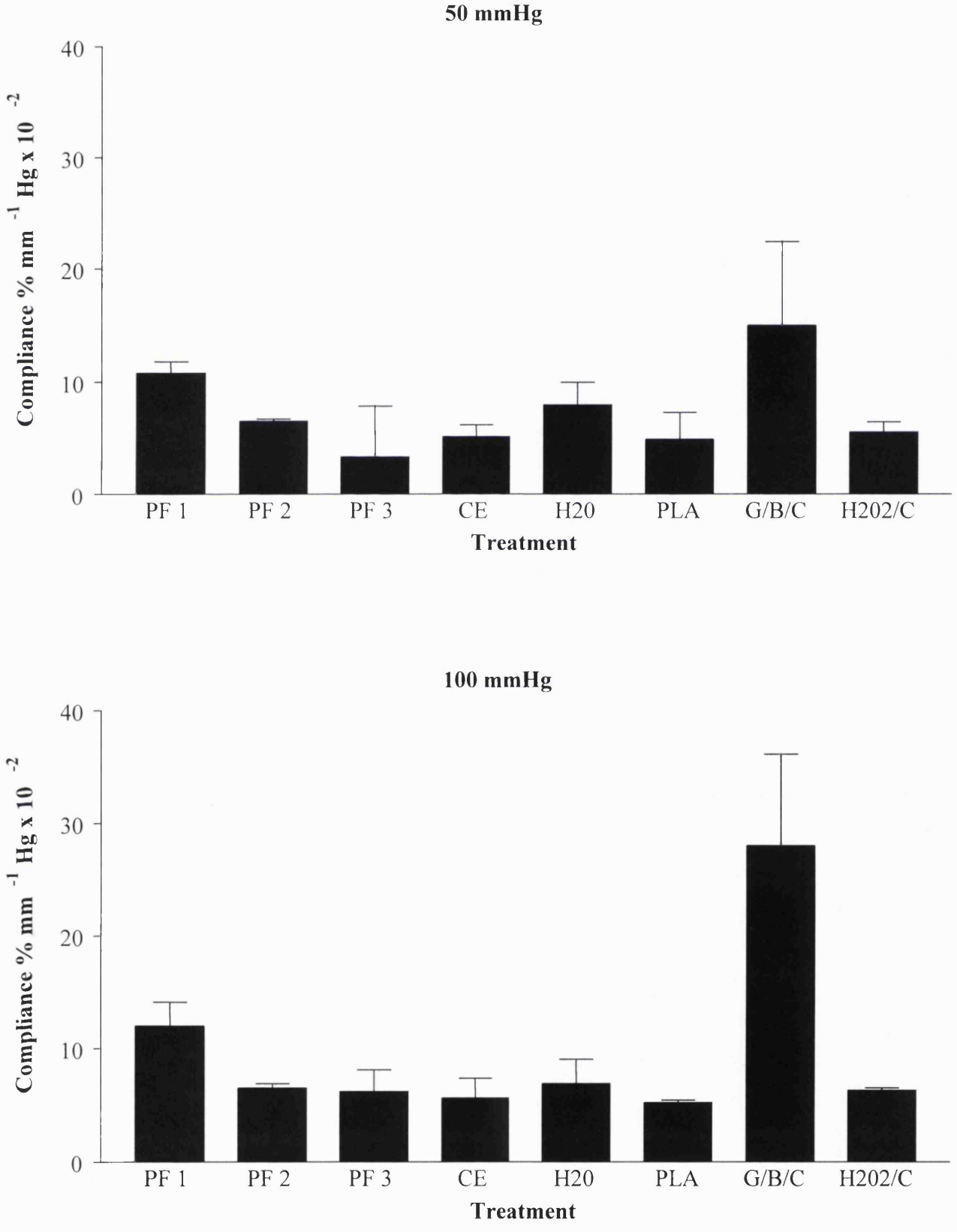
50 mmHg
Compliance % mm -1 Hg x 10 -2
40
30
20
10
0
PF 1
PF 2
PF 3
CE
H20
PLA
G/B/C
H202/C
Treatment
100 mmHg
Compliance % mm -1 Hg x 10 -2
40
30
20
10
0
PF 1
PF 2
PF 3
CE
H20
PLA
G/B/C
H202/C
Treatment

Opposite:

Fig. 5.4. Bar charts depicting (mean ± SD) compliance of poly(ether) grafts, measured at mean pressures of 50 and 100 mmHg, following 70 days immersion in degradative media. Abbreviations: as Fig 5.3.

Figure 5.4.

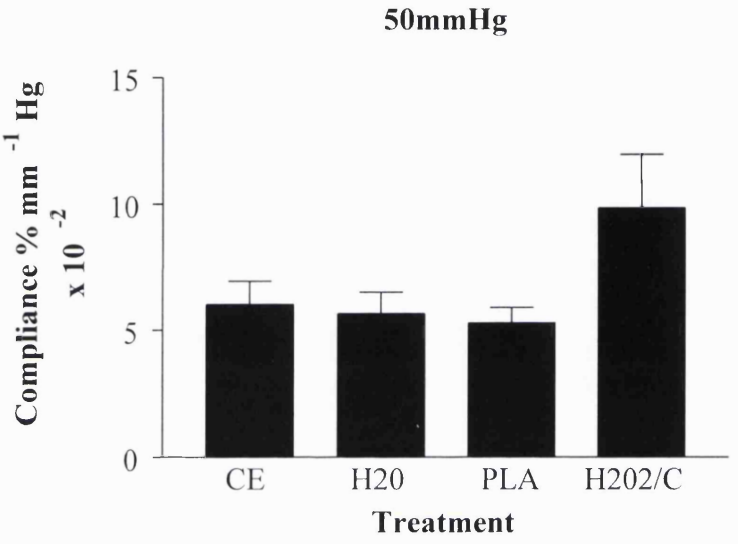
50mmHg
Compliance % mm -1 Hg
x 10 -2
15
10
5
0
CE
H20
PLA
H202/C
Treatment

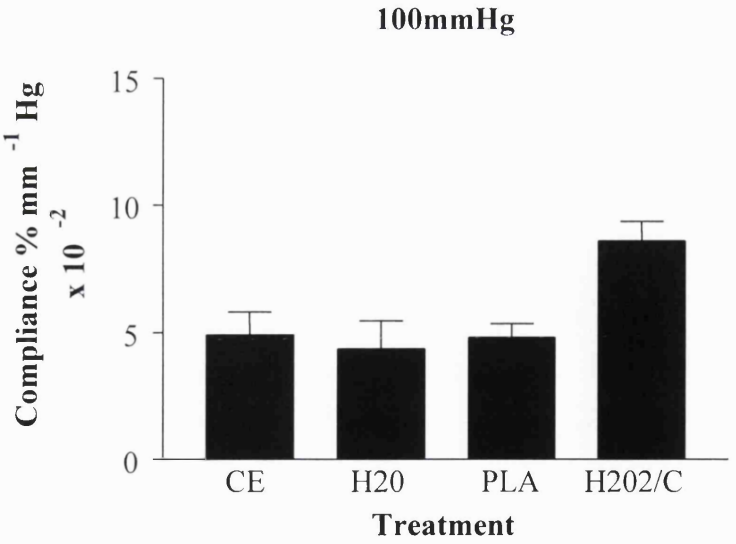
100mmHg
Compliance % mm -1 Hg
x 10 -2
15
10
5
0
CE
H20
PLA
H202/C
Treatment

Table 5.2. Effect of aging media on Chronoflex CPU and poly(ether) graft segments.

Media	ESC observed on SEMs	
	Poly(ether)	*Chronoflex CPU*
H_20	-	-
Plasma Fraction I	+	-
Plasma Fraction II	+	-
Plasma Fraction III	+	-
PLA	-	-
CE	-	-
$H_20_2/CoCl_2$	-	-
t-but/$CoCl_2$	+	+
Glut/t-but/$CoCl_2$	+	-

5.4. Discussion

5.4.1. Mechanisms of degradation

When determining the suitability of a particular polymer for use *in vivo* as an implant it is vital that an assessment has been made of that polymer's susceptibility to biodegradation. This is because post-implantation interaction between the polymer and adjacent tissues may induce change in its chemical and physical properties [225]. Chemical changes may occur by covalent bond cleavage, crosslinking or ionic bond transformation. Physical changes include swelling, plasticisation, crystallisation or decrystallisation, fatigue fracture, creep, stress cracking and kinking. The purpose of assessment is to understand the mechanism of degradation in order to devise strategies to protect the material from such forces, thereby increasing longevity. Three modes of chemical degradation predominate *in vivo* : mineralisation, hydrolysis and oxidation. In recent years it has become apparent that polyurethanes are particularly susceptible to the latter two processes, both of which lead to the phenomenon of environmental stress cracking. The aim of this chapter was to assess how well the new Chronoflex CPU graft resists these forces, with change measured in terms of morphology and elastic behaviour (compliance).

5.4.2. Hydrolysis

Hydrolysis is the fracture of vulnerable chemical bonds with water. *In vitro* experiments have demonstrated that polyurethanes are a potent activator of monocyte-derived macrophages [304] and stimulate the formation of foreign body giant cells [305] – two notable features of the chronic inflammatory response. It is hypothesised that exposure to hydrolysing enzymes released following lysosomal degranulation during the chronic inflammatory reaction is a mechanism of graft biodegradation. Work carried out by Santerre *et al* [306,307] has implicated cholesterol esterase, and more recently, phospholipase A_2 [302] as party to this process of hydrolytic

degradation. CE preferentially attacks the urethane linkage of the soft segment of poly(esters) [307] whereas the specificity of phospholipase A_2 is unknown. In this series, poly(ether) and Chronoflex CPU grafts appeared resistant to both PLA and CE as judged by a lack of ESC or significant difference in compliance compared to water-incubated controls. This result was expected as neither the poly(ether) or Chronoflex polymer contains hydrolytically-vulnerable ester linkages. However, CE has been observed to cause release of breakdown products from poly(ether) urethanes when used at very high concentration [308]. Further, it is known that the biodegradative effect of CE and PLA may be enhanced by co-incubation with mixed micellar solutions of phospatidyl choline and oleic acid [302] as the resulting fatty acid breakdown products act synergistically to further attack susceptible bonds. Neither of these protocols was utilised in these investigations. Thus, although both Chronoflex CPU grafts and poly(ether) grafts appear resistant to hydrolysis, it is not possible to conclude that they are invulnerable merely because they do not contain ester linkages.

5.4.3. Oxidation

Poly(ether) urethanes may have enhanced resistance to hydrolytic attack but are at risk of oxidative degradation [227]; that is the modification of molecular structure via electron transfer reactions [225]. Those sites along the soft-segment backbone that can stabilise a free radical are vulnerable to attack and scission ; the methyl group in the alpha position to the ether oxygen segment has been shown to be particularly susceptible to this type of reaction [224,227,309]. *In vivo*, oxidising free radicals are generated during the inflammatory response by the respiratory burst of activated neutrophils and it is believed that this process leads to oxidation of the polymer [225,228,310].

Oxidation of aliphatic polymer chains usually involves four stages: initiation by hydrogen abstraction; formation of hydroperoxide by molecular oxygen; chain reaction propagation and termination [225] . Free radical formation may be promoted by the aqueous ions of certain

transition metals such as cobalt and molybdenum [311], arising from the *in vivo* corrosion of pacemaker lead assemblies, and has been offered as an additional explanation for the limited lifespan of poly(ether)-insulated pacemaker leads [312]. Attempts to reproduce oxidative degradation of polyurethane *in vitro* have relied upon the use of hydrogen peroxide (H_2O_2) with or without promoting agents. Although treating prestressed poly(ether)urethane tubes with H_2O_2 solution at room or body temperature does not produce stress cracking [313], the surface chemistry and molecular weight are altered [314] and these changes become marked if the urethane is boiled in H_2O_2 solution over several days [303]. Zhao and colleagues promoted the development of ESC in poly(ether) grafts with the use of H_2O_2 / $CoCl_2$ solutions: initially, the protocol involved exposure to human plasma at 37° C, followed by H_2O_2 / $CoCl_2$ at 50° C [229]. The plasma pretreatment stage was then discarded in favour of a pure H_2O_2 / $CoCl_2$ room temperature method that utilised glass wool to enhance the interaction between polyurethane and oxygen species [300]. Using these methods Chronoflex CPU grafts have previously exhibited superior survivability over poly(ether) controls grafts exposed to the same oxidising system [245]. Thus, polyurethanes with soft segments that are oxidatively stable may have lower rates of biodegradation.

In this study grafts were exposed to solutions capable of generating several oxidising free radical species including: hydroxyl (·OH) species from the H_2O_2 / $CoCl_2$ mixture [312]; alkyl (·OR) species from the H_2O_2 / t-butyl peroxide mixture and thiyl (·R) species as a result of the breakdown of glutathione (a free radical scavenger *in vivo*) added to a H_2O_2 / t-butyl peroxide mixture [315]. Such species can be identified and quantified using spin trapping techniques [316] although at the time of the study no attempt was made to verify their presence. ESC was observed in poly (ether) grafts exposed to the H_2O_2 / t-butyl peroxide mixture and the glutathione/ H_2O_2 / t-butyl peroxide mixture and in Chronoflex CPU grafts exposed to the H_2O_2 / t-butyl peroxide mixture. Although poly(ether) appeared resistant to the H_2O_2 / $CoCl_2$ mixture, significant difference in compliance was observed compared to controls, indicating possible

material degradation. Chronoflex CPU grafts showed no such changes with regard to the H_2O_2 / $CoCl_2$ mixture, confirming Zhao's earlier experience with the polycarbonate Corethane when exposed to a glass wool H_2O_2 / $CoCl_2$ system [300]. However, Chronoflex CPU grafts did show significant differences in compliance with regard to the glutathione/t-butyl peroxide/cobalt chloride, although no ESC was observed. Whilst compliance measurements have previously been used to characterise the physical properties of polyurethane grafts in the virgin state [243,317] this result indicates that such measurements also provide a qualitative indicator of change in material character that precedes the development of overt ESC. Ideally, the compliance of a graft mounted within the circulation should not change significantly since this may adversely affect graft function and lead to anastomotic mismatch.

Grafts observed to have ESC did not survive the preclotting process. Whilst preclotting was intended to be a means of preventing graft leakage (as in Chapter 3), distending the graft with blood also acted as a materials test in itself. Preclotting consists of a forceful injection of freshly obtained whole blood into one end of the graft whilst the other end is clamped off [318]. Blood is then forced through the graft interstices, and the process repeated twice at intervals with freshly drawn blood. On the third infusion, the resistance to the passage of blood is high because graft pores are blocked by stable clot. Unharmed grafts distend and permit minimal transmural egress of blood but degraded grafts were noted to rupture during the second or third stage of the preclotting protocol. Consequently it was not possible to obtain compliance measurements for poly(urethane) grafts exposed to plasma fractions I-III, H_2O_2 / t-butyl peroxide mixture and the glutathione/ H_2O_2 / t-butyl peroxide mixture; and in Chronoflex CPU grafts exposed to the H_2O_2 / t-butyl peroxide mixture.

Clearly, Chronoflex CPU grafts were more resistant than poly(urethane) grafts to metal ion oxidative degradation but they were not invulnerable to attack. Two reasons might account for this: firstly, although the aliphatic structure of Chronoflex contains a lower proportion of ether linkages in its soft segment compared to poly(ether) urethanes, some susceptible ether

linkages remain. Secondly, carbonate bonds may be subject to acid catalysed *hydrolysis* if the pH is low enough with the formation of carbon-dioxide and alcohol [319] . Ward has proposed such a mechanism as the main mode of biodegradation of polycarbonate polyurethanes [320]. However, the pH of the H_2O_2 / t-butyl peroxide and the glutathione/ H_2O_2 / t-butyl peroxide mixture was 5.2 ± 0.4 and 5.0 ± 0.3 respectively (n=6), which does not approach the degree of acidity thought necessary to promote such hydrolysis. Further studies are required to elucidate the exact mechanism - whether oxidative or hydrolytic - by which poly(carbonate) urethanes lose their chemical integrity.

5.4.4. The effect of serum proteins

Zhao *et al* found that the ability of oxidising solutions to cause ESC in poly(ether) urethanes was enhanced by pre-treating grafts in human plasma for 7 days [229], with the greatest effect occurring in samples exposed to plasma fraction II . Adsorption of alpha-2-macroglobulin onto graft specimens was confirmed by protein electrophoresis and immunoblotting techniques. Caeruloplasmin, a notable constituent of plasma fraction III was also found to promote ESC. Based on these findings Zhao *et al* proposed that plasma proteins were able to act as ESC promoters, although the mechanism of action remains unknown.

In this study, poly(ether) graft segments incubated in a range of plasma fractions, derived using Zhao's protocol developed ESC. Additionally, such segments did not survive the preclotting process. Notably, none of the Chronoflex segments exhibited ESC or significant difference in compliance compared to water incubated controls. Zhao *et al* found it was necessary to sequentially incubate poly(ether) segments in plasma followed by immersion in H_2O_2 / $CoCl_2$ mixture in order to produce extensive ESC. In this study cracking was produced by exposure to fractionated plasma without additional treatments. This may be because in our protocol graft segments were incubated for an arbitrary period of 10 weeks (70 days) whereas

Zhao *et al* limited exposure to 7 days. There were no consistent trends noted in the effect of different plasma treatments on compliance in Chronoflex CPU grafts.

5.4.5. Methodology

The principal limitations in the experimental protocol are four fold. Firstly, it was not possible to assess the half-life of the ageing solutions that were made and thus the refilling frequency (solutions were changed on a weekly basis) may be insufficient. Secondly, only two means of material assessment were utilised – SEM and compliance testing. More sophisticated means of material assessment include tensile testing [300,312,317] quantification of release of radiolabelled carbon from degraded PU [302,306,307], X-ray photo spectroscopic (XPS) surface characterisation [302], electron dispersive analysis by X-ray (EDAX) [312], Fourier transform infrared surface spectroscopy (FTIR)[307,312,317] and Gel permeation chromatography (GPC) [312]. XPS, EDAX and FTIR are particularly valuable as they allow the specific quantification of the chemical changes that occur following hydrolysis or oxidation. Thirdly, the changes that occurred – particularly with respect to metal-ion oxidation in Chronoflex samples – have not been quantified with parallel animal investigations. Zhao rated the $H_20_2/CoCl_2$ system by comparing the degree of ESC in polyether specimens exposed *in vitro* to that of specimens implanted in rabbits, and tentatively estimated the *in vitro* solution as accelerating ESC by approximately seven fold. No parallel animal data was available in this study and thus an estimate of likely *in vivo* longevity cannot be made. Finally, although the protocol included a number of chemical stressors to provoke ESC in subject grafts, no equivalent mechanical stress was incorporated (excluding the unforeseen side-effect of the graft pre-clotting procedure). The use of oversized mandrels has been discussed [245], but this method was not employed. This is because it was intended to fabricate perfusion equipment that would expose grafts to degenerative media at arterial circulatory pressures whilst subjecting them to simultaneously applied rotational, axial and torsional stresses. Unfortunately it was not

possible to complete the apparatus prior to the conclusion of my research period, and thus the effect of graft exposure to a combination of degenerative and mechanical stress remains unknown.

In summary, previous studies have shown the poly(carbonate) urethanes to possess resistance to $H_2O_2/CoCl_2$ metal ion oxidation solutions. This study supports those findings and also shows that Chronoflex CPU grafts are resistant to plasma protein and hydrolytic enzyme degradation. However, Chronoflex CPU grafts may be vulnerable to some oxidative species. Further work is necessary; to quantify the chemical changes that occur with exposure to these species, to relate these *in vitro* changes to *in vivo* performance and to consider how the chemical structure may be augmented to enhance bioresistance further.

Chapter 6.

Conclusions

Prosthetic grafts perform poorly when used for infrainguinal vascular reconstruction, particularly when used for infragenicular or distal revascularisation. This problem has attracted intensive scientific endeavour as to its causes and possible solutions. However, despite a convincing body of work supporting the compliance hypothesis (as detailed in chapter 1) the bulk of research has been directed at solving the difficulty of graft thrombogenicity. In comparison, biomechanical issues have become an area of relative neglect. The work in this thesis concerns a graft which offers a solution to the problem of compliance mismatch, itself postulated to cause anastomotic intimal hyperplasia and thereby graft failure. The aim of the studies was to quantify the extent to which this graft fulfils its potential as a purportedly compliant, biostable arterial prosthesis capable of retaining and supporting seeded endothelial cells. The purpose of this chapter is to summarise the conclusions from these studies, discuss the chief limitations of compliance matching and consider areas which merit further research.

6.1. Practical constraints to compliance matching

In chapter 3 it was demonstrated that the Chronoflex CPU graft is more compliant than PTFE or Dacron alternatives and match the compliance values of lower-limb artery, although a number of important caveats apply to this conclusion.

6.1.1. The compliance of the infragenicular vessels is unknown

The degree of compliance match possible with Chronoflex CPU in the context of the infragenicular popliteal and distal arteries (peroneal, anterior and posterior tibial arteries) is not known, because it was not possible to study these vessels with sufficient accuracy. Inadequate resolving power in the ultrasound scanner employed prevented reproducible measurements of arterial diameter. The compliance values of the infrapopliteal vessel segments are unknown and further studies will be required.

6.1.2. *Femoropopliteal compliance is highly variable*

The results of the limited *in vivo* study presented in chapter 2 revealed that femoropopliteal compliance values appear to be particular to the anatomical portion of the vessel concerned. Additionally, the mechanical properties of the vessel appear to be specific to the disease-state of the vessel, a parameter that varies within and between individuals. Thus, by implication, a mass-produced compliant graft can only reduce - not eradicate - anastomotic compliance mismatch, since the latter would require individual tailoring of graft compliance to meet the requirements of that portion of the receiving vessel forming the distal part of the anastomosis.

6.1.3. *Arteries exhibit anisotropic deformation*

Furthermore, the study in chapter 2 showed that, as is the case with grafts made from PTFE and Dacron, the Chronoflex CPU graft fails to mimic the anisotropic, non-linear elastomeric character of intact arterial tissue. Therefore, even though the CPU graft is nominally compliant, the degree of compliance match between graft and artery will be dependent upon the operating pressure. The homogenous nature of the graft must be reconfigured if it is to truly exhibit anisotropic behaviour. This is because, in order for a compliant graft to exhibit variable, pressure-dependent elasticity, it must have a heterogeneous, composite structure consisting of elements of differing elastic modulus. An example of a prototype graft designed in this respect is the experimental Casali composite prosthesis[321-322], which consists of poly (ether) urethane fibres (Lycra) buried in a matrix of Pell ethane and a poly (lactic acid) co-polymer. In this type of graft the compliance characteristics are factory-set by changing the reinforcement angle of the investing Lycra fibres and are dependent upon pressure. Thus, although the Chronoflex CPU graft can be accurately described as providing a degree of compliance matching over and above that which can be expected from ePTFE or Dacron, this design fails to offer the ideal of 100% compliance matching.

6.1.4. Is "zero compliance mismatch" the ideal state ?

However, there is no evidence to suggest that composite grafts - supposedly offering the ideal of zero compliance mismatch - provide a greater degree of mitigation against intimal hyperplasia than grafts that provide a partial compliance match. Therefore, it may be misguided to reject the current design in favour of zealously pursuing the ideal of 100% compliance match if such a graft fails to confer significant patency advantage. Unfortunately, there is no data illustrating the mismatch threshold that, if exceeded, triggers anomalous EC and SMC behaviour with the precipitation of AIH.

6.1.5. The problem of graft-tissue incorporation

A further limitation to the degree of *in vivo* compliance-match obtainable is the prospect of progressive reduction in graft distensibility following implantation as tissue incorporation proceeds [88,218]. The relatively thick-walled design of the Chronoflex CPU graft has been designed to act as a buffer to the constraining effect of adventitial scar tissue [243]. Although the problem was not investigated in this thesis, future *in vivo* studies of the Chronoflex CPU graft will be required to address the effect of stiffening due to graft incorporation. Regular observation of grafts that have been implanted within the arterial system of a suitable animal model should allow longitudinal assessment of graft compliance in order to determine if the current design offsets the effect of scar tissue build-up. Comparison of the patency rate between compliant and non compliant (externally stiffened) Chronoflex CPU grafts would allow further validation of the compliance hypothesis, a necessity if the vascular surgical community is to be persuaded to re-examine the issue of compliance and graft failure.

6.1.6. The problem of the sutured anastomosis

It should be noted that however faithfully any compliant graft matches the elasticity of adjacent artery, the suture ring of the anastomosis will disrupt the otherwise smooth transition in

compliance from prostheses to vessel. Current polypropylene suture materials are of low elasticity and thus either new sutures or suturing techniques must be devised to overcome this potential pitfall. One approach, currently under investigation at The Royal Free, is to apply photosensitive tissue glue to the opposed graft and vessel, thereby decreasing the number of sutures required to obtain a satisfactory anastomosis. It is anticipated that a reduced number of sutures will lead to a more distensible suture ring, thereby preserving anastomotic compliance.

6.2. Augmentation of the graft lumen will be necessary to enhance EC adherence

In chapter 4, in order to help define a successful cell seeding protocol, the optimal values for seeding density and incubation time were sought with respect to the Chronoflex graft. It was concluded that the graft saturates at 9.65 x 10^5 cells/cm^2 and to achieve saturation 18 x 10^5 cells/cm^2 must be seeded because a sizable proportion (45%) of cells are not able to resist initial displacement forces and become disattached from the graft. Although the study confirmed that cells adhere more strongly to Chronoflex CPU than ePTFE graft material, the implication of these results is that the graft lumen must be augmented in some way to lower the cell seeding density required to produce saturation. It is speculated that augmentation may also lower the optimal incubation time of 4 hours, as the length of this period will preclude use of this graft in single-stage seeding applications. New research must be directed at exploring which of the many EC adhesion agents provides the best way of jointly achieving these goals. Furthermore, significant difficulties with leakage of perfusate from the graft during initial *in vitro* perfusion necessitated a pre-clotting protocol in order to prevent trans-mural egress of the EC inoculum. If an EC-binding moiety is bound to the graft lumen, further study will be required to determine how leakage can be prevented without recourse to pre-clotting as the latter process may cloak the binding agent.

6.3. *Does the Chronoflex CPU graft degrade in animals ?*

Chapter 5 examined the biodurability of the Chronoflex CPU graft. As expected, the graft resisted degradation by a greater number of media than poly(ether) alternatives. However, somewhat surprisingly, stress cracking and change in compliance properties *was* observed in Chronoflex CPU grafts following 70 days immersion in t-butyl peroxide/cobalt chloride and glutathione/t-butyl peroxide/cobalt chloride mixtures respectively. Correlating these results to *in vivo* data has not been possible since an ongoing animal trial has yet to reach completion. Dr Stephan Bowald of Uppsala, Sweden has implanted 5mm CPU aortic interposition grafts in four adult beagles on behalf of Cardiotech Ltd. At the time of writing, the study is approaching its termination date when grafts will be removed following 30 months implantation. Explant samples will then be available for compliance testing and chemical analyses. If ESC or significant loss of molecular weight is observed in these samples, consideration must be given to additional means of protecting the poly(carbonate) structure from chemical attack [225]. For instance, Labow's group claim to have endowed additional resistance in a poly(ester) urethane by including a fluorinated macromolecular additive that migrates to the luminal surface and inhibits enzymatic hydrolysis [323] .

6.4. *Conclusion of thesis*

Despite the expressed reservations regarding the degree of compliance matching attainable with the Chronoflex CPU graft, it is readily apparent that this prosthesis matches the compliance characteristics of lower-limb arterial vessels considerably more so than ePTFE or Dacron. It may thereby posses the necessary mechanical properties to diminish anastomotic compliance mismatch. Additionally, it exhibits suitable qualities for use in endothelial cell seeded applications and has enhanced biostability relative to second generation poly (ether) urethane. Therefore, these findings are submitted in broad support of the hypothesis as stated at the start of this work.

Appendix

Suggested topics for future research arising from this work

Laboratory research

- *In vitro* assessment of femoral, popliteal and infra-popliteal arterial compliance using ethically obtained cadaveric arterial samples, or samples retrieved from amputated limbs. This would provide the compliance data required to design a Chronoflex CPU graft tailored for femorodistal reconstructions.
- Effect of bonding RGD cell binding residue to Chronoflex CPU grafts in terms of optimal EC seeding density, incubation time and cell retention, with comparison to blood clot and fibronectin.
- Refined assessment of resistance of Chronoflex CPU graft to ESC by exposure to circulating degradative media plus simultaneous mechanical strain in the form of pulsatile pressure. This might be achieved by mounting the graft within a suitably designed pressure circuit containing the media and perfusing it over several weeks. This study could employ more sophisticated methods for quantitative analysis of material degradation (i.e. EDAX, FITR, GPC)

Animal studies

- Use of animal models to observe the effect of balloon angioplasty upon compliance of arterial vessels.
- Randomised, controlled trial of Chronoflex CPU iliac interposition grafts in canine animal model, comparing externally supported (i.e. incompliant) versus unsupported (i.e compliant) grafts to re-assess the veracity of the compliance hypothesis with regard to the Chronoflex CPU graft. A more refined and ambitious study might examine the relative patencies of several different versions of the Chronoflex CPU

graft, each with a specific grade of compliance. This would be feasible as it is relatively easy to vary the compliance of the graft by subtle but straightforward alterations in the manufacturing process.

- Randomised, controlled trial of Chronoflex CPU iliac interposition grafts in Canine animal model, comparing EC seeded versus unseeded grafts to examine if seeding confers significant advantages in patency and clot free-surface area with regard to the Chronoflex CPU graft. EC would be obtained from ongoing work to harvest functional cells from subcutaneous fat samples.
- Assessment of the durability of the elastic properties of the graft during tissue incorporation in an animal model, by regular post-implantation ultrasound imaging and compliance measurement.

Human studies

- Assessment of infrapopliteal arterial compliance in subjects with and without lower-limb peripheral vascular disease. The results from this study would complement data gathered from post-mortem *ex vivo* compliance studies as discussed above.
- Investigation of intra-observer error in the measurement of lower-limb arterial compliance.
- Assessment of compliance of human lower-limb arteries during arterial catheterisation procedures (eg during angioplasty or angiography). Thus, pressure variables local to the arterial site being assessed could be obtained, abolishing the need to use potentially unrepresentative surrogates such as brachial artery pressures. Accuracy of compliance measurement might be further enhanced if intra-luminal ultrasound could be employed to generate the M-Mode Doppler images required to capture vessel wall motion.

Bibliography and references

1. Dormandy J, Mahir M, Ascady G, Balsano F, De Leeuw P, Blombery P *et al.* Fate of the patient with chronic leg ischaemia: a review article. J Cardiovasc Surg 1989; 30: 50-7.
2. Fowkes FGR. Epidemiology of peripheral vascular disease. Springer Verlag, London 1991.
3. Fowkes FGR, Housley E, Cawood EHH, Macintyre CCA, Ruckley CV, Prescott RJ. Edinburgh Artery Study: prevalence of asymptomatic and symptomatic peripheral arterial disease in the general population. Int J Epidem 1991;20: 384-92.
4. The Vascular Surgical Society of Great Britain and Ireland. Critical Limb Ischaemia: management and outcome. Report of a national survey. Eur J Vasc Endovasc Surg 1995; 10: 108-13.
5. European Working Group on Critical Limb Ischaemia. Second European consensus document on chronic critical leg ischaemia. Circulation (Suppl) 1991;84:1-26.
6. Department of Health and Social Security. Office of Population Censuses and Surveys. Hospital Inpatient Enquiry. London: HMSO, 1986.
7. Cotran RS, Kumar V, Robbins SL (Eds). Robbins' pathologic basis of disease. Philadelphia, WB Saunders, 1989:553-595.
8. Fowkes FGR, Housley E, Riemersma RA *et al.* Smoking, lipids, glucose intolerance and blood pressure as risk factors for peripheral artherosclerosis compared with ischaemic heart disease in the Edinburgh Artery Study. Am J Epidemiol 1992; 135: 331-40.
9. Dagenais GR, Maurice S, Robitaille NM, Gingras S, LupeinPJ. Intermittent claudication in Quebec Men from 1974-1986: the Quebec Cardiovascular Study. Clin Invest Med 1991;14: 93-100.

10. Kannel WB, McGhee DL. Update on some epidemiological features of intermittent claudication: The Framingham Study. J Am Ger Soc 1985;33:13-18.

11. Reunanen A, Takkunen H, Aromaa A. Prevalence of intermittent claudication and its effect on mortality. Acta Med Scand 1982; 211 :249-56.

12. Ruffer MA. On arterial lesions found in Egyptian mummies. J Path Bact 1911; 15:453-61.

13. Clowes AW. Theories of atherosclerosis. In: White RA (Ed) Atherosclerosis and arteriosclerosis: human pathology and experimental animal methods and models. Boca Raton, CRC press, 1989: 3-15.

14. Ross R. Pathogenesis of atherosclerosis: an update . N Engl J Med 1986;314:488-500.

15. Glagov S, Weisenberg E, Zarins SK, Stankunavicius R, Kolettis GJ. Compensatory enlargement of human atherosclerotic coronorary arteries. N Engl J Med 1987;316: 1371-1375.

16. Haimovici H. Patterns of arteriosclerotic lesions of the lower extremity. Arch Surg 1967; 95: 918-33.

17. Mavor GE. The pattern of occlusion in atheroma of the lower limb arteries. The correlation of clinical and arteriographic findings. Br J Surg 1956 ; 43: 352.

18. Giddings AEB, Quraishy MS. Management of the acutely ischaemic limb. In: Galland RB, Clyne CAC (Eds). Clinical problems in vascular surgery. Edward Arnold, London 1994. p19-29.

19. Kempczinski RF, Bernhard VM. Management of chronic ischaemia of the lower extremities: introduction and general considerations. In: Rutherford RB (Ed). Vascular surgery. Philadelphia, WB Saunders, 1989. 643-652.

20. Gaines PA, Beard JD. Management of lower-limb ischaemia. In: Beard JD, Gaines PA (Eds) . Vascular and endovascular surgery. London, WB Saunders 1998. p151-171.

21. Quick CRG, Cotton LT. The measured effect of stopping smoking on intermittent claudication. Brit J Surg 1982; 69 (S) : 524-6.

22. Garner AW, Poehlman ET. Exercise rehabilitation programs for the treatment of claudication pain. JAMA 1995; 274: 975-80.

23. Antiplatelet trialists collaboration. Collaboration overview of randomised trials on antiplatelet therapy in various categories of patients. Br Med J 1994;308: 81-106.

24. Goyanes J. Nuevos trabajos de chirugia vascular: sustitucion plastica de as arterias por las venas, o arterioplastica venosa, como nuevo methodo al tratimiento de las aneurismas. Siglo Medico 1906; 53: 546-8, 561-4.

25. Kunlin J . Le Traitement de l'artérite oblitérante par la greffe veineuse longue. Arch Mal Du Coeur 1949; 42: 371-2.

26. DeBakey ME. The development of vascular surgery. Am J Surg 1979;137 : 697-738.

27. Bernhard VM. Bypass to the popliteal and infrapopliteal arteries. In: Rutherford RB (Ed). Vascular Surgery. WB Saunders, Philadelphia 1989. p 692-703

28. Whittemore AD. Infrainguinal bypass. In: Rutherford RB (Ed). Vascular Surgery. WB Saunders, Philadelphia 1995. p 794 –814.

29. Michaels JA. Choice of material for above-knee femoropopliteal bypass graft. Br J Surg 1989;76:7-14.

30. Myhie H, Dahl T, Lundbom J, Saether O, Gronningsaether A. Imaging of the superficial veins for suitability of by-pass surgery. In: Vascular imaging for surgeons. Greenhalgh R.M. (Ed) W.B. Saunders Company Ltd, London, 1995. p 353-60.

31. Veith FJ, Weiser RK, Gupta SK, Ascer E, Scher LA, Samson RH *et al.* Diagnosis and management of failing lower extremity arterial reconstructions. J Cardiovasc Surg 25: 381, 1984.

32. Brewster DC, LaSalle AJ, Robison JG, Strayhorn EC, Darling RC. Femoropopliteal graft failures: clinical consequences and success of secondary reconstruction. Arch Surg 1983; 118:1043-7.

33. Ascer E, Collier P, Gupta SK, Veith FJ. Reoperation for polytetrafluorethylene bypass failure; the importance of distal outflow site and operative technique in determining outcome. J Vasc Surg 1987;5:298-310.

34. Kazmers M, Satiani B, Evans WE. Amputation level following unsuccessful distal limb salvage operations. Surgery 1980; 87: 683-7.

35. Dardik H, Kahn M, Dardik I. Influence of failed vascular bypass procedures on conversion of below knee to above knee amputation levels. Surgery 1982; 91: 63-9.

36. De-Frang RD, Taylor LM, Porter JM. Basic data related to amputations. Ann Vasc Surg 1991;5: 202-7.

37. Houghton AD, Taylor PR, Thurlow S, Rootes E, McColl I. Success rates for rehabilitation of vascular amputees: implications for pre-operative assessment and amputation level. Br J Surg 1992;79: 753-5.

38. Taylor RS, McFarland RJ, Cox MI. An investigation into the causes of failure of PTFE grafts. Eur J Vasc Surg 1987;1: 335-43.

39. Fischer CM, Tew K, Appleberg M. Prevalence and outcome of activated protein C resistance in patients after peripheral arterial bypass grafts. Cardiovasc Surg 1999; 7:519-525.

40. Wiseman S, Powell J, Greenhalgh R, McCollum C, Kenchington G, Alexander C *et al.* The influence of smoking and plasma factors on prosthetic graft patency. Eur J Vasc Surg 1990;4: 57-61.

41. Pevec WC, Darling RC, L'Italien GJ, Abbott WM. Femoro-politeal reconstruction with knitted non-velour dacron versus expanded polytetrafluoroethylene. J Vasc Surg 1992;16:60–65.

42. Mosley JG, Marston A. A 5-year follow-up of Dacron femoropopliteal bypass grafts. Br J Surg 1986; 73: 24-7.

43. US patent 3, 962, 153 (June 8 1976 to W.L.Gore and Associates) Very highly stretched polytetraethylene and process therefore. 1976, p 1-24.

44. Boyce B. Physical characteristics of expanded polytetrafluoroethylene grafts. In : Biologic and Synthetic Vascular Prostheses. Stanley JC (ed). Grune and Stratton, New York 1982. p 553-61.

45. Campbell CD, Goldfarb D, Roe R. A small arterial substitute: Expanded microporous polytetrafluoroethylene for limb salvage: a preliminary report. Surgery 1976; 79: 485-91.

46. Nunn DB, Carter MM, Donohue MT. Postoperative dilatation of knitted Dacron aortic bifurcation graft. J Vasc Surg 1990; 12: 291-6.

47. Lindenauer SM: the fabric vascular prosthesis. In Rutherford RB (Ed) :Vascular Surgery. 3rd ed. WB Saunders, Philadelphia 1989. p450-460.

48. Kottke-Marchant K, Anderson JM, Umemura Y, Marchant RE. Effect of albumin coating on the in-vitro compatibility of Dacron arterial prostheses. Biomaterials 1989;110:14-55.

49. Dardik H, Miller N, Dardik A, Ibrihim C, Sussman B, Berry SM *et al.* A decade of experience with the glutaraldehyde-tanned human umbilical cord vein graft for revascularisation of the lower limb. J Vasc Surg 1988;7:336-46.

50. Eickhoff JH, Broome A, Ericsson BF. Four years' results of a prospective randomised clinical trial comparing polytetrafluroethylene and modified human umbilical vein for below-knee femoropopliteal bypass. J Vasc Surg 1987; 6: 506-11.

51. McCollum C, Kenchington G, Alexander C, Franks PJ, Greenhalgh RM. PTFE or HUV for femoropopliteal bypass: A multi-centre trial. Eur J Vasc Surg 1991; 5: 435-43.

52. Scales JT: Tissue reactions to synthetic materials. Proc R Soc Med 1953; 46: 647.

53. Sauvage LR, Walker MW, Berger K, Robert SB, Lisko MM, Yates SG. Current arterial prosthesis: Experimental evaluation by implantation in the carotid and circumflex coronory arteries of the dog. Arch Surg 1979;114:687-91.

54. Greisler HP: Vascular graft healing - Interfacial phenomena. In: Greisler HP (Ed) New Biologic and Synthetic Vascular Prostheses. RG Landes Austin, Austin,Texas 1991. p 1-19.

55. Herring M, Baughman S, Glover J, Kesler K, Jesseph J, Campbell J *et al.* Endothelial seeding of dacron and polytetraethylene grafts: the cellular events of healing. Surgery 1984; 96: 745-753.

56. Schneider PA, Kotze HF, Heyns AD, Hanson SR. Thomboembolic potential of synthetic vascular grafts in baboons. J Vasc Surg 1989;10: 75-82.

57. Shoenfeld NA, Connolly R, Ramberg K, Valeri CR, Eldrup-Jorgensen J, Callow AD. The systemic activation of platelets by Dacron grafts. Surg Gyn Obs 1988;166: 454-7.

58. Kalman PG, Rotstein OD, Niven J, Glynn MF, Romaschin AD. Differential stimulation of macrophage activity by vascular grafts. J Vasc Surg 1993; 17:531-7.

59. Goldman M, Norcott HC, Hawker RJ, Drolc Z, McCollum CN. Platelet accumulation on mature Dacron grafts in man. Brit J Surg 1982; 69: Suppl:s38-40 .

60. Berger K, Sauvage LR, Rao AM, Wood SJ. Healing of arterial prostheses in man: Its incompleteness. Ann Surg 1972;175:118- 27.

61. Guidon R, Chafke N, Maurel S, How T, Batt M, Marois M *et al.* Expanded polytetrafluoroethylene arterial prostheses in humans: histopathological study of 298 surgically excised grafts. Biomaterials 1993;14:678-93.

62. Tunstall A, Eberhart RC, Prager MD. Endothelial cells on Dacron vascular prostheses: adherence, growth, and susceptibility to neutrophils. J Biomed Mater Res 1995; 29: 1193-9.

63. Shepard AD, Gelfand JA, Callow AD, O'Donnell TF Jr. Complement activation by synthetic vascular prostheses. J Vasc Surg 1984;1: 829-38.

64. Kent KC, Shindo S, Ikemoto T, Whittemore AD. Speices variation and the success of endothelial cell seeding. J Vasc Surg 1989; 9: 271-6.

65. Sottiurai VS, Yao JTS, Flinn WR, Batson WC. Intimal hyperplasia and neointima; an ultrastructural analysis of thrombosed grafts in humans. Surgery 1983; 93:809-817.

66. Neville RF, Sidawy AN. Myointimal hyperplasia: basic science and clinical considerations. Seminars in Vascular Surgery 1998; 11: 142-8.

67. Antelmo NL, Quist WC, LoGerfo FW. Quantitative analysis of anastomotic intimal hyperplasia in paired Dacron and PTFE grafts. J Cardiovasc Surg 1989; 30: 910-915

68. Mehta D, George SJ, Jeremy JY, Izzat MB, Southgate KM, Bryan AJ *et al.* External stenting reduces long-term medial and neointimal thickening and platelet derived growth factor expression in a pig model of arteriovenous bypass grafting. Nat Med 1998 ;4: 235-239.

69. Kamiya A, Togowa T. Adaptive regulation of wall-shear stress to flow change in the canine carotid artery. Am J Physiol 1980;239: H14-H21.

70. Zarins CK, Zatina MA, Giddens Sp, Ku DN, Glagov S. Shear-stress regulation of artery lumen diameter in experimental atherogenesis. J Vasc Surg 1987; 5:413-420.

71. Langille BL. Blood flow-induced remodelling of the artery wall. In: Bevan JA, Kaley G, Rubanyi G (Eds). Flow dependent regulation of vascular function. Oxford University Press, New York 1995. 277-299.

72. Ishida T, Takahashi M, Corson MA, Berk BC. Fluid shear stress-mediated signal transduction: How do endothelial clls transduce mechanical force into biological responses ? New York Acad Sci 1997; 811:12-24.

73. Gimbrone MA Jr, Nagel T, Topper JN. Biomechanical activation: an emerging paradigm in endothelial adhesion biology. Perspectives series: Cell adhesion in vascular biology. J Clin Invest 1997; 99: 1809-1813.

74. Topper JN, Cai J, Falb D, Gimbrone MA Jr. Identification of vascular endothelial genes differentially responsive to fluid mechanical stimuli: cyclooxygenase-2, manganese superoxide dismutase, and endothelial cell nitric oxide synthase are selectively upregulated by steady laminar shear stress. Proc Natl Acad Sci USA 1996; 93: 10417-10422.

75. Papadaki M, Tilton RG, Eskin SG, Mcintyre LV. Effects of shear-stress on nitric oxide production by human aortic smooth muscle cells. Am J Physiol 1998; 273: H616-H626.

76. Mondy JS, Lindner V, Miyashiro JK, Berk BC, Dean RH, Geary RL. Platelet-derived growth factor ligand and receptor expression in reponse to altered blood-flow *in vivo*. Circ Res1997; 81: 320-7.

77. Resnick N, Collins T, Atkinson W, Bonthron DT, Dewey CF Jr, Gimbrone MA Jr. Platelet derived growth factor B chain promoter contains a cis-acting fluid shear stress responsive element. Proc Natl Acad Sci USA 1993;90: 4591-4595.

78. Krais LW, Kirkman TR, Kohler TR, Zieler B, Clowes AW. Shear stress regulates smooth muscle proliferation and neointimal thickening in porous polytetrafluoroethylene grafts. Arterioscler Thromb 1991;11 :1844 –1851.

79. Bassiouny HS, White S, Glagov S, Choi E, Giddens DP, Zarins CK. Anastomotic intimal hyperplasia; mechanical injury or flow induced. J Vasc Surg 1991; 15: 708-717.

80. White SS, Zarins CK, Giddens DP, Bassiouny H, Loth F, Jones SA *et al.* Haemodynamic patterns in a model of end-to-side vascular graft anastomoses: effect of pulsatility, flow division and Reynolds number and hood length. J Biomech Eng 1993;115: 105-111.

81. Sottiurai VS, Yao JST, Batson RC, Sue SI, Jones R, Nakamura YA. Distal anastomotic intimal hyperplasia: histopathologic character and biogenesis. Ann Vasc Surg 1989; 24: 711-722.

82. Stonebridge PA, Prescott RJ, Ruckley CV on behalf of the Joint Vascular Research Group. Randomised trial comparing infrainguinal PTFE bypass grafting with and without interposition cuff at the distal bypass. J Vasc Surg 1997; 26:543-550.

83. Raptis S, Miller JH. Influence of a vein cuff on polytetrafluoroethylene grafts for primary popliteal bypass. Br J Surg 1995;82: 487-491.

84. Da Silva AF, Carpenter T, How TV, Harris PL. Stable vortices within vein cuffs inhibit anastomotic myointimal hyperplasia. Eur J Vasc Endovasc Surg 1997; 14: 157-163.

85. Caro CG, Pedley TJ, Schroter RC, Seed WA. Solid mechanics and the properties of blood vessel walls. In: The mechanics of the circulation. Oxford University Press, Oxford1978. p 86-105 .

86. Strandness DE, Sumner DS. Mechanical properties of the blood vessel wall. In: Blood flow for surgeons. Grune and Stratton, New York 1975 . p 161-205.

87. M. O' Rourke . Arterial compliance and wave reflection. Arch Mal Coeur 1991; 84 :45-8

88. Santiago MD, Chatamra K, Taylor DEM. Haemodynamic aspects of lower-limb arterial reconstruction using Dacron and Goretex prostheses. Ann R Coll Surg Eng 1981; 63 : 253-56.

89. Hasson JE, Abbott WM. Complications of artery-graft compliance mismatch. In: Bernhard VM, Towne JB (Eds) :Complications in vascular surgery. Grune and Stratton , New York; 1985. p 545-559.

90. Walden R, L'Italien G, Megerman J, Abbott WM. Matched elastic properties and successful arterial grafting. Arch Surg 1980; 115: 1166-1169.

91. Kidson IG. The effect of wall mechanical properties on patency of arterial grafts. Ann R Coll Surg Eng 1983; 65:24-9.

92. Lehmann E, Hopkins KD, Gosling RG. Definitions of cardiac/ventricular and vascular/arterial compliance are different. Clin Sci 1996; 90:143-4.

93. Kok WEM, Sipkema P, Peters RJG. Compliance, a cardiologist's view ? Clin Sci 1996;90:144-6.

94. Lehmann E, Hopkins KD, Gosling RG. Multiple definitions of "compliance". Clin Sci 1996; 90: 433-434.

95. Peterson LH, Jensen RE, Parnell J. Mechanical properties of arteries *in vivo* . Circ Res 1960; 8: 622-639.

96. Schmitz-Rixen T, Hamilton G. Compliance: a critical parameter for maintenance of arterial reconstruction ? In: Greenhalgh RM, Hollier LH (Eds) The maintenance of arterial reconstruction. WB Saunders, London 1991. 23-43.

97. Baird RN, Abbott WM. Pulsatile blood flow in arterial grafts. Lancet 1976; 30: 948-949.

98. Giron F, Birtwell WS, Soroff HS, Deterling RA. Haemodynamic effects of pulsatile and nonpulsatile flow. Arch Surg 1966;93: 902-810.

99. Abbott WM, Megermann JM. Adaptive responses of arteries to grafting. J Vasc Surg 1989; 9: 377-379.

100. Hasson JE, Megermann JM, Abbott WM. Increased compliance near vascular anastomosis. J Vasc Surg 1985; 2: 419-23.

101. Yano Y, Saito Y, Narumiya S, Sumpio B. involvement of rho p21 cyclic strain induced tyrosine phosphorylation of focal adhesion kinase (pp 125FAK), morphological changes and migration of endothelial cells. Biochem Biophys Res Commun 1996;224: 508-515.

102. Cohen C, Mills I, Du W, Sumpio B. Activation of adenylate cyclase, cAMP, PKA pathway in endothelial cells exposed to cyclic strain. Exp Cell Res 1997; 231: 184-189.

103. Sumpio BE, Du W, Galagher G, Wang X, Khachigian L, Collins T *et al.* Regulation of PDGF-B in endothelial cells exposed to cyclic change. Arterioscler Thromb Vasc Biol 1998;18: 349.

104. Sottirai VS, Sue SI, Feinberg EL, Bringaze WL, Tran AT, Batson RC. Distal anastomotic intimal hyperplasia: biogenesis and aetiology. Eur J Vasc Endovasc Surg 1988; 2: 245-56

105. Predel HG, Yang Z, von Segesser, Turina M, Buhler FR, Luscher TF. Implication of pulsatile stretch on growth of saphenous vein and mammary artery smooth muscle. Lancet 1992; 340: 878-9.

106. Weston MW. Rhee K. Tarbell JM. Compliance and diameter mismatch affect the wall shear rate distribution near an end-to-end anastomosis. J Biomechanics. 1996; 29:187-98.

107. Stewart SF, Lyman DJ. Effects of a vascular graft/natural artery compliance mismatch on pulsatile flow. J Biomech 1992; 25: 297-310.

108. Vyalov S, Langille BL, Gotlieb AI. Decreased blood flow disrupts endothelial repair *in vivo*. Am J Path 1996;149: 2107-18.

109. Wakefield TW. Haemostasis. In: Greenfield LJ (Ed). Surgery: scientific principles and practice. JB Lippincott, Philadelphia , 1993. pp 102-124.

110. Najjar FB, Gott VL. The use of small diameter Dacron Grafts with wall-bonded heparin for venous and arterial replacement: canine studies and preliminary clinical experience. Surgery 1970; 68 :1053-63.

111. Rembaum A, Yen SP, Ingram M, Newton JF, Hu CL. Platelet adhesion to heparin-bonded and heparin-free surfaces. Biomat Med Dev Artif Org 1973;1: 99-119.

112. Lagergren H, Larsson R, Olsson P, Radegran K, Swedenborg J. Decreased platelet adhesion as a characteristic of non-thrombogenic heparinised polymer surfaces. Thromb Diath Haem 1975; 34:557.

113. Esquivel CO, Bjorck CG, Bergantz SE, Bergqvist D, Larsson R, Carson SN *et al.* Reduced thrombogenic characteristics of expanded polytetraethylene and polyurethane arterial grafts after heparin bonding. Surgery 1984; 95; 102-7.

114. Norjiri C, Park KD, Grainger DW, Jacobs HA, Okanu T, Koyanagj H. *In vivo* nonthrombogenicity of heparin-immobilised polymer surfaces. ASAIO Transactions 1990; 36: M168-172.

115. Ritter EF, Kim YB, Reischl HP, Serafin D, Rudner AM, Klitzman B. Heparin coating of vascular prostheses reduces thromboemboli. Surgery 1997;122: 888-892.

116. Lambert AW, Fox AD, Williams DJ, Horrocks M, Budd JS. Experience with heparin-bonded collagen coated grafts for infrainguinal bypass. Cardiovasc surg 1999; 7: 491-4.

117. Rubens FD, Weitz JL, Kinlough-Rathbone RL. The effect of antithrombin III-independent thrombin inhibitors and heparin on fibrin accretion onto fibrin-coated polyethylene. Thromb Haemost 1993; 69 :130-134.

118. Swartbol P, Norgren L. Quantitative analysis of heparin retention on heparin bonded knitted Dacron grafts after exposure to shear stress *in vitro*. Int Angio 1996;15 : 232-5.

119. Becquemin JP, Riff Y, Kovarsky S, Ardaillou N, Benhaien-Sigaux N. Evaluation of a polyester collagen-coated heparin-bonded vascular graft. J Cardiovasc Surg 1997; 38: 7-14.

120. Almeida JI, Liem TK, Silver D. Heparin-bonded grafts induce platelet aggregation in the presence of heparin-associated antiplatelet antibodies. Journal of Vascular Surgery. 1998; 27:896-900.

121. Christenson JT, Thulesius O, Owunwanne A, Nazzal M. Forskolin impregnation of small calibre PTFE grafts lowers early platelet graft sequestation and improves patency in a sheep model. Eur J Vasc Surg 1991; 5: 271-275.

122. Hall JD, Rittgers SE, Schmidt SP. Effect of controlled local acetylsalicylic acid release on *in vitro* platelet adhesion to vascular grafts. J Biomed App 1994; 8: 361-84.

123. Van der Lei B, Bartels HL, Robison PH, Bakker WW. Reduced thrombogenicity of vascular prostheses by coating with ADP-ase. Int Angio 1992; 11: 268-271.

124. Greco RS, Kim HC, Donetz AP, Harvey RA. Patency of a small vessel prosthesis bonded to tissue plasminogen activator and iloprost. Ann Vasc Surg 1995; 9: 140-5.

125. Kusserow BK, Larrow R, Nichols J. The urokinase-heparin bonded synthetic surface. An approach to the creation of a prosthetic surface possessing composite antithrombogenic and thrombolytic properties. Trans ASAIO 1971;17: 1-5.

126. Miller RM, Taylor DE, Ringrose BS. Biotolerant and haemodynamic effects of copolymerisation with acrylic acid on Dacron arterial prostheses. Ann R Coll Surg Eng 1986; 68: 85-8 .

127. Tsuchida H, Cameron BL, Marcus CS, Wilson SE. Modified polytetrafluoroethylene: indium 111-labelled platelet deposition on carbon-lined and high-porosity polytetrafluoroethylene grafts. J Vasc Surgery. 1992;16:643-9 .

128. Bird RL, Hall B, Hobbs KE, Chapman D. New haemocompatible polymers assessed by thromboelastography. J Biomed Engineer 1989;11:231-4 .

129. Schlosser E, Simler R, Hormann H. Retention of thrombin by polytetrafluororethylene: influence on the adsorption of fibrinogen/fibrin. Biomaterials 1993;14: 365-70.

130. Bacourt F. Prospective randomized study of carbon-impregnated polytetrafluoroethylene grafts for below-knee popliteal and distal bypass: results at 2 years. Anns Vasc Surg 1997;11:596-603.

131. Kalman PG, McCullough DA, Ward CA. Evacuation of microscopic air bubbles from Dacron reduces complement activation and platelet aggregation. J Vasc Surg 1990;11:591-8.

132. Vann RD, Ritter EF, Plunkett MD, Wyble CW Jr, Bensen CV, Gerth WA. Patency and blood flow in gas denucleated arterial prostheses. J Biomed Mat Res. 1993; 27:493-8.

133. Ritter EF, Fata MM, Rudner AM, Klitzman B. Heparin bonding increases patency of long microvascular prostheses. Plas Reconstructive Surg 1998;101:142-146 .

134. LeBlanc J. Albus R. Williams WG. Moes CA. Wilson G. Freedom RM. Trusler GA. Serous fluid leakage: a complication following the modified Blalock-Taussig shunt. J Thoracic Cardiovasc Surg 1984; 88: 259-62.

135. Cronenwett JL. Arterial Haemodynamics. In: Greenfield LJ (Ed). Surgery: scientific principles and practice. JB Lippincott, Philadelphia , 1993.

136. Simionescu M, Simionescu N. Functions of the endothelial cell surface. Ann Rev Physiol 48: 279-93 1986

137. Shireman PK, Pearce WH. Endothelial cell function in health and disease. AJR 166:7-13 1996.

138. Clagett GP. Occlusive disease: thrombosis. In: Greenfield LJ (Ed). Surgery: scientific principles and practice. JB Lippincott, Philadelphia , 1993. p 1470-1478.

139. Edwards WS: The effect of porosity in solid plastic grafts. Surg Forum 1957; 8: 446.

140. Weslowski SA, Fries CC, Karlson KE, De Bakey M, Sawyer PN. Porosity: primary determinant of ultimate fate of synthetic vascular grafts. Surgery 1961; 50: 91-96.

141. Ottinger LW, Darling RC, Wirthlin LS, Linton RR. Failure of ultra-lightweight knitted dacron grafts in arterial reconstruction. Arch Surg 1976; 111:146-149.

142. Cambell CD, Godfarb D, Roe R. A small arterial substitute : expanded microporous polytetrafluoroethylene : patency vs porosity. Ann Surg 1975; 182:138-143.

143. Cameron BL, Tsuchida H, Connal TP, Nagae T, Furukawa K, Wilson SE. High porosity PTFE improves endothelialisation of arterial grafts without increasing early thrombogenicity. J Cardiovasc Surg 1993; 34: 281-5.

144. Akers DL, Du YH, Kempczinski RF. The effect of carbon coating and porosity on early patency of expanded polytetrafluoroethylene grafts: an experimental study. J Vasc Surg. 1993; 18:10-15.

145. Clowes AW, Zacharias RK, Kirkman TR. Early endothelial coverage of synthetic arterial grafts: porosity re-visited. Am J Surg 1987; 153: 501-4.

146. Kohler TR, Stratton JR, Kirkman TR, Johansen KH, Zierler BK, Clowes AW. Conventional versus high-porosity polytetrafluoroethylene grafts: clinical evaluation. Surgery 1992; 112:901-7.

147. Martokas P, Karwoski T. Healing characteristics of hybrid and conventional polytetrafluoroethylene vascular grafts. ASAIO 1995; 41:735-740.

148. Gray JL, Kang SS, Zenni GC, Kim DU, Kim PI, Burgess WH *et al.* FGF-1 affixation stimulates ePTFE endothelialization without intimal hyperplasia. J Surg Res 1994; 57: 596-612.

149. Doi K, Matsuda T. Enhanced vascularisation in a microporous polyurethane graft impregnated with basic fibroblast growth factor and heparin. J Biomed Mater Res 1997; 34:361-70.

150. Greisler HP, Gosselin C, Ren D, Kang SS, Kim DU. Bioactive polymers and tissue engineered blood vessels. Biomater 1996; 17; 329-36.

151. Herring MD, Gardner A, Glover J. A single-staged technique for seeding vascular grafts with autogenous endothelium. Surgery 1978; 84: 498-504.

152. Hunter TJ, Schmidt SP, Sharp WV, Malindzak GS. Controlled flow-studies in 4mm endothelialised dacron grafts. Trans Am Soc Artif Org 1983; 29 :177-182.

153. Allen BT, Long JA, Clark RE, Sicard GA, Hopkins KT, Welch MJ. Influence of endothelial cell seeding on platelet deposition and patency in small-diameter Dacron arterial grafts. J Vasc Surg 1984 ;1: 224-33.

154. Kempczinski RF, Rosenman JE, Pearce WH, Roedersheimer LR, Berlatzky Y, Ramalanjaona GJ. Endothelial cell seeding of a new PTFE vascular prosthesis. J Vasc Surg 1985; 2: 424-429.

155. Pannell RC, Hollier LH, Solis E, Kaye MP. Xenograft seeding of Dacron grafts in dogs. J Surg Res 1986; 40: 332-339 .

156. Shepard AD, Eldrup-Jorgensen J, Keough EM, Foxall TF, Ramberg K, Connolly RJ *et al.* Endothelial cell seeding of small-caliber synthetic grafts in the baboon. Surgery 1986; 99:318-326

157. Budd JS, Allen KE, Hartley G, Bell PR. The effect of preformed confluent endothelial cell monolayers on the patency and thrombogenicity of small calibre vascular grafts. Eur J Vasc Surg 1991; 5: 397-405.

158. Sicard GA, Allen BT, Long JA, Welch MJ, Griffin A, Clark RE *et al.* Prostaglandin production and platelet reactivity of small-diameter grafts. J Vasc Surg 1984; 1:774 - 781.

159. Jensen N, Lindblad B, Ljungberg J, Leide S, Bergqvist D. Early attachment of platelets, leukocytes and fibrinogen in endothelial cell-seeded Dacron grafts. Ann Vasc Surg 1996;10:530-536.

160. Budd JS, Allen K, Hartley J, Walsh A, James RF, Bell PR. Prostacyclin production from seeded prosthetic vascular grafts. Br J Surg 1992; 79: 1151-1153.

161. Lewis DA, Lowell RC, Cambria RA, Roche PC, Gloviczki P, Miller VM. Production of endothelium-derived factors from sodded expanded polytetrafluoroethylene grafts. J Vasc Surg 1997; 25: 187-97.

162. Birinyi LK, Douville EC, Lewis SA, Bjornsen HS, Kempczinski RF. Increased resistance to bacteremic graft infection after endothelial cell seeding. J Vasc Surg 1987; 5: 193-7.

163. Keller JD, Falk J, Bjornson HS, Silberstein EB, Kempczinski RF. Bacterial infectibility of chronically implanted endothelial cell-seeded expanded polytetrafluoroethylene vascular grafts. J Vasc Surg 1988; 7: 524-30.

164. Herring MB, Compton RS, LeGrand DR, Gardner AL, Madison DL, Glover JL. Endothelial seeding of polytetrafluoroethylene popliteal bypasses. A preliminary report. J Vasc Surg 1987; 6: 114-148.

165. Herring MB, Baughman S, Glover J. Endothelium develops on seeded human arterial prosthesis: a brief clinical note. J Vasc Surg 1985; 2: 727-730.

166. Herring MB, Smith J, Dalsing M, Glover J, Compton R, Etchberger K *et al.* Endothelial seeding of polytetrafluoroethylene femoral popliteal bypasses: The failure of low-density seeding to improve patency. J Vasc Surg 1994; 20;650-5.

167. Ortenwall P, Wadenvik H, Kutti J, Risberg B. Reduction in deposition of indium 111-labelled platelets after autologous endothelial cell seeding of Dacron aortic bifurcation grafts in humans : a preliminary report. J Vasc Surg 1987; 6 :17-25.

168. Ortenwall P, Wadenvik H, Risberg B. Reduced platelet deposition on seeded versus unseeded segments of expanded polytetrafluoroethylene grafts : clinical observations after a 6-month follow-up. J Vasc Surg1989; 10:374-380.

169. Jensen N, Lindblad B, Bergqvist D. Endothelial cell seeded dacron aortobifurcated grafts : Platelet deposition and long-term follow-up. J Cardiovasc Surg 1994; 35: 425-429

170. Smyth JV, Welch M, Carr HM, Dodd PD, Eisenberg PR, Walker MG. Fibrinolysis profiles and platelet activation after endothelial cell seeding of prosthetic vascular grafts. Ann Vasc Surg 1995; 9: 542-546.

171. Magometschnigg H, Kadletz M, Vodrazka M, Dock W, Grimm M, Grabenwoger M *et al.* Prospective clinical study with *in-vitro* endothelial cell lining of expanded

polytetrafluoroethylene grafts in crural repeat reconstruction. J Vasc Surg 1992; 15: 527-535.

172. Zilla P, Fasol R, Deutsch M, Fischlein T, Minar E, Hammerle A *et al.* Endothelial cell seeding of polytetrafluoroethylene vascular grafts in humans: A preliminary report. J Vasc Surg 1987; 6 : 535-41.

173. Zilla P, Deutsch M, Meinhart J, Puschmann R, Eberl T, Minar E *et al.* Clinical *in vitro* endothelialisation of femoropopliteal bypass grafts : An acturarial follow-up over three years. J Vasc Surg 1994;19 : 540-548.

174. Zilla P, Deutsch M, Meinhart J, Fischlein T, Hofman G. Long-term effects of clinical *in vitro* endothelialisation on grafts. J Vasc Surg 1997; 25: 1110-1112.

175. Schneider P, Hanson S, Price T, Harker L. Durability of confluent endothelial cell monolayers on small-caliber vascular prostheses *in vitro*. Surgery 1988; 103 : 456-462.

176. Sharp WV, Schmidt SP, Meerbaum SO, Pippert TR. Derivation of human microvascular endothelial cells for prosthetic vascular graft seeding. Ann Vasc Surg 1989; 3; 104-7.

177. Jarrell BE, Williams SK, Stokes G, Hubbard FA, Carabasi RA, Koolpe E *et al.* Use of freshly isolated capillary endothelial cells for the immediate establishment of a monolayer on a vascular graft at surgery. Surgery 1986;100: 392-9.

178. Williams SK, Jarrell BE, Rose DG, Pontell J, Kapelan BA, Park PK *et al.* Human microvessel endothelial cell isolation and vascular graft sodding in the operating room. Ann Vasc Surg 1989; 3: 146-52.

179. Schmidt SP, Monnajjem N, Evancho MM, Pippert TR, Sharp WV. Microvascular endothelial cell seeding of small-diameter Dacron vascular grafts. J Invest Surg 1988;1: 35-44.

180. Stansby G, Shukla N, Hamilton G, Jeremy J. Comparison of prostanoid synthesis in cultured human vascular endothelial cells derived from omentum and umbilical vein. Eur J Vasc Surg 1991; 5; 501-506.

181. Pasic M, Muller-Glauser W, Odermatt B, Lachat M, Seifert B, Turina M. Seeding with omental cells prevents late neointimal hyperplasia in small-diameter Dacron grafts. Circulation 1995;92 : 2605-2616.

182. Williams SK, Rose DG, Jarrell BE. Microvascular endothelial cell sodding of ePTFE vascular grafts: Improved patency and stability of the cellular lining. J Biomed Mater Res 1994; 28: 203-12.

183. Hewett PW, Clifford Murray J. Immunomagnetic purification of human microvessel endothelial cells using Dynabeads coated with monoclonal antibodies to PECAM-1. Eur J Cell Biol 1993; 62: 451-454.

184. Springhorn JP, Madri JA, Squinto SP. Human capillary endothelial cells from abdominal wall adipose tissue: isolation using an anti-PECAM antibody. In Vitro Cell Dev Biol - Animal 1995; 31: 473-481.

185. Bull HA, Pittilo RM, Drury J, Pollock JG, Clarke JM, Woolf N *et al.* Effects of autologous mesothelial cell seeding on prostacyclin production within Dacron arterial prostheses. Br J Surg 1988; 75:671-4.

186. Verhagen HJ, Heinen-Snyder GJ, Pronk A, Vroom TM, van Vroonhoven TJ, Eikelboom BC *et al.* Thrombomodulin activity on mesothelial cells: perspectives for mesothelial cells as an alternative for endothelial cells for cell seeding on vascular grafts. Br J Haem 1996; 95 : 542-549.

187. Pronk A, de Groot PG, Hoynck van Papendrecht AA, Verbrugh HA, Leguit P, van Vroonhoven TJ *et al.* Thrombogenicity and procoagulant activity of human mesothelial cells. Arterioscler Thromb 1992;12:1428-36

188. Hedeman Joosten PP, Verhagen HJ, Heijnen-Snyder GJ, van Vroonhoven TJ, Sixma JJ, de Groot PG *et al.* Thrombogenesis of different cell types seeded on vascular grafts and studied under blood-flow conditions. J Vasc Surg 1998; 28:1094-1103.

189. Verhagen HJM, Blankensteijn JD, de Groot PG, Heijnen-Snyder GJ, Pronk A, Vroom TM *et al. In vivo* experiments with mesothelial cell seeded ePTFE vascular grafts. Eur J Vasc Endovasc Surg 1998;15: 489-496.

190. van Wechem PB, Stronck JW, Koers-Zuideveld R, Dijk F, Wildevuur CR. Vacuum cell seeding: a new method for the fast application of an evenly distributed cell layer on porous vascular grafts. Biomater 1990; 11: 602-606

191. Bowlin GL, Rittgers SE. Electrostatic endothelial cell seeding technique for small-diameter (<6mm) vascular prostheses: feasibility testing. Cell Transplant 1997; 6 :623-629

192. Bowlin GL, Rittgers SE. Electrostatic endothelial cell transplantation within small-diameter (<6mm) vascular prostheses: a prototype apparatus and procedure. Cell Transplant 1997; 6: 631-7

193. Rosenman JE, Kempczinski RF, Pearce WH, Silberstein EB. Kinetics of endothelial cell seeding. J Vasc Surg 1985; 2 : 778-784

194. Kent KC, Oshima A, Whittemore AD. Optimal seeding conditions for human endothelial cells. Anns Vasc Surg 1992; 6:258-264.

195. Carr HM, Vohra R, Sharma H, Smyth JV, Rooney OB, Dodd PD *et al.* Endothelial cell seeding kinetics under chronic flow in prosthetic grafts. Ann Vasc Surg 1996;10 : 469-75.

196. Ramalanjaona G, Kempczinski RF, Rosenman JE, Douville EC, Silberstein EB. The effect of fibronectin coating on endothelial cell kinetics in polytetrafluoroethylene grafts. J Vasc Surg 1986; 3:264-72.

197. Ivarsson BL, Cambria RP, Megerman J, Abbott WM. Fibronectin enhances early shear stress resistance of seeded adult human venous endothelial cells. J Surg Res 1989; 47:203-7.

198. Thomson GJ, Vohra RK, Carr MH, Walker MG. Adult human endothelial cell seeding using expanded polytetrafluoroethylene vascular grafts: a comparison of four substrates. Surgery 1991;109:20-7.

199. Stansby G, Shukla N, Fuller B, Hamilton G. Seeding of human microvascular endothelial cells onto polytetrafluoroethylene graft material. Br J Surg 1991; 78:1189-92.

200. Li JM, Menconi MJ, Wheeler HB, Rohrer MJ, Klassen VA, Ansell JE *et al.* Precoating expanded polytetrafluoroethylene grafts alters production of endothelial cell-derived thrombomodulators. J Vasc Surg 1992; 15: 1010-1017.

201. Walluscheck KP, Steinhoff G, Kelm S, Haverich A. Improved endothelial cell attachment on ePTFE vascular grafts pretreated with synthetic RGD-containing peptides. Eur J Vasc Endo Surg 1996;12:321-30.

202. Dekker A, Poot AA, van Mourik JA, Workel MP, Beugeling T, Bantjes A *et al.* Improved adhesion and proliferation of human endothelial cells on polyethylene precoated with monoclonal antibodies directed against cell membrane antigens and extracellular matrix proteins. Thromb-Haemost 1991; 66 :715-24.

203. Gosselin C, Vorp DA, Warty V, Severyn DA, Dick EK, Borovetz HS *et al.* ePTFE coating with fibrin glue, FGF-1, and heparin: effect on retention of seeded endothelial cells. J Surg Res 1996; 60:327-32.

204. Schneider A, Chandra M, Lazarovici G, Vlodavsky I, Merin G, Uretzky G *et al.* Naturally produced extracellular matrix is an excellent substrate for canine endothelial cell proliferation and resistance to shear stress on PTFE vascular grafts. Thromb Haemost 1997; 78:1392-8.

205. Ott MJ, Ballerman BJ. Shear-stress conditioned, endothelial cell-seeded vascular grafts: improved cell adherence in response to *in vitro* shear-stress Surgery 1995;17: 334-9.

206. Dardik A, Liu A, Ballerman BJ. Chronic *in vitro* shear stress stimulates endothelial cell retention on prosthetic vascular grafts and reduces subsequent *in vivo* neointimal thickness. J Vasc Surg 1999; 29:157-167.

207. Shayani V, Newman KD, Dichek DA. Optimization of recombinant tPA secretion from seeded vascular grafts. J Surg Res 1994; 57:495-504.

208. Robinson KA, Candal FJ, Scott NA, Ades EW. Seeding of vascular grafts with an immortalised human dermal microvascular endothelial cell line. Angiology 1995; 46: 107-13.

209. Sackman JE, Freeman MB, Petersen MG, Allebban Z, Niemeyer GP, Lothrop CD Jr. Synthetic vascular grafts seeded with genetically modified endothelium in the dog: evaluation of the effect of seeding technique and retroviral vector on cell persistence *in vivo*. Cell Trans 1995; 4: 219-35.

210. Dunn PF, Newman KD, Jones M, Yamuda I, Shayani V, Virmani R, Dichek DA. Seeding of vascular grafts with genetically modified endothelial cells. Secretion of recombinant TPA results in decreased seeded cell retention in-vitro and in-vivo. Circulation 1996; 93: 1439-46.

211. Jankowski RJ, Severyn DA, Vorp DA, Wagner WR. Effects of retroviral transduction on human endothelial cell phenotype and adhesion to Dacron vascular grafts. J Vasc Surg 1997; 26: 676-84.

212. Kaufman BR, Fox PL, Graham LM. Platelet-derived growth factor production by canine aortic grafts seeded with endothelial cells. J Vasc Surg 1992;15: 699-706.

213. Shindo S, Tada Y, Egami J, Yamamoto K, Sato O, Takagi A *et al.* Perianastomotic findings in canine endothelial cell seeded grafts at 3 months. ASAIO Journal 1993; 39:132-6.

214. L'Italien GJ, Megerman J, Hasson JE, Meyer AE, Baier RE, Abbott WM. Compliance changes in glutaraldehyde-treated arteries. J Surg Res 1986; 41; 182-8.

215. Abbott WM, Megerman JM, Hasson JE, L'Italien G, Warnock D. Effect of compliance mismatch upon vascular graft patency J Vasc Surg 1987; 5: 376-382.

216. Trubel W, Schima H, Moritz A, Raderer F, Windisch A, Ullrich R *et al.* Compliance mismatch and formation of distal anastomotic intimal hyperplasia in externally stiffened and lumen adapted venous grafts. Eur J Vasc Endovasc Surg 1995;10: 415-423.

217. Zenni GC, Gray JL, Appelgren EO, Kim DU, Bercelli S, Ligush J *et al.* Modulation of myofibrobalst proliferation by vascular prosthesis biomechanics. ASAIO J 1993; 39: M496-M500.

218. Uchida N, Kambic H, Emoto H, Chen JF, Hsu SH, Murabayshi S *et al.* Compliance effect on small diameter vascular graft patency . J Biomed Mater Res 1993; 27:1269-1279.

219. Wu MH, Shi Q, Sauvage LR, Kaplan S, Hayashida N, Patel MD *et al* . The direct effect of compliance mismatch *per se* on development of host arterial intimal hyperplasia at the anastomotic interface. Anns Vasc Surg 1993; 7;156-168.

220. Usui Y, Goff SG, Sauvage LR, Wu HD, Robel SB, Walker M. Effect of healing on compliance of porous Dacron grafts. Anns Vasc Surg 1988; 2; 120-6.

221. Kenney DA, Tu R, Peterson RC. Evaluation of compliant and noncompliant PTFE vascular prostheses. Trans Am Soc Artif Org 1988;34: 661-662.

222. White RA, Klein SK, Shors EC. Preservation of compliance in a small diameter microporous silicone rubber prosthesis. J Cardiovasc Surg 1987; 28:485-490.

223. Whalen RL, Cardona RR, Kantrwitz A. A new all silicone rubber small vessel prosthesis. ASAIO journal 1992; 38: M207-212.

224. Zdrahala RJ. Small caliber vascular grafts. Part II: polyurethanes revisisted. J Biomater Appl 1996; 11: 37-61.

225. Coury AJ. Biostable polymers as durable scaffolds for tissue engineered vascular prostheses. In: Zilla P, Greisler HP (Eds). Tissue engineering of prosthetic vascular grafts. RG Landes, Austin, Texas 1999. p469-488.

226. Santerre JP, Labow RS, Adams GA: Enzyme-biomaterial interactions: effect of biosystems on degradation of polyurethanes. J Biomed Mater Res 1993;27: 97-109

227. Szycher M. Surface fissuring of polyurethanes following *in vivo* exposure . Fraker and Griffin (Eds): ASTM STP 859. Philadelphia 1983 p 308-321.

228. Phua SK, Anderson JM. Biodegradation of a polyurethane *in vitro*. J Biomed Mater Res 1987; 21:231-246.

229. Zhao Q, McNally AK, Rubin KR, Renier M, Wu Y, Rose-Capara J *et al.* Human plasma alpha-2-macroglobulin promotes oxidative stress cracking of pellathane 2363-80A: *in vivo* and *in vitro* correlations. J Biomater Res 1993; 27: 379-389.

230. De Cossart L, How TV, Annis D. A two year study of the performance of a small diameter polyurethane (Biomer) arterial prosthesis. J Cardiovasc Surg 1989;30: 388-394.

231. Martz H, Paynter R, Forest JC, Downs A, Guidon R. Microporous hydrophillic polyurethane vascular grafts as substitutes in the abdominal aorta of dogs. Biomaterials 1987; 8:3-11.

232. Martz H, Paynter R, Ben Slimane S, Beaudoin G, Guidon R *et al.* Hydrophillic microporous polyurethane versus expanded PTFE grafts as substitutes in the carotid arteries of dogs. A limited study. J Biomed Mater Res 1988; 22: 63-69

233. Marois Y, Guidon R, Boyer D, Assayed F, Doillon CJ, Paynter R *et al. In vivo* evaluation of hydrophobic and fibrillar microporous polyurethane urea graft. Biomaterials 1989; 10: 521-531.

234. Marois Y, Akoum A, King M, Guidon R, von Maltzahn W, Kowligi R *et al.* A novel microporous polyurethane vascular graft: *in vivo* evaluation of the UTA prosthesis implanted as infra-renal aortic replacement in dogs. J Invest Surg 1993; 6: 273-288.

235. Bull PG, Denck H, Guidon R, Gruber H. Preliminary clinical experience with polyurethane vascular prostheses in femoro-popliteal reconstruction. Eur J Vasc Surg 1992; 6: 217-224

236. Zhang Z, King M, Guidon R, Therrien M, Doillon C, Diehl-Jones WL *et al. In vitro* exposure of novel polyesterurethane graft to enzymes: a study of the biostability of the vascugraft arterial prosthesis. Biomaterials 1994; 15: 1129-1144.

237. Marois Y, Paris E, Zhang A, Doillon CJ, King MW, Guidoin RG. Vascugraft microporous polyesterurethane arterial prosthesis as a thoraco-abdominal bypass in dogs. Biomaterials 1996; 17: 1289-1300.

238. Zhang Z, Marois Y, Guidoin RG, Bull P, Marois M, How T *et al* . Vascugraft polyurethane arterial prosthesis as femoro-popliteal and femoro-peroneal bypass in humans: pathological, structural and chemical analyses of four excised grafts. Biomaterials 1997; 18:113-124.

239. Wilson GJ, MacGregor DC, Klement P, Dereume JP, Weber BA, Binnington AG *et al.* The composite Corethane/Dacron vascular prosthesis. Canine *in vivo* evaluation of 4mm diameter grafts with 1 year follow-up. ASAIO Trans 1991; 37: M475-M476.

240. Dereume JP, van Romphey A, Vincent G, Engelmann E. Femoropopliteal bypass with a compliant composite polyurethane/Dacron graft: short-term results of a multicentre trial. Cardiovasc Surg 1993;1:499-503.

241. Reed AM, Potter J, Szycher M. A solution grade biostable polyurethane elastomer: Chronoflex AR. J Biomed App 1994; 8: 210-36.

242. Methods and apparatus for making a polymer material. Euro Patent: 0286220. USA Patent: 5132066. Japanese Patent: 63-78318.

243. Edwards A, Carson RJ, Bowald S, Quist WC. Developmant of a microporous compliant small bore vascular graft. J Biomater Apps 1995; 10:171-87.

244. Coury AJ, Slaikeu P, Calahan P, Stokes KB, Hobot CM *et al.* Factors and interactions affecting the performance of polyurethane elastomers in medical devices. J Biomater App 1988; 2:130-179.

245. Edwards A, Carson RJ, Szycher M, Bowald S. *In vitro* and *in vivo* biodurability of a compliant microporous vascular graft. J Biomater Apps 1998; 13:23-45.

246. Giudiceandrea A, Seifalian AM, Krijgsman B, Hamilton G. Effect of prolonged pulsatile shear stress *in vitro* on endothelial cell seeded PTFE and compliant poyurethane vascular grafts . Eur J Vasc Endovasc Surg 1998; 15:147-154.

247. Benetos A, Laurent S, Hoeks AP, Boutouyrie PH, Safar ME. Arterial alterations with ageing and high blood pressure - a noninvasive study of carotid and femoral arteries. Arterioscler Thromb 1993; 13 : 90-97.

248. Van Merode T, Brands PJ, Hoeks APG, Reneman RS. Different effects of aging on elastic and muscular arterial bifurcations in men. J Vasc Res 1996; 33:47-52.

249. Laogun AA, Gosling RG. *In vivo* arterial compliance in man. Clin Phys Physiol Meas 1982 ;3:201-212.

250. Hofstra L, Willigers JM, Huvers FC, Schaper NC, Kester AD, Kitslaan PJ. Short-term variation in the elastic properties of a muscular artery in humans. Clin Sci 1994; 86: 567-574.

251. Glasser SP, Arnett DK, McVeigh GE, Finkelstein SM, Bank AJ, Morgan DJ *et al.* Vascular compliance and cardiovascular disease: a risk factor or a marker ? Am J Hypertension 1997;10:1175-1189.

252. Newman DL, Gosling RG, Bowden NLR. Changes in aortic distensibility and area ratio with the development of atherosclerosis. Atherosclerosis 1973 ;14: 231-234.

253. Kawasaki T, Sasayama S, Yagi SI, Asakawa T, Hirai T. Non-invasive assessment of the age-related changes in stiffness of major branches of the human arteries. Cardiovasc Res 1987; 21:678-687.

254. Sonesson B, Hansen F, Stale H, Lanne T. Compliance and diameter in the human abdominal aorta - the influence of age and sex. Eur J Vasc Surg 1993; 7: 690-697

255. Wada T, Fujishiro K, Fukomoto T, Yamazaki S. Relationship between ultrasound assessment of arterial wall properties and blood pressure. Angiology 1997;48: 893-900.

256. Dahlberg G. Statistical methods for medical and biological students. 2nd Edition. Allen and Unwin Ltd, London 1948.

257. Bland JM, Altman DG. Statistical methods for assessing agreement between two methods of clinical measurement. Lancet 1986;1: 307-310.

258. Hoeks APG, Brands PJ, Reneman RS. Assessment of the arterial distension waveform using doppler signal processing. J Hypertension 1992; 10: S19-S22

259. Hoeks APG, Reneman RS. Biophysical principles of vascular diagnosis. J Clin Ultrasound 1995;23:71-79

260. Seifalian AM, Giudiceandrea A, Schmitz-Rixen T, Hamilton G. Noncompliance: the silent acceptance of a villain. In: Zilla P, Greisler HP (Eds). RG Landes, Philadelphia, 1999. p45-58.

261. Lanne T, Stale H, Bengtsson H, Gustafsson D, Bergquist D, Sonesson B *et al.* Noninvasive measurement of diameter changes in the distal abdominal aorta in man. Ultrasound Med Biol 1992; 18: 451-457.

262. Reneman RS, Van Merode T, Hick P, Muytjens AMM, Hoeks APG. Age-related changes in carotid arterial wall properties in men. Ultrasound Med Biol 1986 ;12:465 – 471.

263. Van Merode T, Lodder J, Smeets FAM, Hoeks APG, Reneman RS. Accurate non-invasive method to diagnose minor atherosclerotic lesions in the carotid artery bulb. Stroke 1989;20: 1336-40.

264. Hansen F, Mangell P, Sonesson B, Lanne T. Diameter and compliance in the human common carotid artery - variations with age and sex. Ultrasound Med Biol 1995; 21:1-9.

265. Kool MJF, Van Merode T, Reneman RS, Hoeks APG, Struyker Boudier HAJ, Van Bortel LMAB. Evaluation of reproducibility of a vessel wall movement detector system for assessment of large artery properties. Cardiovasc Res 1994; 28 : 610-614.

266. Hansen F, Berggvist D, Mangell P, Ryden A, Sonesson B, Lanne T. Non-invasive measurement of pulsatile vessel diameter change and elastic properties in human arteries: a methodological study. Clin Physiology 1993; 13 :631-643.

267. Farrar DJ, Bond MG, Riley WA, Sawyer JK. Anatomic correlates of aortic pulse wave velocity, and carotid artery elasticity during atherosclerosis progression and regression in monkeys. Circulation 1991;83:1754 -1763.

268. Dart AM, Lacombe F, Yeoh JK, Cameron JD, Jennings GL, Laufer E *et al.* Aortic distensibility in patients with isolated hypercholesterolaemia, coronary artery disease or cardiac transplant. Lancet 1991;338: 270-273.

269. Lehmann ED, Hopkins KD, Jones RL, Rudd AG, Gosling RG. Aortic distensibility in patients with cerebrovascular disease. Clin Sci 1995 ; 89: 247-253.

270. Aviolo AP, Chen SG, Wang RP, Zang CL, Li MF, O'Rourke MF. Effects of aging on changing arterial compliance and left ventricular load in a northern chinese urban community. Circulation 1983; 68: 50-58.

271. Schultz RD, Hokanson DE, Strandness DR Jr. Pressure-flow and stress-strain measurements of normal and diseased aortoiliac segments. Surg Gynecol Obstet 1967;124:1267.

272. Clowes AW. Arteriosclerosis and the pathogenesis of occlusive disease. In: Greenfield LJ, Mulholland MW, Oldham KT, Zelenock GB, (Eds). Surgery: Scientific principles and practice.: J B Lippincott Company, Philadelphia 1993. p 1447-1458.

273. Relationship of structure to function of the tissues of the wall of blood vessels. Physiol Rev 1953;34: 619-642.

274. Roach MR, Burton AC. The reason for the shape of the distensibility curves of arteries. Can J Biochem Physiol 1967; 35 :691-90.

275. Jaffe EA, Nachman RL, Becker CG, Minick CR. Culture of human endothelial cells derived from umbilical veins . Identification by morpologic and and immunologic criteria. J Clin Invest 1973; 52:2745-56.

276. Sharefkin JB, Lather C, Smith M, Rich NM. Endothelial cell labeling with indium-111 oxine as a marker of cell attachment to bioprosthetic surfaces. J Biomed Mater Res 1983;17: 345-57.

277. Budd JS, Bell PRF, James RF. Attachment of indium-111 labelled endothelial cells to pretreated polytetrafluoroethylene vascular grafts. Br J Surg 1989;76:1259-61.

278. Anderson JS, Price TM, Hanson SR, Harker LA. *In vitro* endothelialisation of small-caliber vascular grafts. Surgery 1987;101:577-86.

279. Stansby G, Shukla G, Berwanger C, Seifalian AM, Fuller B, Hamilton G. 111 Indium labeling of endothelial cells: potential problems when applied to studies of vascular graft seeding. International J Angiology 1994;3:86-89.

280. Wolf S, Werthessen NT. Fluid mechanics of arterial flow. In: Dynamics of arterial flow. (Advances in experimental medicine and biology volume 115). Plenum Press, New York, 1978. p55-103.

281. Sclichting H. Boundary layer theory. McGraw-Hill, New York, 1968. p536-562.

282. Chang C, Atabek H. The inlet length for oscillatory flow and its effect on the determination of rate of flow in artery. Phys Med Biol 1961;6: 303-317.

283. Sank A, Rostami K, Weaver F, Ertl D, Yellin A, Nimni M, Tuan TL. New evidence and new hope concerning endothelial cell seeding of vascular grafts. Am J Surg 1992; 164:199-204.

284. Stansby G, Berwanger C, Shukla N, Hamilton G. Endothelial cell seeding of vascular grafts: status and prospects. Cardiovascular Surgery 1994;2:543-548.

285. Miwa H, Matsuda T, Tani N, Kondo K, Iida F. An *in vitro* endothelialised compliant vascular graft minimises anastomotic hyperplasia. ASAIO Journal 1993; 39: M501-5.

286. Poole-Warren LA, Schindhelm K, Grahma AR, Slowiaczek PR, Noble KR. Performance of small diameter synthetic vascular prostheses with confluent autologous endothelial cell linings. J Biomed Biomater Res 1996 ; 30:221-29.

287. Williams SK, Carter T, Park PK, Rose DG, Schneider T, Jarrell BE. Formation of a multicellular lining on a polyurethane vascular graft following endothelial cell sodding. J Biomedical Mater Res 1992; 26:103-17.

288. Lin HB, Sun W, Mosher DF, Garcia-Echeverria C, Schaufeflberger K, Lelkes PI, Cooper SL. Synthesis, surface and cell-adhesion properties of polyurethanes containing covalently grafted RGD-peptides. J Biomedica Mater Res 1994; 28: 329-342.

289. Stansby G, Berwanger C, Shukla N, Schmitz-Rixen T, Hamilton G. Endothelial seeding of compliant polyurethane vascular graft material. Brit J Surg 1994; 81: 1286-1289.

290. Consigny PM, Vitali NJ. Resistance of freshly adherent endothelial cells to detachment by shear stress is matrix and time dependent. JVIR 1998;9:479-485.

291. Vohra R, Thomson GJL, Carr HMH, Sharma H, Walker MG. Comparison of different vascular prostheses and matrices in relation to endothelial seeding. Br J Surg 1991;78: 417-420.

292. Curti T, Pasuinelli G, Preda P, Frerie A, Laschi R, D' Addato M. An ultrastructural and immunocytochemiacl analysis of human endothelial cell adhesion on coated vascular grafts. Ann Vasc Surg 1989;4:351-363.

293. Suguwara Y, Pasuinelli G, Preda P, Frerie A, Laschi R, D'Addato M. An ultrastructural and immunocytochemical analysis of human endothelial cell adhesion on coated vascular grafts. Ann Vasc Surg 1989;4:351-363

294. Thomson JL, Vohra R, Walker MG. Cell seeding for small diameter ePTFE vascular grafts: a comparison between adult human endothelial cells and mesothelial cells. Ann Vasc Surg 1989; 2:140-145.

295. Thompson MM, Budd JS, Eady SL, James RFL, Bell PRF. Effect of pulsatile shear stress on endothelial attachment to native vascular surfaces. Brit J Surg 1994; 81: 1121-1127.

296. Kesler KA, Herring M, Arnold MP, Glover JL, Park HM, Helmes MN *et al.* Enhanced strength of endothelial cell attachment on polyester elastomer and polytetrafluoroethylene graft surfaces with fibronectin substrate. J Vasc Surg 1986; 3: 58-64.

297. Jensen N, Lindblad B, Leide S, Bergqvist D. Loss of seeded endothelial cells *in vivo*. A study of Dacron grafts under different flow conditions. Eur J Vasc Endovasc Surg 1994;8:690-693.

298. Page B, Page M, Noel C. A new fluorometric assay for cytotoxicity measurements *in vitro*. Int J Oncol 1993;3:473-476.

299. Nikolaychik VV, Samet MM, Lelkes PI. A new method for continual quantitation of viable cells on endothelized polyurethanes. J Biomater Sci Polymer Edn 1996;7:881-891

300. Zhao Q, Casas-Bejar J, Urbanski P, Stokes K. Glass wool-$H_2O_2/CoCl_2$ test system for *in vitro* evaluation of biodegradative stress cracking in polyurethane elastomers. J Biomed Mater Res 1995;29:467-475

301. Hao YL, Ingham KC, Wickerhauser M. Fractional precipitation of proteins with polyethylene glycol. In: Curling JM (Ed). Methods of plasma protein fractionation. Academic Press, New York, 1980. p57-74.

302. Labow RS, Santerre JP, Waghray G. The effect of phospholipids on the biodegradation of polyurethanes by lysosomal enzymes. J Biomater Sci Polymer Edn 1997;8: 779-795.

303. Meijs GF, McCarthy SJ, Rizzardo E, Chen Y, Chatelier RC, Brandwood A, Schindhelm K: Degradation of medical grade polyurethane elastomers: The effect of hydrogen peroxide *in vitro.* J Biomed Mater Res 1993;27:345-356.

304. Labow RS, Meek E, Santerre JP. Differential synthesis of cholesterol esterase by monocyte-derived macrophages cultured on poly(ether or ester) - based poly(urethane)s. J Biomed Mater Res 1998;39 : 469-477.

305. Kao WJ, Hiltner A, Anderson JM, Lodoen GA. Theoretical analysis of *in vivo* macrophage adhesion and foreign body giant cell formation on strained poly(etherurethane urea) elastomers. J Biomed Mater Res 1994; 28: 819-829

306. Santerre JP, Labow RS, Adams GA. Enzyme-biomaterial interactions: effect of biosystems on degradation of polyurethanes. J Biomed Mater Res 1993; 27:97-109.

307. Santerre JP, Labow RS, Duguay DG, Erfle D, Adams GA. Biodegradation evaluation of polyether and polyester-urethanes with oxidative and hydrolytic enzymes. J Biomed Mater Res 1994; 28: 1187-1199.

308. Labow RS, Meek E, Santerre JP. Synthesis of cholesterol esterase by monocyte-derived macrophages: a potential role in the biodegradation of poly(urethane)s. J Biomaterials Apps 1999;13: 187-205.

309. Schubert MA, Wiggins MJ, Schaefer MP, Hiltner A, Anderson JM. Oxidative biodegradation mechanisms of biaxially strained poly(etherurethane urea) elastomers. J Biomed Mater Res 1995;29:337-347.

310. Sutherland K, Mahoney JR, Coury AJ. Degradation of materials by phagocyte derived oxidants. J Clin Invest 1993;92:2360-2367.

311. Moorhouse CP, Halliwell B, Grootveld M, Gutteridge JMC. Cobalt (II) ion as promoter of hydroxyl radical and possible crypto-hydroxyl radical formation under physiological conditions: Differential effects of hydroxyl radical scavengers. Biochem. Biophys. Acta. 1983; 843: 261-268.

312. Stokes K, Urbanski P, Upton J. The *in vivo* auto-oxidation of polyether polyurethane by metal ions. J Biomater Sci Polymer Edn 1990;1:207-230.

313. Stokes K, Urbanski P, Cobian K: New test methods for the evaluation of stress cracking and metal-catalyzed oxidation in implanted polymers. In: Planck H, Syre I, Dauner M, Egbers G (Eds.) Polyurethanes in Biomedical Engineering II, Elsevier Science Publishers, Amsterdam 1987. pp.109-127.

314. Tyler BJ, Ratner BD: Variation between Biomer lots II. The effect of differences between lots on *in vitro* enzymatic and oxidative degradation of a commercial polyurethane. J Biomed Mater Res 1993;27:327-334.

315. Shi X, Dala NS, Kasprzak KS. Generation of free radicals from model lipid hydroperoxides and H_2O_2 by Co (II) in the presence of cysteineyl and histdyl chelators. Chem Res Roxicol 1993; 6:277-283.

316. Buettner GR. Spin trapping: ESR parameters of spin adducts. Free Rad Biol Med 1987;3:246-250.

317. Martz H, Beuadoin G, Paynter R, King M, Marceau D, Guidoin R. Physiochemical characterization of a hydrophillic microporous polyurethane vascular graft. J Biomed Mater Res 1987;21:399-412.

318. Harris PL. Arteries. In: Kirk RM (Ed). General Surgical Operations (Third Edition). Churchill Livingstone, Edinburgh 1994. p529-572.

319. Hegarty AF. Derivatives of carbon dioxide. In: Sutherland IO (Ed). Comprehensive Organic Chemistry Vol.2. Pergamon Press, Oxford, 1979; p.1067-1103.

320. Ward RS: Surface modification prior to surface formation. Control of polymer surface properties via bulk modification. Med. Plastics Biomater. Spring:1995; 34-41.

321. Gershon B, Cohn D, Marom G. Utilization of composite laminate theory in the design of synthetic soft tissues for biomedical prostheses. Biomaterials 1990;11:548-52.

322. Hellener G, Cohn D, Marom G. Elastic response of filament wound arterial prostheses under internal pressure. Biomaterials 1994;15:1115-21.

323. Tang YW, Santerre JP, Labow RS, Taylor DG. Application of macromolecular additives to reduce the hydrolytic degradation of polyurethanes by lysosomal enzymes. Biomaterials 1997; 18:37-45.

324. Lancaster MV, Fields RD. Patent publication number WO 90/08/96. Patent application number PCT/US90/0049 1990

325. O'Brien J, Wilson I, Orton T. Pognan F. Investigation of the Alamar Blue (resazurin) fluorescent dye for the assessment of mammalian cell cytotoxicity. European Journal of Biochemistry 2000; 267:5421-6.

326. Ahmed SA, Gogal RM Jr., Walsh JE. A new rapid and simple non-radioactive assay to monitor and determine the proliferation of lymphocytes: an alternative to [3H] thymidine incorporation assay. Journal of Immunological Methods1994: 170:211-24.

327. DeForge LE. Billeci KL. Kramer SM. Effect of IFN-gamma on the killing of S. aureus in human whole blood. Assessment of bacterial viability by CFU determination and by a new method using alamar Blue. Journal of Immunological Methods 2000; 245:79-89.

328. Voytik-Harbin SL, Brightman AO, Waisner B, Lamar CH, Badylak SF. Application and evaluation of the alamar Blue assay for cell growth and survival of fibroblasts. In Vitro Cellular & Developmental Biology. Animal 1998; 34:239-46.

329. Back SA. Khan R. Gan X. Rosenberg PA. Volpe JJ. A new Alamar Blue viability assay to rapidly quantify oligodendrocyte death. Journal of Neuroscience Methods 1999; 91:47-54.

330. de Fries R,Mitsuhashi M. Quantification of mitogen induced human lymphocyte proliferation: comparison of alamarBlue assay to 3H-thymidine incorporation assay. Journal of Clinical Laboratory Analysis 1995; 9:89-95.